EUROPEAN ORGANIZATION FOR NUCLEAR RESEARCH

CERN–EP/98–95

10 June 1998

# $\pi^{\pm}$, $\mathrm{K}^{\pm}$, p and $\overline{\mathrm{p}}$ production in $\mathrm{Z}^0 \to q\overline{q}$ , $\mathrm{Z}^0 \to b\overline{b}$ , $\mathrm{Z}^0 \to u\overline{u}, d\overline{d}, s\overline{s}$

DELPHI Collaboration

**Abstract**

The DELPHI experiment at LEP uses Ring Imaging Cherenkov detectors for particle identification. The good understanding of the RICH detectors allows the identification of charged pions, kaons and protons, covering the full momentum range from $0.7 < p < 45.6$ GeV/$c$. The $\pi^{\pm}$, $\mathrm{K}^{\pm}$, p and $\overline{\mathrm{p}}$ normalised production rates, their differential cross sections, multiplicities and the maxima $\xi_p^*$ of the $\xi_p = \ln(1/X_p)$ distributions are measured for three event samples $\mathrm{Z}^0 \to q\overline{q}$ , $\mathrm{Z}^0 \to b\overline{b}$ and $\mathrm{Z}^0 \to u\overline{u}, d\overline{d}, s\overline{s}$ , selected from $\sim 1\,400\,000$ $\mathrm{Z}^0$ decays collected by DELPHI in 1994. The results are compared to the predictions of the JETSET string fragmentation model and the HERWIG cluster fragmentation model. The Modified Leading Logarithm Approximation with Local Parton-Hadron Duality is tested. The $\xi_p^*$ dependence on the primary quark flavour is investigated and quantified for the different particle distributions. The $\pi^{\pm}$, $\mathrm{K}^{\pm}$, p and $\overline{\mathrm{p}}$ multiplicities are measured with precisions from $\pm 4\%$ to $\pm 6\%$. For the $\mathrm{Z}^0 \to q\overline{q}$ and $\mathrm{Z}^0 \to b\overline{b}$ event samples, these improve on previous measurements. The $\pi^{\pm}$, $\mathrm{K}^{\pm}$, p and $\overline{\mathrm{p}}$ multiplicities for $\mathrm{Z}^0 \to u\overline{u}, d\overline{d}, s\overline{s}$ are presented for the first time.

(Submitted to E. Phys. J. C)

P.Abreu[21], W.Adam[50], T.Adye[36], P.Adzic[11], I.Ajinenko[42], G.D.Alekseev[16], R.Alemany[49], P.P.Allport[22], S.Almehed[24], U.Amaldi[9], S.Amato[47], E.G.Anassontzis[3], P.Andersson[44], A.Andreazza[9], P.Antilogus[25], W-D.Apel[17], Y.Arnoud[14], B.Åsman[44], J-E.Augustin[25], A.Augustinus[9], P.Baillon[9], P.Bambade[19], F.Barao[21], G.Barbiellini[46], R.Barbier[25], D.Y.Bardin[16], G.Barker[9], A.Baroncelli[38], M.Battaglia[15], M.Baubillier[23], K-H.Becks[52], M.Begalli[6], P.Beilliere[8], Yu.Belokopytov[9,53], K.Belous[42], A.C.Benvenuti[5], C.Berat[14], M.Berggren[25], D.Bertini[25], D.Bertrand[2], M.Besancon[39], F.Bianchi[45], M.Bigi[45], M.S.Bilenky[16], M-A.Bizouard[19], D.Bloch[10], M.Bonesini[27], W.Bonivento[27], M.Boonekamp[39], P.S.L.Booth[22], A.W.Borgland[4], G.Borisov[39], C.Bosio[41], O.Botner[48], E.Boudinov[30], B.Bouquet[19], C.Bourdarios[19], T.J.V.Bowcock[22], I.Boyko[16], I.Bozovic[11], M.Bozzo[13], P.Branchini[38], T.Brenke[52], R.A.Brenner[48], P.Bruckman[35], J-M.Brunet[8], L.Bugge[32], T.Buran[32], T.Burgsmueller[52], P.Buschmann[52], S.Cabrera[49], M.Caccia[27], M.Calvi[27], A.J.Camacho Rozas[40], T.Camporesi[9], V.Canale[37], M.Canepa[13], F.Carena[9], L.Carroll[22], C.Caso[13], M.V.Castillo Gimenez[49], A.Cattai[9], F.R.Cavallo[5], Ch.Cerruti[10], V.Chabaud[9], Ph.Charpentier[9], L.Chaussard[25], P.Checchia[35], G.A.Chelkov[16], M.Chen[2], R.Chierici[45], P.Chliapnikov[42], P.Chochula[7], V.Chorowicz[25], J.Chudoba[29], P.Collins[9], M.Colomer[49], R.Contri[13], E.Cortina[49], G.Cosme[19], F.Cossutti[39], J-H.Cowell[22], H.B.Crawley[1], D.Crennell[36], G.Crosetti[13], J.Cuevas Maestro[33], S.Czellar[15], B.Dalmagne[19], G.Damgaard[28], M.Davenport[9], W.Da Silva[23], A.Deghorain[2], G.Della Ricca[46], P.Delpierre[26], N.Demaria[9], A.De Angelis[9], W.De Boer[17], S.De Brabandere[2], C.De Clercq[2], B.De Lotto[46], A.De Min[35], L.De Paula[47], H.Dijkstra[9], L.Di Ciaccio[37], A.Di Diodato[37], A.Djannati[8], J.Dolbeau[8], K.Doroba[51], M.Dracos[10], J.Drees[52], K.-A.Drees[52], M.Dris[31], A.Duperrin[25], J-D.Durand[25,9], R.Ehret[17], G.Eigen[4], T.Ekelof[48], G.Ekspong[44], M.Ellert[48], M.Elsing[9], J-P.Engel[10], B.Erzen[43], M.Espirito Santo[21], E.Falk[24], G.Fanourakis[11], D.Fassouliotis[11], J.Fayot[23], M.Feindt[17], P.Ferrari[27], A.Ferrer[49], S.Fichet[23], A.Firestone[1], P.-A.Fischer[9], U.Flagmeyer[52], H.Foeth[9], E.Fokitis[31], F.Fontanelli[13], B.Franek[36], A.G.Frodesen[4], R.Fruhwirth[50], F.Fulda-Quenzer[19], J.Fuster[49], A.Galloni[22], D.Gamba[45], M.Gandelman[47], C.Garcia[49], J.Garcia[40], C.Gaspar[9], M.Gaspar[47], U.Gasparini[35], Ph.Gavillet[9], E.N.Gazis[31], D.Gele[10], J-P.Gerber[10], L.Gerdyukov[42], N.Ghodbane[25], I.Gil[49], F.Glege[52], R.Gokieli[51], B.Golob[43], P.Goncalves[21], I.Gonzalez Caballero[40], G.Gopal[36], L.Gorn[1,54], M.Gorski[51], Yu.Gouz[42], V.Gracco[13], J.Grahl[1], E.Graziani[38], C.Green[22], A.Grefrath[52], P.Gris[39], K.Grzelak[51], M.Gunther[48], J.Guy[36], F.Hahn[9], S.Hahn[52], S.Haider[9], A.Hallgren[48], K.Hamacher[52], F.J.Harris[34], V.Hedberg[24], S.Heising[17], R.Henriques[21], J.J.Hernandez[49], P.Herquet[2], H.Herr[9], T.L.Hessing[34], J.-M.Heuser[52], E.Higon[49], S-O.Holmgren[44], P.J.Holt[34], D.Holthuizen[30], S.Hoorelbeke[2], M.Houlden[22], K.Huet[2], K.Hultqvist[44], J.N.Jackson[22], R.Jacobsson[44], P.Jalocha[9], R.Janik[7], Ch.Jarlskog[24], G.Jarlskog[24], P.Jarry[39], B.Jean-Marie[19], E.K.Johansson[44], P.Jonsson[24], C.Joram[9], P.Juillot[10], F.Kapusta[23], K.Karafasoulis[11], S.Katsanevas[25], E.C.Katsoufis[31], R.Keranen[17], B.A.Khomenko[16], N.N.Khovanski[16], A.Kiiskinen[15], B.King[22], N.J.Kjaer[30], O.Klapp[52], H.Klein[9], P.Kluit[30], D.Knoblauch[17], P.Kokkinias[11], M.Koratzinos[9], C.Kourkoumelis[3], O.Kouznetsov[16], M.Krammer[50], C.Kreuter[9], E.Kriznic[43], Z.Krumstein[16], P.Kubinec[7], W.Kucewicz[18], K.Kurvinen[15], J.W.Lamsa[1], L.Lanceri[46], D.W.Lane[1], P.Langefeld[52], V.Lapin[42], J-P.Laugier[39], R.Lauhakangas[15], G.Leder[50], F.Ledroit[14], V.Lefebure[2], L.Leinonen[44], A.Leisos[11], R.Leitner[29], J.Lemonne[2], G.Lenzen[52], V.Lepeltier[19], T.Lesiak[18], M.Lethuillier[39], J.Libby[34], D.Liko[9], A.Lipniacka[44], I.Lippi[35], B.Loerstad[24], J.G.Loken[34], J.H.Lopes[47], J.M.Lopez[40], R.Lopez-Fernandez[14], D.Loukas[11], P.Lutz[39], L.Lyons[34], J.MacNaughton[50], J.R.Mahon[6], A.Maio[21], A.Malek[52], T.G.M.Malmgren[44], V.Malychev[16], F.Mandl[50], J.Marco[40], R.Marco[40], B.Marechal[47], M.Margoni[35], J-C.Marin[9], C.Mariotti[9], A.Markou[11], C.Martinez-Rivero[33], F.Martinez-Vidal[49], S.Marti i Garcia[22], F.Matorras[40], C.Matteuzzi[27], G.Matthiae[37], F.Mazzucato[35], M.Mazzucato[35], M.Mc Cubbin[22], R.Mc Kay[1], R.Mc Nulty[9], G.Mc Pherson[22], C.Meroni[27], A.Miagkov[42], E.Migliore[45], L.Mirabito[25], W.A.Mitaroff[50], U.Mjoernmark[24], T.Moa[44], R.Moeller[28], K.Moenig[9], M.R.Monge[13], X.Moreau[23], P.Morettini[13], G.Morton[34], K.Muenich[52], M.Mulders[30], C.Mulet-Marquis[14], R.Muresan[24], W.J.Murray[36], B.Muryn[14,18], G.Myatt[34], T.Myklebust[32], F.Naraghi[14], F.L.Navarria[5], S.Navas[49], K.Nawrocki[51], P.Negri[27], S.Nemecek[12], N.Neufeld[9], W.Neumann[52], N.Neumeister[50], R.Nicolaidou[14], B.S.Nielsen[28], M.Nieuwenhuizen[30], V.Nikolaenko[10], M.Nikolenko[10,16], V.Nomokonov[15], A.Normand[22], A.Nygren[24], V.Obraztsov[42], A.G.Olshevski[16], A.Onofre[21], R.Orava[15], G.Orazi[10], K.Osterberg[15], A.Ouraou[39], P.Paganini[19], M.Paganoni[27], S.Paiano[5], R.Pain[23], R.Paiva[21], J.Palacios[34], H.Palka[18], Th.D.Papadopoulou[31], K.Papageorgiou[11], L.Pape[9], C.Parkes[34], F.Parodi[13], U.Parzefall[22], A.Passeri[38], M.Pegoraro[35], L.Peralta[21], M.Pernicka[50], A.Perrotta[5], C.Petridou[46], A.Petrolini[13], H.T.Phillips[36], G.Piana[13], F.Pierre[39], M.Pimenta[21], E.Piotto[27], T.Podobnik[43], M.E.Pol[6], G.Polok[18], P.Poropat[46], V.Pozdniakov[16], P.Privitera[37], N.Pukhaeva[16], A.Pullia[27], D.Radojicic[34], S.Ragazzi[27], H.Rahmani[31], D.Rakoczy[50], J.Rames[12], P.N.Ratoff[20], A.L.Read[32], P.Rebecchi[9], N.G.Redaelli[27], M.Regler[50], D.Reid[9], R.Reinhardt[52], P.B.Renton[34], L.K.Resvanis[3], F.Richard[19], J.Ridky[12], G.Rinaudo[45], O.Rohne[32], A.Romero[45], P.Ronchese[35], E.I.Rosenberg[1], P.Rosinsky[7], P.Roudeau[19], T.Rovelli[5], V.Ruhlmann-Kleider[39], A.Ruiz[40], H.Saarikko[15], Y.Sacquin[39], A.Sadovsky[16], G.Sajot[14], J.Salt[49], D.Sampsonidis[11], M.Sannino[13], H.Schneider[17], Ph.Schwemling[23], U.Schwickerath[17], M.A.E.Schyns[52], F.Scuri[46], P.Seager[20], Y.Sedykh[16], A.M.Segar[34], R.Sekulin[36], V.Senko[42], R.C.Shellard[6], A.Sheridan[22], R.Silvestre[39], L.Simard[39], F.Simonetto[35], A.N.Sisakian[16], T.B.Skaali[32], G.Smadja[25], O.Smirnova[24], G.R.Smith[36], O.Solovianov[42], A.Sopczak[17], R.Sosnowski[51], T.Spassov[21], E.Spiriti[38], P.Sponholz[52], S.Squarcia[13], D.Stampfer[50], C.Stanescu[38], S.Stanic[43], S.Stapnes[32], K.Stevenson[34], A.Stocchi[19], J.Strauss[50], R.Strub[10], B.Stugu[4], M.Szczekowski[51], M.Szeptycka[51], T.Tabarelli[27], F.Tegenfeldt[48], F.Terranova[27], J.Thomas[34], A.Tilquin[26], J.Timmermans[30], L.G.Tkatchev[16], T.Todorov[10], S.Todorova[10], D.Z.Toet[30], A.Tomaradze[2], B.Tome[21], A.Tonazzo[27], L.Tortora[38], G.Transtromer[24], D.Treille[9], G.Tristram[8],

A.Trombini[19], C.Troncon[27], A.Tsirou[9], M-L.Turluer[39], I.A.Tyapkin[16], S.Tzamarias[11], B.Ueberschaer[52], O.Ullaland[9], V.Uvarov[42], G.Valenti[5], E.Vallazza[46], C.Vander Velde[2], G.W.Van Apeldoorn[30], P.Van Dam[30], W.K.Van Doninck[2], J.Van Eldik[30], A.Van Lysebetten[2], I.Van Vulpen[30], N.Vassilopoulos[34], G.Vegni[27], L.Ventura[35], W.Venus[36], F.Verbeure[2], M.Verlato[35], L.S.Vertogradov[16], V.Verzi[37], D.Vilanova[39], N.Vishnevsky[42], L.Vitale[46], E.Vlasov[42], A.S.Vodopyanov[16], G.Voulgaris[3], V.Vrba[12], H.Wahlen[52], C.Walck[44], C.Weiser[17], A.M.Wetherell[9], D.Wicke[52], J.H.Wickens[2], G.R.Wilkinson[9], M.Winter[10], M.Witek[18], T.Wlodek[19], G.Wolf[9], J.Yi[1], O.Yushchenko[42], A.Zaitsev[42], A.Zalewska[18], P.Zalewski[51], D.Zavrtanik[43], E.Zevgolatakos[11], N.I.Zimin[16,24], G.C.Zucchelli[44], G.Zumerle[35]

[1] Department of Physics and Astronomy, Iowa State University, Ames IA 50011-3160, USA
[2] Physics Department, Univ. Instelling Antwerpen, Universiteitsplein 1, BE-2610 Wilrijk, Belgium
and IIHE, ULB-VUB, Pleinlaan 2, BE-1050 Brussels, Belgium
and Faculté des Sciences, Univ. de l'Etat Mons, Av. Maistriau 19, BE-7000 Mons, Belgium
[3] Physics Laboratory, University of Athens, Solonos Str. 104, GR-10680 Athens, Greece
[4] Department of Physics, University of Bergen, Allégaten 55, NO-5007 Bergen, Norway
[5] Dipartimento di Fisica, Università di Bologna and INFN, Via Irnerio 46, IT-40126 Bologna, Italy
[6] Centro Brasileiro de Pesquisas Físicas, rua Xavier Sigaud 150, BR-22290 Rio de Janeiro, Brazil
and Depto. de Física, Pont. Univ. Católica, C.P. 38071 BR-22453 Rio de Janeiro, Brazil
and Inst. de Física, Univ. Estadual do Rio de Janeiro, rua São Francisco Xavier 524, Rio de Janeiro, Brazil
[7] Comenius University, Faculty of Mathematics and Physics, Mlynska Dolina, SK-84215 Bratislava, Slovakia
[8] Collège de France, Lab. de Physique Corpusculaire, IN2P3-CNRS, FR-75231 Paris Cedex 05, France
[9] CERN, CH-1211 Geneva 23, Switzerland
[10] Institut de Recherches Subatomiques, IN2P3 - CNRS/ULP - BP20, FR-67037 Strasbourg Cedex, France
[11] Institute of Nuclear Physics, N.C.S.R. Demokritos, P.O. Box 60228, GR-15310 Athens, Greece
[12] FZU, Inst. of Phys. of the C.A.S. High Energy Physics Division, Na Slovance 2, CZ-180 40, Praha 8, Czech Republic
[13] Dipartimento di Fisica, Università di Genova and INFN, Via Dodecaneso 33, IT-16146 Genova, Italy
[14] Institut des Sciences Nucléaires, IN2P3-CNRS, Université de Grenoble 1, FR-38026 Grenoble Cedex, France
[15] Helsinki Institute of Physics, HIP, P.O. Box 9, FI-00014 Helsinki, Finland
[16] Joint Institute for Nuclear Research, Dubna, Head Post Office, P.O. Box 79, RU-101 000 Moscow, Russian Federation
[17] Institut für Experimentelle Kernphysik, Universität Karlsruhe, Postfach 6980, DE-76128 Karlsruhe, Germany
[18] Institute of Nuclear Physics and University of Mining and Metalurgy, Ul. Kawiory 26a, PL-30055 Krakow, Poland
[19] Université de Paris-Sud, Lab. de l'Accélérateur Linéaire, IN2P3-CNRS, Bât. 200, FR-91405 Orsay Cedex, France
[20] School of Physics and Chemistry, University of Lancaster, Lancaster LA1 4YB, UK
[21] LIP, IST, FCUL - Av. Elias Garcia, 14-1°, PT-1000 Lisboa Codex, Portugal
[22] Department of Physics, University of Liverpool, P.O. Box 147, Liverpool L69 3BX, UK
[23] LPNHE, IN2P3-CNRS, Univ. Paris VI et VII, Tour 33 (RdC), 4 place Jussieu, FR-75252 Paris Cedex 05, France
[24] Department of Physics, University of Lund, Sölvegatan 14, SE-223 63 Lund, Sweden
[25] Université Claude Bernard de Lyon, IPNL, IN2P3-CNRS, FR-69622 Villeurbanne Cedex, France
[26] Univ. d'Aix - Marseille II - CPP, IN2P3-CNRS, FR-13288 Marseille Cedex 09, France
[27] Dipartimento di Fisica, Università di Milano and INFN, Via Celoria 16, IT-20133 Milan, Italy
[28] Niels Bohr Institute, Blegdamsvej 17, DK-2100 Copenhagen Ø, Denmark
[29] NC, Nuclear Centre of MFF, Charles University, Areal MFF, V Holesovickach 2, CZ-180 00, Praha 8, Czech Republic
[30] NIKHEF, Postbus 41882, NL-1009 DB Amsterdam, The Netherlands
[31] National Technical University, Physics Department, Zografou Campus, GR-15773 Athens, Greece
[32] Physics Department, University of Oslo, Blindern, NO-1000 Oslo 3, Norway
[33] Dpto. Fisica, Univ. Oviedo, Avda. Calvo Sotelo s/n, ES-33007 Oviedo, Spain
[34] Department of Physics, University of Oxford, Keble Road, Oxford OX1 3RH, UK
[35] Dipartimento di Fisica, Università di Padova and INFN, Via Marzolo 8, IT-35131 Padua, Italy
[36] Rutherford Appleton Laboratory, Chilton, Didcot OX11 OQX, UK
[37] Dipartimento di Fisica, Università di Roma II and INFN, Tor Vergata, IT-00173 Rome, Italy
[38] Dipartimento di Fisica, Università di Roma III and INFN, Via della Vasca Navale 84, IT-00146 Rome, Italy
[39] DAPNIA/Service de Physique des Particules, CEA-Saclay, FR-91191 Gif-sur-Yvette Cedex, France
[40] Instituto de Fisica de Cantabria (CSIC-UC), Avda. los Castros s/n, ES-39006 Santander, Spain
[41] Dipartimento di Fisica, Università degli Studi di Roma La Sapienza, Piazzale Aldo Moro 2, IT-00185 Rome, Italy
[42] Inst. for High Energy Physics, Serpukov P.O. Box 35, Protvino, (Moscow Region), Russian Federation
[43] J. Stefan Institute, Jamova 39, SI-1000 Ljubljana, Slovenia and Department of Astroparticle Physics, School of Environmental Sciences, Kostanjeviska 16a, Nova Gorica, SI-5000 Slovenia,
and Department of Physics, University of Ljubljana, SI-1000 Ljubljana, Slovenia
[44] Fysikum, Stockholm University, Box 6730, SE-113 85 Stockholm, Sweden
[45] Dipartimento di Fisica Sperimentale, Università di Torino and INFN, Via P. Giuria 1, IT-10125 Turin, Italy
[46] Dipartimento di Fisica, Università di Trieste and INFN, Via A. Valerio 2, IT-34127 Trieste, Italy
and Istituto di Fisica, Università di Udine, IT-33100 Udine, Italy
[47] Univ. Federal do Rio de Janeiro, C.P. 68528 Cidade Univ., Ilha do Fundão BR-21945-970 Rio de Janeiro, Brazil
[48] Department of Radiation Sciences, University of Uppsala, P.O. Box 535, SE-751 21 Uppsala, Sweden
[49] IFIC, Valencia-CSIC, and D.F.A.M.N., U. de Valencia, Avda. Dr. Moliner 50, ES-46100 Burjassot (Valencia), Spain
[50] Institut für Hochenergiephysik, Österr. Akad. d. Wissensch., Nikolsdorfergasse 18, AT-1050 Vienna, Austria
[51] Inst. Nuclear Studies and University of Warsaw, Ul. Hoza 69, PL-00681 Warsaw, Poland
[52] Fachbereich Physik, University of Wuppertal, Postfach 100 127, DE-42097 Wuppertal, Germany
[53] On leave of absence from IHEP Serpukhov
[54] Now at University of Florida

# 1 Introduction

The measurement of the composition of hadronic final state particles in electron-positron annihilation is fundamental to the understanding of the fragmentation of quarks and gluons into hadrons. Only phenomenological models, which need to be tuned to the data, are available to describe this fragmentation process with high accuracy. Two models commonly used are the JETSET string fragmentation model [1] and the HERWIG cluster fragmentation model [2].

During the 1994 LEP run, DELPHI collected $\sim$1 400 000 $Z^0$ events, having the Ring Imaging Cherenkov (RICH) detectors operational in optimal and stable conditions. The DELPHI experiment and its RICH detectors are described in detail elsewhere ([3–5]).

Three event samples were considered for this analysis, a sample containing all quark flavours i.e. *udscb* (referred to as the '$q\overline{q}$ - sample'), a sub-sample of $b$ - flavour enriched events (the '$b$ - sample') and a *uds* - flavour enriched sub-sample (the '*uds* - sample').

With the barrel RICH detector offering the possibility of a complete $\pi^{\pm}$, $K^{\pm}$, p and $\overline{p}$[1] identification, DELPHI is able to perform precision measurements on $\pi^{\pm}$, $K^{\pm}$ *and* $p\overline{p}$ spectra in hadronic $Z^0$ decays covering the full momentum range from 0.7 up to 45 GeV/$c$. The data distributions are compared with the predictions of JETSET and HERWIG fragmentation models. The $\pi^{\pm}$, $K^{\pm}$ and $p\overline{p}$ multiplicities are obtained by integrating over fits to the measured $\xi_p$ distributions ($\xi_p = -\ln X_p$, $X_p = p/p_{beam}$) based on the Modified Leading Logarithm Approximation under the assumption of Local Parton-Hadron Duality. More details of the analysis can be found in [6]. In addition, the maxima $\xi_p^*$ of the $\xi_p$ distributions are determined. The obtained multiplicities and $\xi_p^*$ results are compared with the JETSET and HERWIG predictions and with previously published measurements.

# 2 Event and charged particle selection criteria

Charged particles were selected according to the following criteria:

- The particle momentum had to be greater than 0.3 GeV/$c$ and lower than 70 GeV/$c$.
- The relative uncertainty on the measured momentum had to be smaller than 50% and the absolute uncertainty had to be less than 5 GeV/$c$.
- The measured track length was required to be larger than 30 cm.
- The impact parameter had to be less than 10 cm transverse to the beam axis ($R_\phi$) and less than 20 cm along the beam axis ($R_z$).
- The track had to have a polar angle between 15° and 165°.

Hadronic events were then defined as:

- Events containing at least 5 charged particles.
- The total energy of the charged particles in the event had to be larger than 15 GeV.

Since this analysis is based on data measured by the barrel RICH detector, only those hadronic events were selected which had at least one charged particle with $p > 0.7$ GeV/$c$ inside the DELPHI barrel region (polar angle to the beam between 47° and 133°). In addition, a run-selection was performed, removing small data taking periods which were potentially unstable.

Of the $\sim$1 400 000 hadronic $Z^0$ decays collected by DELPHI in 1994, $\sim$1 068 000 hadronic events were selected after the above criteria. Out of $\sim$2 380 000 generated

[1] Protons and anti-protons (i.e. p and $\overline{p}$) will be represented by the symbol $p\overline{p}$.

Monte Carlo events with full detector simulation [4,7], $\sim$2 027 000 events passed the same selection criteria. The contributions from beam-gas scattering, two-photon events and $Z^0 \to \tau^+\tau^-$ events were estimated to be less than 0.3%.

Finally, charged particle tracks used in the analysis had to pass the following criteria:

- The track polar angle had to be between 47° and 133°.
- The particle momentum had to be larger than 0.7 GeV/$c$.
- Time Projection Chamber (TPC) information was used for the track reconstruction.
- Particles with $p < 2.7$ GeV/$c$ had to be negatively charged, suppressing particles coming from secondary interactions ($\sim$95% reduction of secondary protons).

# 3 Tagging $b\overline{b}$ and $u\overline{u}, d\overline{d}, s\overline{s}$ events

To separate $b$ - and $uds$ - flavour enriched sub-samples from the $q\overline{q}$ - sample, a topological lifetime $b$ - tagging was applied. The method defines an event-probability '$\mathcal{P}_E^+$' (based on the positive lifetime-signed impact parameter significances of tracks in the event) for the tracks to be consistent with the primary vertex [4]. Cutting on $\mathcal{P}_E^+$ can then be used to select (or suppress) $b$ - events.

Requiring $\mathcal{P}_E^+$ to be less than 0.01 resulted in a sub-sample of $\sim$198 000 $b$ - enriched events from the data. From the Monte Carlo simulation $\sim$424 000 events were selected, giving a sub-sample of 78.5% $b$ - purity. The contamination of $uds$ and $c$ flavour was respectively 6.8% and 14.7%.

A $uds$ - flavour enriched event sample was obtained by using the $b$ - tagging information to suppress $b$ - events (i.e. anti $b$ - tagging). Requiring $\mathcal{P}_E^+$ to be bigger than 0.15 selected $\sim$668 000 events from the data and $\sim$1 243 000 from the Monte Carlo, with a $uds$ - purity of 81.7%. The contamination of $b$ - and $c$ - flavour was respectively 3.8% and 14.5%.

# 4 The experimental method

The real particle content of a sample was obtained from the measured particle content by inverting the tagging efficiency matrix[2]:

$$\begin{pmatrix} N_\pi \\ N_{\mathrm{K}} \\ N_{\mathrm{p}} \end{pmatrix}^{\mathrm{Real}}(x) = \begin{pmatrix} \mathcal{E}_\pi^\pi & \mathcal{E}_{\mathrm{K}}^\pi & \mathcal{E}_{\mathrm{p}}^\pi \\ \mathcal{E}_\pi^{\mathrm{K}} & \mathcal{E}_{\mathrm{K}}^{\mathrm{K}} & \mathcal{E}_{\mathrm{p}}^{\mathrm{K}} \\ \mathcal{E}_\pi^{\mathrm{p}} & \mathcal{E}_{\mathrm{K}}^{\mathrm{p}} & \mathcal{E}_{\mathrm{p}}^{\mathrm{p}} \end{pmatrix}^{-1} \cdot \begin{pmatrix} N_\pi \\ N_{\mathrm{K}} \\ N_{\mathrm{p}} \end{pmatrix}^{\mathrm{Meas.}}(x) \qquad (1)$$

where, for $i, j = \pi^\pm$, $\mathrm{K}^\pm$ or $\mathrm{p\overline{p}}$, the vector element $N_i$ stands for the (normalised) number of particles of type $i$ and the matrix element $\mathcal{E}_i^j$ represents the efficiency of tagging a particle of true identity $i$ as a particle of type $j$. The tagging efficiency matrix is derived from the simulation. In principle, any observable can be taken for $x$ e.g. momentum $p$, $X_p = p/p_{beam}$, $\xi_p$, rapidity $y$ etc.. The method implicitly accounts for particle misidentification, provided the full detector simulation describes the data well.

The NEWTAG package [8] was used for $\pi^\pm$, $\mathrm{K}^\pm$ *and* $\mathrm{p\overline{p}}$ identification using barrel RICH data. For each particle hypothesis, NEWTAG provides different levels of *tagging quality* and of RICH *track quality* (i.e. 'very loose', 'loose', 'standard' or 'tight' in each case). This is done by allowing the measured Cherenkov angle, $\theta_{\check{c}}^{\mathrm{meas.}}$, and its uncertainty, $\sigma_{\mathrm{ring}}^{\mathrm{exp.}}$, to vary within different windows. Thus various $\pi^\pm, \mathrm{K}^\pm, \mathrm{p\overline{p}}$ samples of different

[2] The RICH $\pi^\pm$ identification in most cases cannot differentiate $\pi^\pm$ from $e^\pm$ and $\mu^\pm$. An explicit correction for the $e^\pm$ and $\mu^\pm$ contamination will be applied in section 5.2 below.

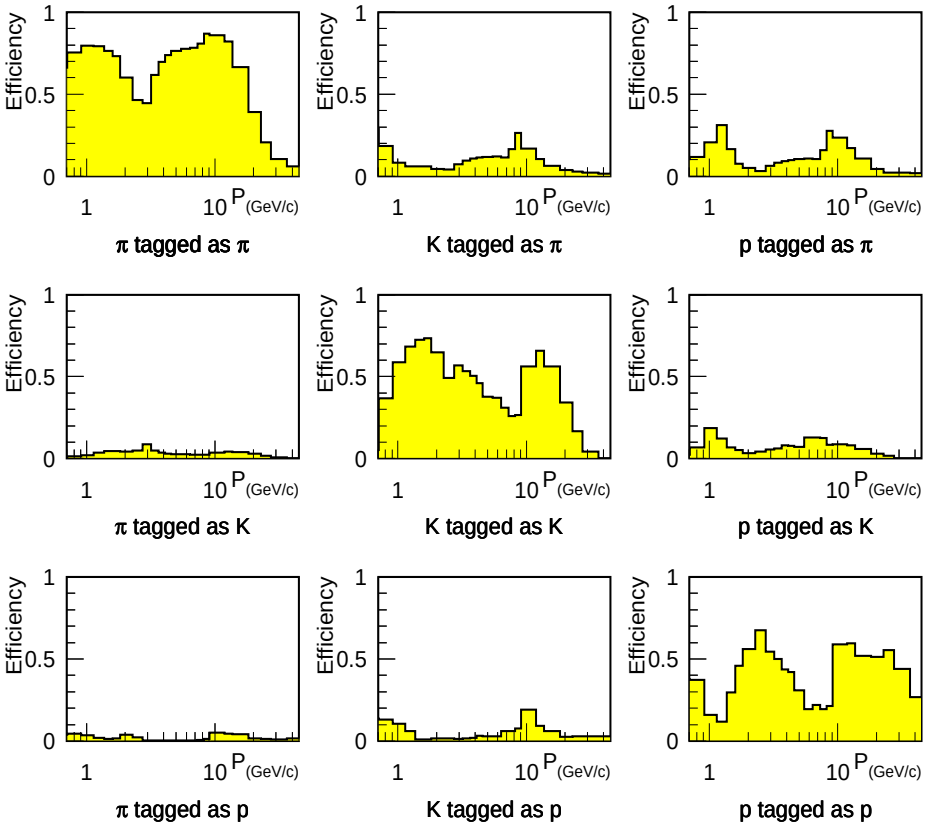


Figure 1: The tagging efficiency matrix for standard NEWTAG output and very loose track quality selection versus momentum (for tracks with Outer Detector information).

purity and efficiency can be selected. The loose tagging and loose track quality criteria were chosen for the central values of the measurements in this analysis. The results obtained in the same way using the very loose and standard criteria were used to estimate the systematic uncertainties. Figure 1 illustrates the tagging efficiency matrix for the standard tag and very loose track quality for $x \equiv p$ in equation 1.

In the momentum window between 2.7 and 8.5 GeV/$c$, NEWTAG offers two options for tagging kaons and protons. Either using positive RICH identification for both $K^{\pm}$ and $p\overline{p}$ through the combined use of liquid and gas radiator information, or not distinguishing $K^{\pm}$ from $p\overline{p}$ by using only the gas radiator 'veto-information' – the so called heavy particle ($Hv^{\pm}$) tag[3]. Including the heavy particle tag in this analysis offers the following advantages for $2.7 < p < 8.5$ GeV/$c$:

- It is significantly more efficient than the sum of the $K^{\pm}$ and $p\overline{p}$ tags (see for example fig. 3, 'p tagged as p' compared to 'p tagged as Hv').
- By comparing the heavy-tag result with the sum of $K^{\pm}$ and $p\overline{p}$, systematic effects caused by the identification based on the liquid radiator (since it is used for $K^{\pm}$, $p\overline{p}$ but omitted in the heavy-tag) can be quantified.
- It simplifies the method of matrix inversion. The 3x3 matrix equation (eq.1) is reduced to a 2x2 matrix equation[4]:

$$\begin{pmatrix} N_{\pi} \\ N_{\mathrm{Hv}} \end{pmatrix}^{\mathrm{Real}}(x) = \begin{pmatrix} \mathcal{E}_{\pi}^{\pi} & \mathcal{E}_{\mathrm{Hv}}^{\pi} \\ \mathcal{E}_{\pi}^{\mathrm{Hv}} & \mathcal{E}_{\mathrm{Hv}}^{\mathrm{Hv}} \end{pmatrix}^{-1} \cdot \begin{pmatrix} N_{\pi} \\ N_{\mathrm{Hv}} \end{pmatrix}^{\mathrm{Meas.}}(x) \qquad (2)$$

[3] Heavy particles $Hv^{\pm}$ are defined as particles which are heavier than pions.

[4] From here onwards, the 3x3 matrix inversion method will be referred to as the '3x3-method' and the 2x2 matrix inversion method will be referred to as the '2x2-method'.

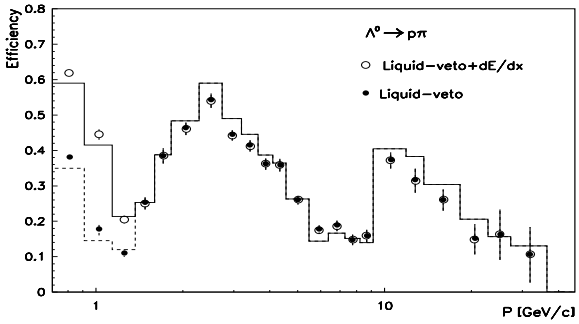


Figure 2: The gain in proton tagging efficiency due to including the $\mathrm{d}E/\mathrm{d}x$ measurement of the TPC at low momenta, tested on data (open and closed points) and Monte Carlo (line and dashed histograms) with protons from $\Lambda^0$ decay.

At low momenta ($p < 1.3$ GeV/$c$), the RICH proton tag is based on the liquid-veto information which has a low efficiency due to the background. The efficiency can be increased by using also the TPC $\mathrm{d}E/\mathrm{d}x$ measurement, defining similar tagging and track quality levels. The $\mathrm{d}E/\mathrm{d}x$ proton tag for particle momenta between 0.7 and 1.3 GeV/$c$ is based on the scaled difference between the measured and expected $\mathrm{d}E/\mathrm{d}x$ for a proton:

$$\sigma_{\mathrm{acc}} = \frac{\mid (\mathrm{d}E/\mathrm{d}x)^{\mathrm{meas.}} - (\mathrm{d}E/\mathrm{d}x)^{\mathrm{exp.(p)}} \mid}{\sigma_{\mathrm{d}E/\mathrm{d}x}} \tag{3}$$

A particle is tagged as a proton if the $\mathrm{d}E/\mathrm{d}x$ measurement is within 3 ('very loose'), 2.5 ('loose'), 2 ('standard') or 1.5 ('tight') standard deviations of the proton hypothesis. Protons are then selected if tagged by either $\mathrm{d}E/\mathrm{d}x$ or NEWTAG. Figure 2 illustrates the gain in efficiency compared with the RICH-only proton tag for data and Monte Carlo for the standard tag and the very loose track quality selection.

To avoid biases due to the different compositions of the event samples, the efficiency matrix was computed separately for each sample. Choosing the loose tagging and track quality criteria, the agreement between data and Monte Carlo using pions from $\mathrm{K}^0_{\mathrm{S}} \to \pi^+\pi^-$ and protons from $\Lambda^0 \to \mathrm{p}\pi^-$ decays, is shown in figure 3. The pion purity was estimated from the $\mathrm{K}^0_{\mathrm{S}}$ sample to be $\sim$94% and the proton purity from the $\Lambda^0$ sample to be $\sim$75%. The right-hand side of the figure appears to show that a proton is more likely to be misidentified as a pion than as a kaon. This can be understood from the relatively low purity of the proton sample. The dashed lines in the right-hand side column represent the correctly tagged part of the Monte Carlo, e.g. the dashed line in the top right plot ('p tagged as $\pi$') represents real pions which the $\Lambda^0$ reconstruction indicated were protons. However, the important point is that the detector simulation describes the data well.

The final stage deals with the primary quark flavour impurities in the $b$ - sample and $uds$ - sample. With a purity of 78.5% for the $b$ - sample and 81.7% for the $uds$ - sample, corrections must be made for the 21.5% $udsc$ and 18.3% $bc$ flavour impurity respectively. This was achieved by purity matrix inversion, as follows:

$$\begin{pmatrix} N_i^b \\ N_i^{udsc} \end{pmatrix}^{\mathrm{Real}}(x) = \begin{pmatrix} \mathcal{P}_b & 1-\mathcal{P}_{udsc} \\ 1-\mathcal{P}_b & \mathcal{P}_{udsc} \end{pmatrix}^{-1} \cdot \begin{pmatrix} N_i^b \\ N_i^{udsc} \end{pmatrix}^{\mathrm{Meas.}}(x) \qquad \text{(a)}$$

$$\begin{pmatrix} N_i^{bc} \\ N_i^{uds} \end{pmatrix}^{\mathrm{Real}}(x) = \begin{pmatrix} \mathcal{P}_{bc} & 1-\mathcal{P}_{uds} \\ 1-\mathcal{P}_{bc} & \mathcal{P}_{uds} \end{pmatrix}^{-1} \cdot \begin{pmatrix} N_i^{bc} \\ N_i^{uds} \end{pmatrix}^{\mathrm{Meas.}}(x) \qquad \text{(b)} \tag{4}$$

For $i = \pi^{\pm}$, $\mathrm{K}^{\pm}$, $\mathrm{p\overline{p}}$ or $\mathrm{Hv}^{\pm}$, the vector element $N_i^b$ stands for the real (normalised) number of particles of type $i$ from the $b$ - sample and $N_i^{udsc}$ represents the equivalent for

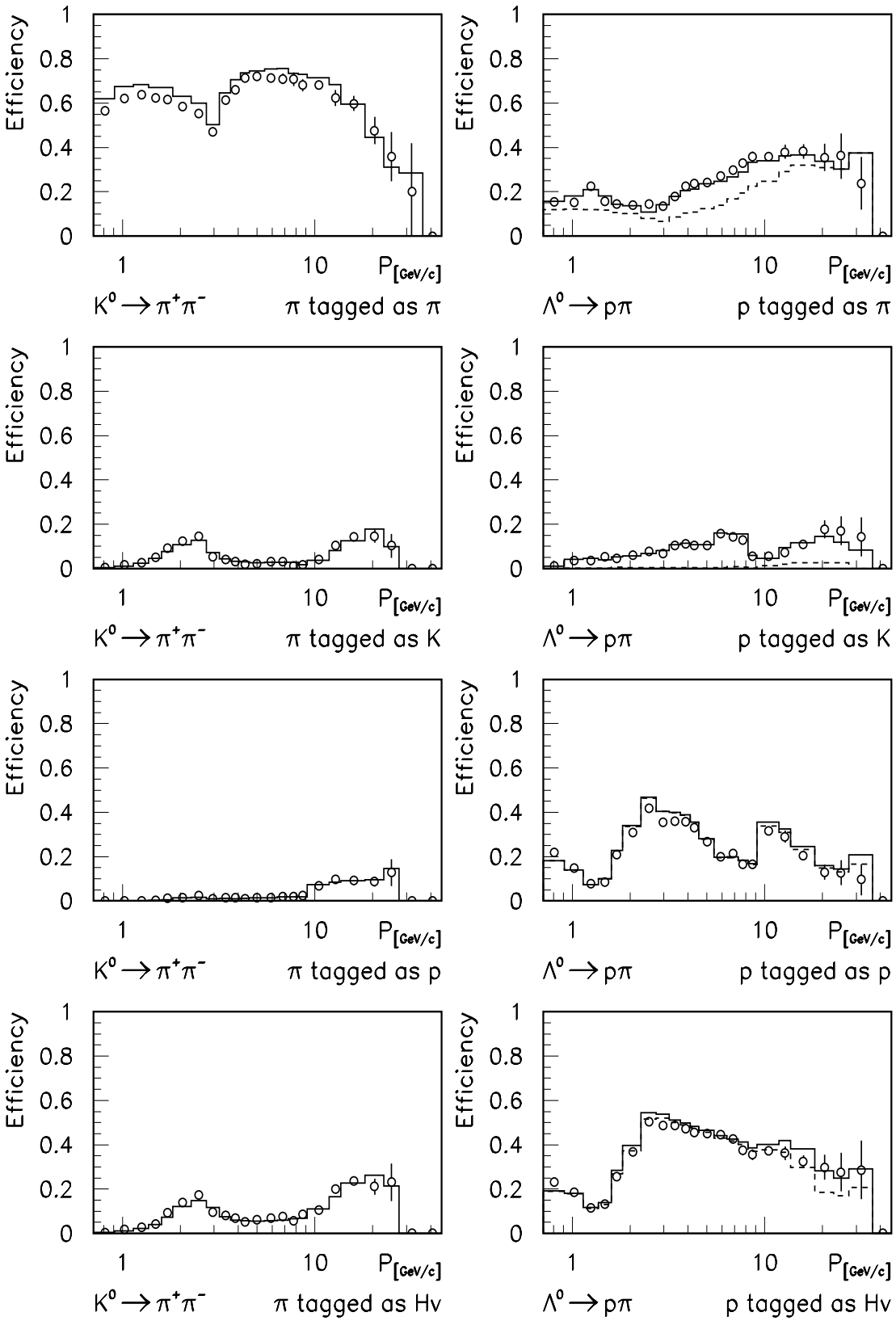


Figure 3: The NEWTAG comparison of efficiency versus momentum between data (points) and Monte Carlo (histograms) for loose tagging and loose track quality selection with pions from $K^0_S$ decay candidates and protons from $\Lambda^0$ decay candidates in $Z^0 \to q\overline{q}$ events. The dashed histograms correspond to correctly tagged (non)-proton tracks in the $\Lambda^0$ Monte Carlo sample.

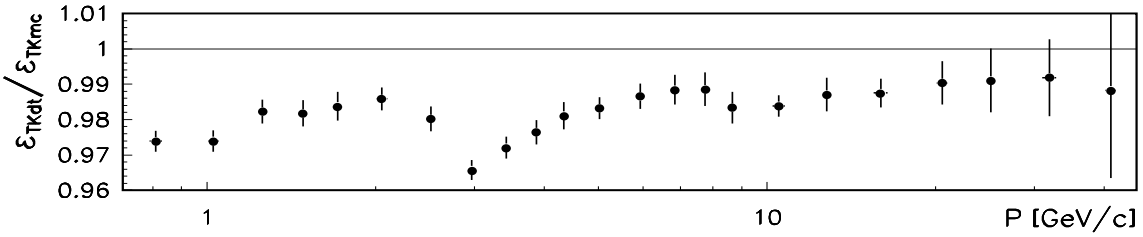


Figure 4: The data-Monte Carlo ratio of the loose track selection efficiency $\mathcal{E}_{\rm sel}^{\rm data}/\mathcal{E}_{\rm sel}^{\rm m.c.}$.

non $b$ - tagged events. Likewise, $N_i^{uds}$ stands for the real (normalised) number of particles of kind $i$ from the $uds$ - sample and $N_i^{bc}$ represents the equivalent for non $uds$ - tagged events. The elements of the purity matrix $\mathcal{P}_{b(c)}$ and $\mathcal{P}_{uds(c)}$ were determined from full detector simulation. The difference between the two equations lies in the treatment of the $c$-flavour contribution, which is the main impurity in both the $b$ - and the $uds$ - sample.

# 5 Corrections and uncertainties

In this section an overview of the corrections which have been applied to obtain the final distributions will be presented first, followed by a discussion on the statistical and systematic uncertainties. Corrections, other than those performed implicitly by the matrix inversion methods from the previous section, were separated into two groups. A group of 'local corrections' and a group of 'global corrections'. Both groups rely on the Monte Carlo simulation.

## 5.1 Local corrections

Local corrections are linked to the TPC and RICH detectors and their particle identification. Two local correction factors were applied, one to the track selection efficiency based on the track quality and one to the tagging efficiency.

We define the track selection efficiency as:

$$\mathcal{E}_{\rm sel} = \frac{\text{the number of tracks of a certain quality in the barrel region}}{\text{the total number of tracks in the barrel region}} \qquad (5)$$

For the loose track quality, the ratio of data to Monte Carlo for $\mathcal{E}_{\rm sel}$ versus momentum is illustrated in figure 4. The correction was applied bin-by-bin to the measured distributions and for most bins it was of order 1–2%.

The tagging efficiency matrix elements determined from the simulation as a function of momentum are illustrated in figure 1. To determine whether corrections to this matrix are needed, data and simulation were compared using pions from $\rm K_S^0$ and protons from $\Lambda^0$, as shown in figure 3. Unfortunately, not all bins of the individual elements of the efficiency matrix can be verified. Since no equivalent kaon sample is available, only the matrix elements for pion and proton tagging can be considered. Moreover, especially for the $\rm K_S^0$, they can be compared only for momenta below $\sim 10$ GeV/$c$. This is mainly because at higher momenta the statistics are too low, but is also to avoid a bias due to the topology of the $\rm K_S^0$ decay. At high momenta, the opening angle between the two outgoing tracks is usually very small and the Cherenkov ring reconstruction is more complicated because the rings overlap.

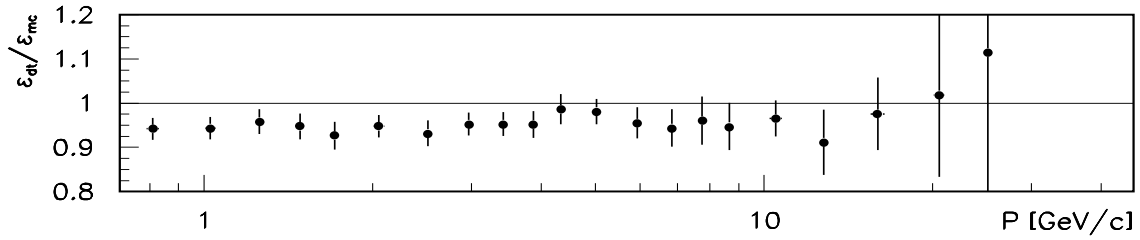


Figure 5: The data-Monte Carlo ratio of $\mathcal{E}_\pi^{\rm data}/\mathcal{E}_\pi^{\rm m.c.}$ versus momentum for loose track quality selection and loose pion tagging for $\pi^\pm$ from $\mathrm{K}^0_\mathrm{S}\to\pi^+\pi^-$.

With one exception (discussed below), the correction factors were derived only for the diagonal elements of the tagging probability matrix (i.e. for '$\pi$ tagged as $\pi$', 'p tagged as p' and 'p tagged as Hv' in figure 3). This strategy was chosen because the diagonal elements are the most important and to overcome a potential bias due to the impurity of the samples (especially the $\Lambda^0$ sample). To maintain the unitarity of the probability matrix, a correction applied to a diagonal element was propagated to the off-diagonal elements of the same column.

The one exception concerned the discrepancy between data and Monte Carlo in five momentum bins around 2 GeV/$c$ for the $\pi^\pm$ misidentification. Of all off-diagonal matrix elements, the elements $\mathcal{E}_\pi^{\rm K}$ in the 3x3-method and $\mathcal{E}_\pi^{\rm Hv}$ in the 2x2-method have the most significant influence on the matrix inversion method, especially around 2 GeV/$c$ where the pion production rate is high.

As an example, figure 5 shows the ratio of the pion tagging efficiency for data and Monte Carlo for the top-left distributions '$\pi$ tagged as $\pi$' in figure 3. From this ratio, an average correction factor was computed for each of three momentum ranges: 0.7–2.7 GeV/$c$, 2.7–5.5 GeV/$c$, and over 5.5 GeV/$c$. Between 0.7 and 2.7 GeV/$c$, only liquid radiator information is used for pion tagging. Above 2.7 GeV/$c$ only gas information is used for tagging pions, but the ranges below and above 5.5 GeV/$c$ were considered separately in order to allow for the difference in curvature of the tracks and its influence on the Cherenkov angle resolution, even though the effects are small.

For the proton and heavy particle tagging an equivalent procedure was followed. The corrections for the liquid radiator ranges were typically of order $\sim 5\%$. For the gas radiator ranges the corrections were typically of order $\sim 3\%$.

## 5.2 Global corrections

Global corrections refer to overall detector effects and general selection cuts. They are derived from Monte Carlo by comparing the distributions at the hadronic level *before* detector simulation (generator level) with the distributions *after* the detailed detector simulation. The correction factors $c^{(f,i)}$ can be obtained from

$$c^{(f,i)} = \frac{N_{gen}^{(f,i)}}{N_{sim}^{(f,i)}}, \tag{6}$$

where $i = \pi^\pm$, $\mathrm{K}^\pm$, $\mathrm{p\overline{p}}$ or $\mathrm{Hv}^\pm$ and $f$ represents the event flavour, i.e. the $q\overline{q}$ -, $b$ - or $uds$ -sample, and $N_{gen}^{(f,i)}$ stands for the distributions at the hadronic level before detector simulation while $N_{sim}^{(f,i)}$ stands for the distributions after the detailed simulation of the

DELPHI detector, including all steps of the analysis[5]. The factor $c^{(f,i)}$ basically corrects for effects caused by the event and track selection, track losses, secondary interactions, detector geometry and resolution effects. The suppression of particles coming from secondary interactions, by accepting only negative charged particles below 2.7 GeV/$c$, is also included in $c^{(f,i)}$.

The simulation of hadronic $Z^0$ decays before detector simulation is provided by a Monte Carlo program which is based on JETSET 7.3 [4,7]. To obtain the values for $N_{gen}^{(f,i)}$, 2.5 million $Z^0 \to q\overline{q}$ events were used. In the case of the $b$ - events for particle momenta above 10 GeV/$c$, an additional 2.5 million $Z^0 \to b\overline{b}$ events were produced. Finally, the corrected data distributions were obtained from

$$N_{cor}^{(f,i)} = c^{(f,i)} \cdot N_{data}^{(f,i)} \tag{7}$$

In the case of $i = \pi^{\pm}$, an additional correction factor which took care of the lepton contribution was obtained from the ratio $N_{gen}^{(f,\pi^{\pm})}/N_{gen}^{(f,\pi^{\pm}+e^{\pm}+\mu^{\pm})}$.

A correction to $N_{sim}^{(f,i)}$ is applied to account for the presence of so called 'ghost' particles. These are incorrectly reconstructed tracks which have no counterpart simulated track. They occur only above 20 GeV/c and increase with momentum. Additional corrections due to ghost particles were measured to be $\sim$0.3% at 20 GeV/$c$, slowly rising to $\sim$5% at 45 GeV/$c$.

## 5.3 Systematic uncertainties

Due to the high statistics, the systematic uncertainties usually dominate. The result of a detailed study of the uncertainties for the final $\pi^{\pm}, \mathrm{K}^{\pm}, \mathrm{p\overline{p}}, \mathrm{Hv}^{\pm}$ normalised production rates is shown in figure 6. For each event sample, the systematic uncertainty on each distribution has four different sources: the analysis method, the event selection, the particle identification, and the correction factors.

### 5.3.1 Uncertainties due to the analysis method

The systematic uncertainty due to the analysis method can be estimated by comparing the result for $\pi^{\pm}$ from the 3x3-method (eq.1) with the result for $\pi^{\pm}$ from the simplified 2x2-method (eq.2). Likewise the sum of the results on $\mathrm{K}^{\pm}$ and $\mathrm{p\overline{p}}$ can be compared with the resulting $\mathrm{Hv}^{\pm}$ distribution. For these, the effects due to the different application of the RICH information for particle identification are important for a part of the momentum window.

### 5.3.2 Uncertainties due to the event selection

To study the systematic uncertainties due to the flavour tagging and the purity matrix inversion method (eq.4), two additional $b$ - samples and $uds$ - samples of higher and lower purity were selected. The event probability cuts applied and the compositions of the resulting samples are listed in table 1, where the middle row represents the values used for the measurement. Thus the $b$ - purity was varied by $\sim \pm 5\%$ and the $uds$ - purity by $\sim \pm 1\%$ and the analysis was repeated for every event sample, using these new purities.

The uncertainty due to the general hadronic event selection is very small and is treated in section 5.3.4 below.

[5] At the generator level ($N_{gen}$) particles with lifetimes less than $10^{-9}$ $s$ are considered unstable. Particles with longer lifetimes are taken as stable particles. Thus $\Lambda^0$ and $\mathrm{K_S^0}$ decay, while $\mathrm{K_L^0}$ is considered stable. This is not the case for $N_{sim}$, where lifetimes are properly taken into account.

| $\mathcal{P}_E^+$ | $b$ - purity | $c$ - purity | $\mathcal{P}_E^+$ | $uds$ - purity | $c$ - purity |
|---|---|---|---|---|---|
| $< 0.005$ | 82.3% | 12.8% | $> 0.20$ | 82.5% | 14.0% |
| $< 0.010$ | 78.5% | 14.7% | $> 0.15$ | 81.7% | 14.5% |
| $< 0.020$ | 73.3% | 16.7% | $> 0.10$ | 80.3% | 15.3% |

Table 1: $b$ -, $c$ - and $uds$ - purities for various cuts on the event probability $\mathcal{P}_E^+$.

### 5.3.3 Uncertainties due to particle identification

The NEWTAG package provides different levels of tagging and of track quality selections. To study systematic effects due to the tagging, the very loose and standard tagging were also selected for each identification hypothesis ($\pi^\pm, \mathrm{K}^\pm, \mathrm{p\overline{p}}, \mathrm{Hv}^\pm$) in addition to the loose selection used for the central values.

Likewise for the track quality, the very loose and standard track quality selection were included to study systematic effects on the particle identification from the detector point of view. This was done for each of the three tag-samples and again for each hypothesis and each event sample. Requiring the Outer Detector (OD) information to be used in the track reconstruction leads to higher purities after particle identification, since it lies behind the RICH.

For each hypothesis ($\pi^\pm, \mathrm{K}^\pm, \mathrm{p\overline{p}}, \mathrm{Hv}^\pm$), the whole procedure used 18 (2x3x3) different sub-samples for $q\overline{q}$ - events (i.e. with or without the OD requirement; very loose, loose, and standard tag; and very loose, loose, and standard track quality selection). Consequently, for the three $b$ - and three $uds$ - event samples (sec. 5.3.2, table 1), the procedure used 54 (3x18) sub-samples.

The tight options were not applied, in order to avoid introducing fake systematic effects due to statistical fluctuations, especially for higher momenta.

The systematic uncertainty was computed for each mass hypothesis, on a bin-by-bin basis, as being half of the maximum deviation from the central value.

### 5.3.4 Uncertainties due to corrections

Local and global corrections contribute approximately equally to the systematic uncertainty. Since they operate mainly on the track quality and reconstruction efficiency, they also account for the uncertainty due to the general hadronic event selection.

The largest contribution to the local correction factors is due to the corrections on the efficiency matrix (eqs. 1 and 2). By increasing the corrections by 10%, an average relative contribution of the order of 15% for the $q\overline{q}$ - and $uds$ - sample and 20% for the $b$ - sample was estimated. Assuming an uncertainty of 5% on the track selection efficiency correction (derived from $\mathcal{E}_{\mathrm{sel}}^{\mathrm{data}}/\mathcal{E}_{\mathrm{sel}}^{\mathrm{m.c.}}$) gave a relative contribution to the total systematic uncertainty of $\sim 2\%$.

The global factors $c^{(f,i)}$ contain corrections for several effects. The average relative contribution to the total uncertainty was estimated to be 15% for the $q\overline{q}$ - sample and 20% for the $b$ - and $uds$ - sample. Some effects were much smaller than this. For example, assuming an uncertainty of 5% on the effect of secondary interactions indicated the relative contributions to be $\ll 1\%$. An extra uncertainty of 5% was introduced to account for the uncertainty in accepting only negative charged particles below 2.7 GeV/$c$.

Assuming a 10% uncertainty on the correction for ghost particles, the relative contribution was estimated to be $\ll 1\%$ at 20 GeV/$c$ slowly rising to $\sim 10\%$ at 45 GeV/$c$.

| source $i$ of systematic uncertainty | $Z^0 \to q\overline{q}$ $\frac{\epsilon_i^2}{\sum_{i=1}^4 \epsilon_i^2} \times 100\%$ | $Z^0 \to b\overline{b}$ $\frac{\epsilon_i^2}{\sum_{i=1}^4 \epsilon_i^2} \times 100\%$ | $Z^0 \to u\overline{u}, d\overline{d}, s\overline{s}$ $\frac{\epsilon_i^2}{\sum_{i=1}^4 \epsilon_i^2} \times 100\%$ |
|---|---|---|---|
| 1. analysis method | 4 % | 2 % | 3 % |
| 2. event selection | 2 % | 9 % | 5 % |
| 3. particle identification | 63 % | 49 % | 57 % |
| 4. correction factors | 31 % | 40 % | 35 % |

Table 2: The sources of systematic uncertainty squared and their average relative contribution to the total uncertainty for $Z^0 \to q\overline{q}$ , $Z^0 \to b\overline{b}$ and $Z^0 \to u\overline{u}, d\overline{d}, s\overline{s}$ .

### 5.3.5 The uncertainty distributions

Figure 6 shows the final result of the total uncertainty distributions ($\epsilon_{\rm tot}$) versus momentum for the $\pi^\pm, \mathrm{K}^\pm, \mathrm{p\overline{p}}, \mathrm{Hv}^\pm$ normalised production rates in $q\overline{q}$ - , $b$ - and $uds$ - events. Here, $\epsilon_{\rm tot}$ is split into a systematic part ($\epsilon_{\rm syst}$) and a statistical part ($\epsilon_{\rm stat}$) and it can be seen that the systematic uncertainties dominate in most cases.

The shapes of the distributions reflect the characteristics of the RICH particle identification. For example, the $\mathrm{K}^\pm$ distributions show successively three rising slopes. This is because the $\pi^\pm/\mathrm{K}^\pm$ and $\mathrm{K}^\pm/\mathrm{p\overline{p}}$ separations slowly decrease with increasing momentum. If the reconstructed Cherenkov angle were to be slightly *over*-estimated (or the angle resolution slightly under estimated), then a certain number of kaons would systematically be misidentified as pions (the opposite case will be discussed below). The first rising slope is determined by the $\pi^\pm/\mathrm{K}^\pm$ separation in the region where only liquid radiator information is used for identification ($0.7 < p < 2.7$ GeV/$c$). The second slope, for $2.7 < p < 8.5$ GeV/$c$, is determined by the $\mathrm{K}^\pm/\mathrm{p\overline{p}}$ separation in the liquid radiator. Here, the pion hypothesis has been ruled out by the gas veto-identification and the liquid radiator is needed only to separate $\mathrm{K}^\pm$ from $\mathrm{p\overline{p}}$. Had the $\pi^\pm$ hypothesis not been ruled out, $\mathrm{K}^\pm$ identification using liquid information would have been impossible (especially for $4 < p < 8.5$ GeV/$c$), and the second slope would have been steeper, rising to significantly higher values. The third slope ($\sim 10 < p < 45$ GeV/$c$) can be explained in the same way as the first one, but now for the gas radiator instead of the liquid radiator.

The opposite effect i.e. if the reconstructed Cherenkov angle were to be slightly *under*-estimated (or the angle resolution slightly over estimated), is suppressed because for a particle of momentum $p$, the separation with respect to a heavier mass hypothesis is always larger than the separation with respect to a lighter mass hypothesis. This explains the less steep first slope in the case of the $\pi^\pm$ distributions.

The first slope is missing for the $\mathrm{p\overline{p}}$ distributions because, at low momenta, the protons are either identified in liquid veto-mode (below the proton radiation threshold), or the $\mathrm{K}^\pm/\mathrm{p\overline{p}}$ separation is always larger than five standard deviations. Variations between the patterns can be understood by considering a change in the background for particle identification due to differences in the overall event topology (e.g. track density, particle multiplicity) for the three samples.

The systematic uncertainty is dominated by the RICH track quality and the RICH particle identification. Table 2 shows the average relative contribution to the systematic uncertainty squared from the four sources (sec. 5.3.1 - 5.3.4) for the normalised production rates in $Z^0 \to q\overline{q}$ , $Z^0 \to b\overline{b}$ and $Z^0 \to u\overline{u}, d\overline{d}, s\overline{s}$ .

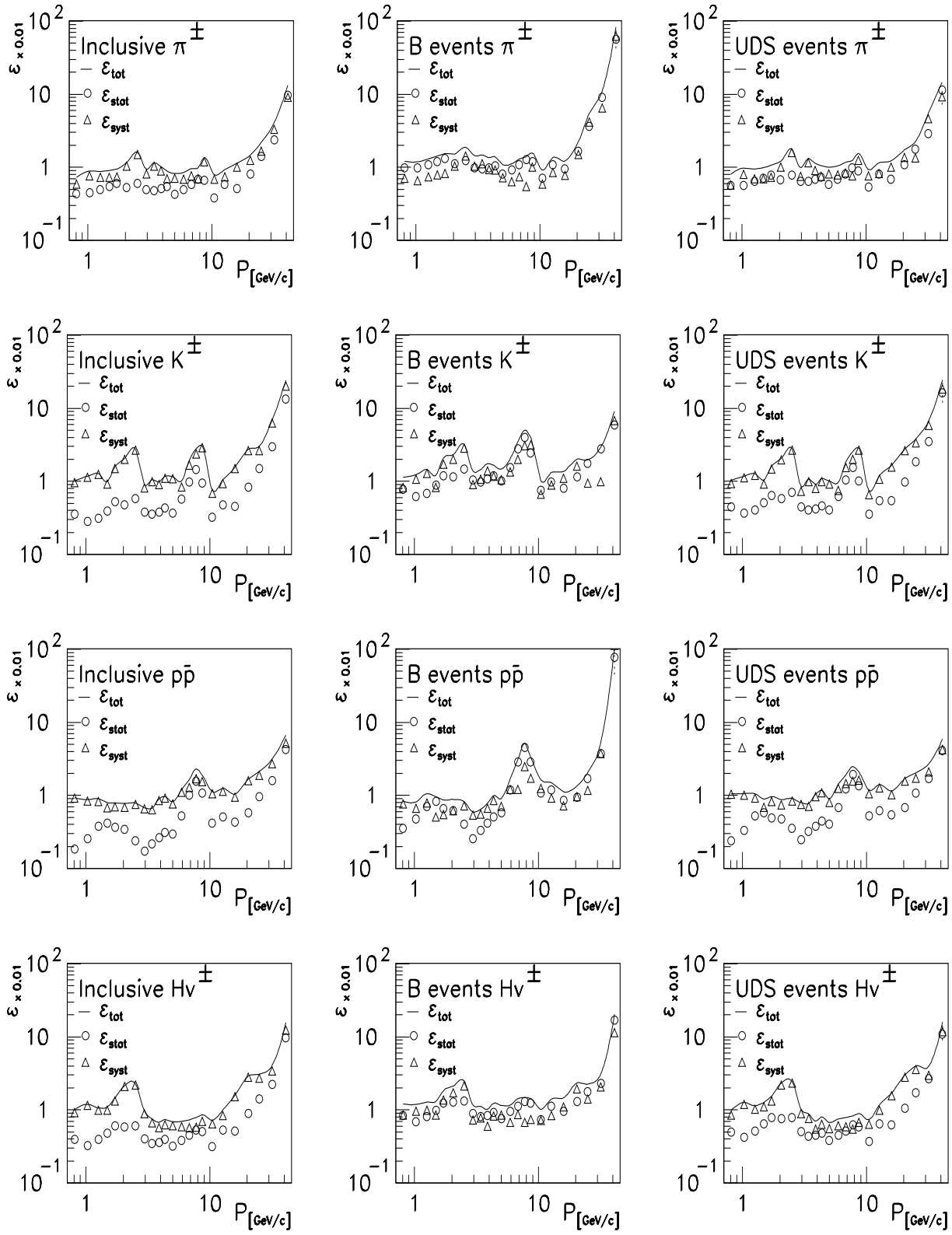


Figure 6: Statistical and systematic uncertainties versus momentum for the normalised $\pi^{\pm}$, $\mathrm{K}^{\pm}$, $\mathrm{p\overline{p}}$ rates for $\mathrm{Z}^0 \to q\overline{q}$ , $\mathrm{Z}^0 \to b\overline{b}$ and $\mathrm{Z}^0 \to u\overline{u}, d\overline{d}, s\overline{s}$ events.

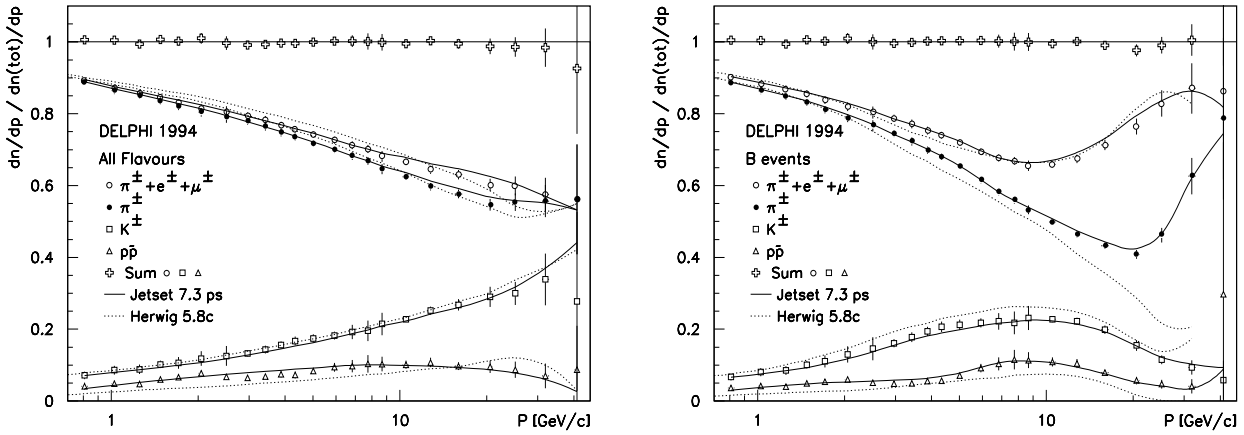


Figure 7: The normalised production rates of $\pi^{\pm}$, $K^{\pm}$ *and* $p\overline{p}$ in $Z^0 \to q\overline{q}$ , $Z^0 \to b\overline{b}$ and $Z^0 \to u\overline{u}, d\overline{d}, s\overline{s}$ . The open symbols are the measured distributions (acceptance corrected). The closed circles indicate $\pi^{\pm}$ after having accounted for $e^{\pm}$ and $\mu^{\pm}$. The distributions have been obtained without constraining the sum of the fractions to equal unity, allowing the consistency test indicated by the open crosses. Compared to *uds* - events, the production of high momentum $K^{\pm}$ ($p > 20$ GeV/$c$) is suppressed in $b$ - events, whereas $K^{\pm}$ production for $3 < p < 20$ GeV/$c$ is clearly higher in $b$ - events.

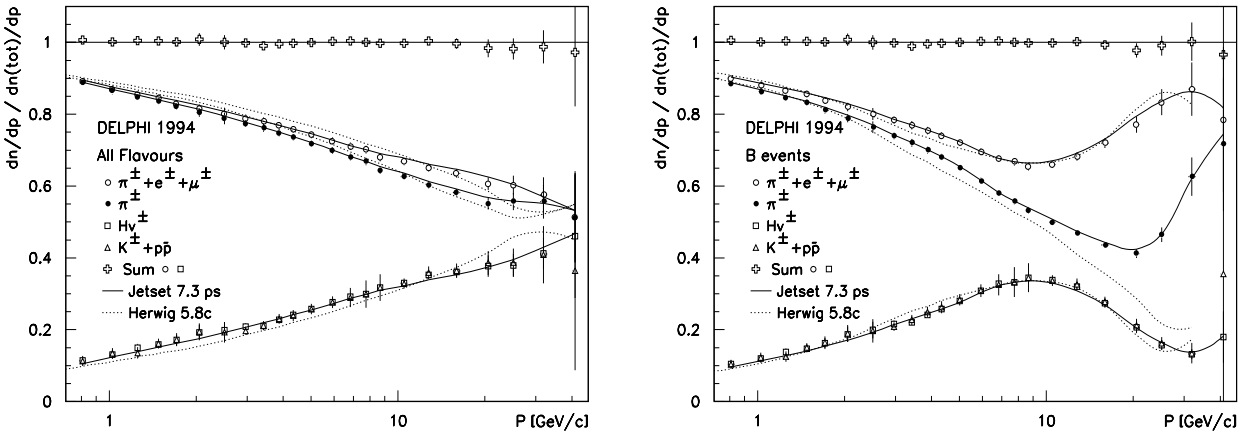


Figure 8: The normalised production rates of $\pi^{\pm}$ and heavy particles ($Hv^{\pm}$) in $Z^0 \to q\overline{q}$ , $Z^0 \to b\overline{b}$ and $Z^0 \to u\overline{u}, d\overline{d}, s\overline{s}$ . The distributions have been obtained without constraining the sum of the fractions to equal unity, allowing the consistency test indicated by open crosses. The open triangles indicate the summation of the results obtained for $K^{\pm}$ and $p\overline{p}$ from figure 7.

# 6 Normalised production rates

The normalised production rates $f_i$ are expressed as follows, where $\mathcal{E}^i_j$ represents the efficiency matrix elements from equation 1,

$$f_i = \sum_j \left( (\mathcal{E}^i_j)^{-1} \cdot \frac{N^{\text{Meas.}}_j}{N^{\text{Meas.}}_{\text{total}}} \right) \qquad ; \qquad i,j = \pi e \mu, \text{K}, \text{p}. \tag{8}$$

For a self-consistent efficiency matrix the condition $\sum_i f_i = 1$ must also hold and provides a useful cross-check of the analysis method and the particle identification. Figure 7 shows the normalised $\pi^{\pm}$, $\text{K}^{\pm}$, $\text{p}\overline{\text{p}}$ production rates derived by the 3x3-method from the $q\overline{q}$ - , $b$ - and $uds$ - samples. The open circles represent the pion distribution before correction for the lepton contribution, to enable the test $\sum_i f_i = 1$. The closed circles depict the pions after the lepton correction. In the case of the $uds$ - events the open and closed circles coincide, indicating a very low lepton production. Also included are the predictions from JETSET 7.3 and HERWIG 5.8C both tuned by DELPHI [7].

For all three event samples, JETSET gives a good description of the data. For $\pi^{\pm}$ and $\text{K}^{\pm}$ in $q\overline{q}$ - events and for $\text{K}^{\pm}$ in $uds$ - events, the HERWIG prediction is also good. However in all other cases HERWIG seems to fail, especially for protons.

Comparing the $b$ - sample with the $uds$ - sample, the distributions show approximately the same behaviour in the momentum region below $\sim 3$ GeV/$c$. However, clear differences occur for very high momenta ($p > 20$ GeV/$c$). In $b$ - events, high momentum $\text{K}^{\pm}$ production seems to be suppressed whereas high momentum $\pi^{\pm}$ production prevails. Conversely, the $\text{K}^{\pm}$ production in the intermediate momentum window ($3 < p < 20$ GeV/$c$) is clearly higher in $b$ - events than in $uds$ - events. For $p > 20$ GeV/$c$, the $\text{K}^{\pm}$ production rate is about a factor three higher in $uds$ - events, which may indicate that those kaons contain a primary $u(\overline{u})$-quark or $s(\overline{s})$-quark. This will be discussed again in section 9.

The $\pi^{\pm}$ and $\text{Hv}^{\pm}$ distributions acquired from the 2x2-method are shown in figure 8. To illustrate the consistency of the matrix inversion method, an overlay of the sum of $\text{K}^{\pm}$ and $\text{p}\overline{\text{p}}$ from the 3x3-method (triangles) is included. The values and their uncertainties corresponding to the different figures are listed in Appendix I (tables 10–21).

# 7 Differential cross-sections

From the normalised production rates, the differential cross-sections for $\pi^{\pm}$, $\text{K}^{\pm}$ and $\text{p}\overline{\text{p}}$ production can be obtained through multiplication with the measured total charged particle differential cross-section. Figure 9 shows the $\pi^{\pm}, \text{K}^{\pm}, \text{p}\overline{\text{p}}$ differential cross-sections versus momentum (bottom, left hand axes) and versus scaled momentum $X_p$ (top, right hand axes), for $\text{Z}^0 \to q\overline{q}$ , $\text{Z}^0 \to b\overline{b}$ and $\text{Z}^0 \to u\overline{u}, d\overline{d}, s\overline{s}$ as obtained from the 3x3-method. Since the LEP beam energy during the 1994 data taking was fixed at the peak of $\text{Z}^0$ resonance, the difference between the top and bottom axes is a constant factor $E_{beam}$.

The systematic uncertainties for the total charged particle distributions (Appendix II) were adopted from the inclusive DELPHI measurement performed on 1991, 1992 and 1993 data [7]. The inclusive total charged particle distributions are in good agreement with these previous DELPHI measurements. The open circles in figure 9 represent the pions *after* the lepton correction. The full lines are the predictions from JETSET 7.3 and the dotted lines represent HERWIG 5.8C. Although not shown in figure 9, it was verified that the sum of the identified-particle distributions agreed with the distribution for all charged particles.

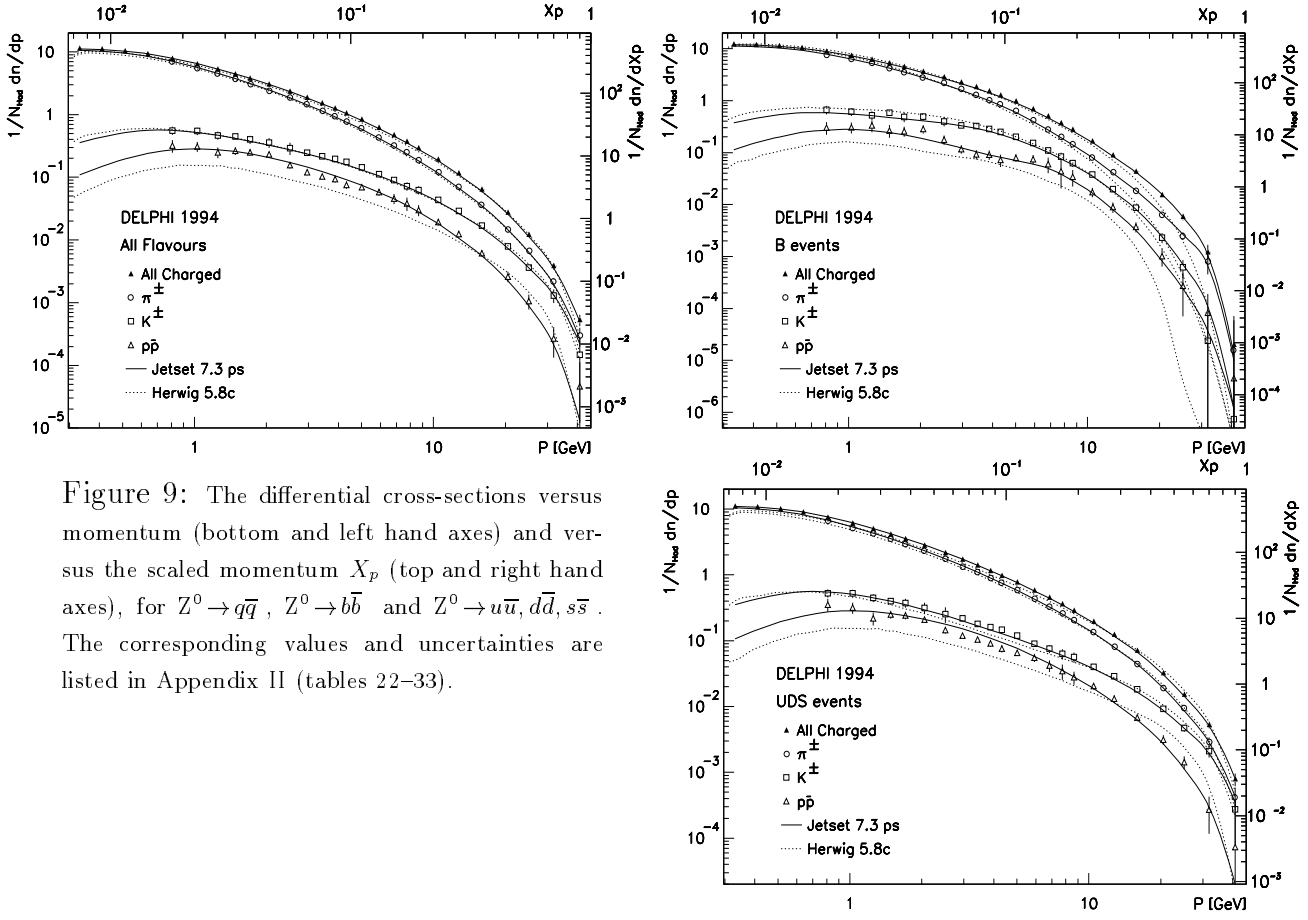


Figure 9: The differential cross-sections versus momentum (bottom and left hand axes) and versus the scaled momentum $X_p$ (top and right hand axes), for $Z^0 \to q\overline{q}$ , $Z^0 \to b\overline{b}$ and $Z^0 \to u\overline{u}, d\overline{d}, s\overline{s}$ . The corresponding values and uncertainties are listed in Appendix II (tables 22–33).

The differential cross-sections as a function of $\xi_p$ are illustrated separately for each distribution in figure 10, together with the predictions of JETSET and HERWIG. Here, the discrepancy between the data and HERWIG becomes very clear. For all three event samples, JETSET describes the measured spectra better than HERWIG, which fails to describe the proton spectra and generally over estimates the spectra for $b$ - events and under estimates them for $uds$ - events. The overall JETSET description is rather good. The only serious discrepancy is in the proton distributions. The proton distribution in $b$ - events shows two distinct local maxima. This will be discussed in section 9.

# 8 Testing the LPHD-MLLA

The advantage of the observable $\xi_p$ is the Gaussian-like shape of its distributions for particle differential cross-sections. Based on the Modified Leading Logarithm Approximation under the assumption of Local Parton Hadron Duality (LPHD-MLLA), an approximation to this Gaussian-like shape is given by a 5 parameter expression [9]:

$$\mathcal{G}(\delta, \sigma, s, \kappa, N) = \frac{N}{\sigma\sqrt{2\pi}} \cdot \exp\left(\frac{1}{8}\kappa - \frac{1}{2}s\delta - \frac{1}{4}(2+\kappa)\delta^2 + \frac{1}{6}s\delta^3 + \frac{1}{24}\kappa\delta^4\right) \qquad (9)$$

where $\delta = (\xi_p - \overline{\xi}_p)/\sigma$ and $\overline{\xi}_p$, $\sigma$, $s$, $\kappa$ are respectively the mean, the width, the skewness and the kurtosis of the distribution and $N$ is a normalisation factor. This so called 'distorted Gaussian' expression (for a normal Gaussian $k = s = 0$) can be tested by performing a fit to each of the measured $\xi_p$ distributions. Figure 11 gives an overview of the fits performed on the data. In most cases the fit procedure based on equation 9 gives a

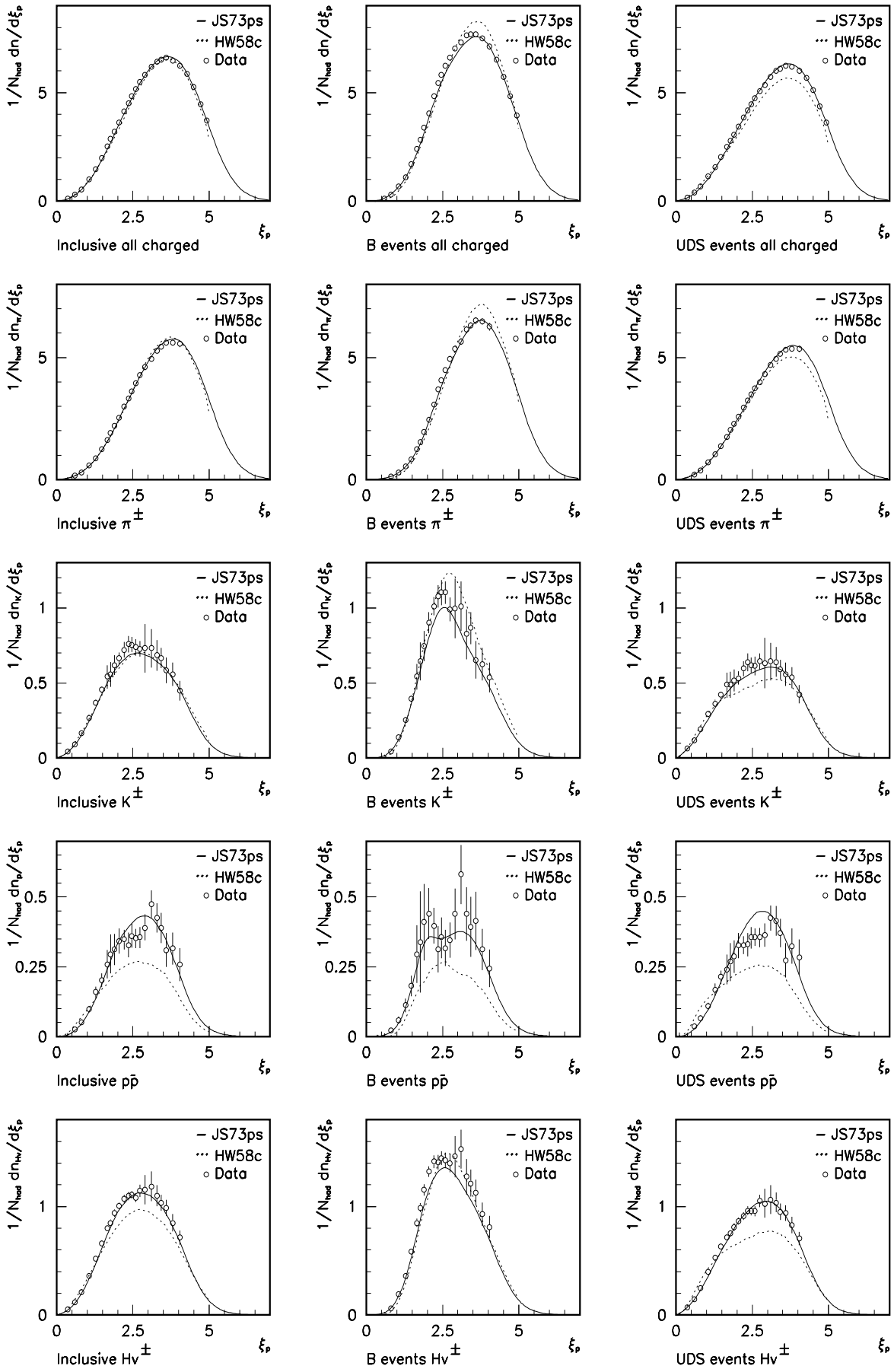


Figure 10: The DELPHI $\xi_p$ distributions compared with JETSET 7.3 and HERWIG 5.8c in $Z^0 \to q\overline{q}$, $Z^0 \to b\overline{b}$ and $Z^0 \to u\overline{u}, d\overline{d}, s\overline{s}$ events.

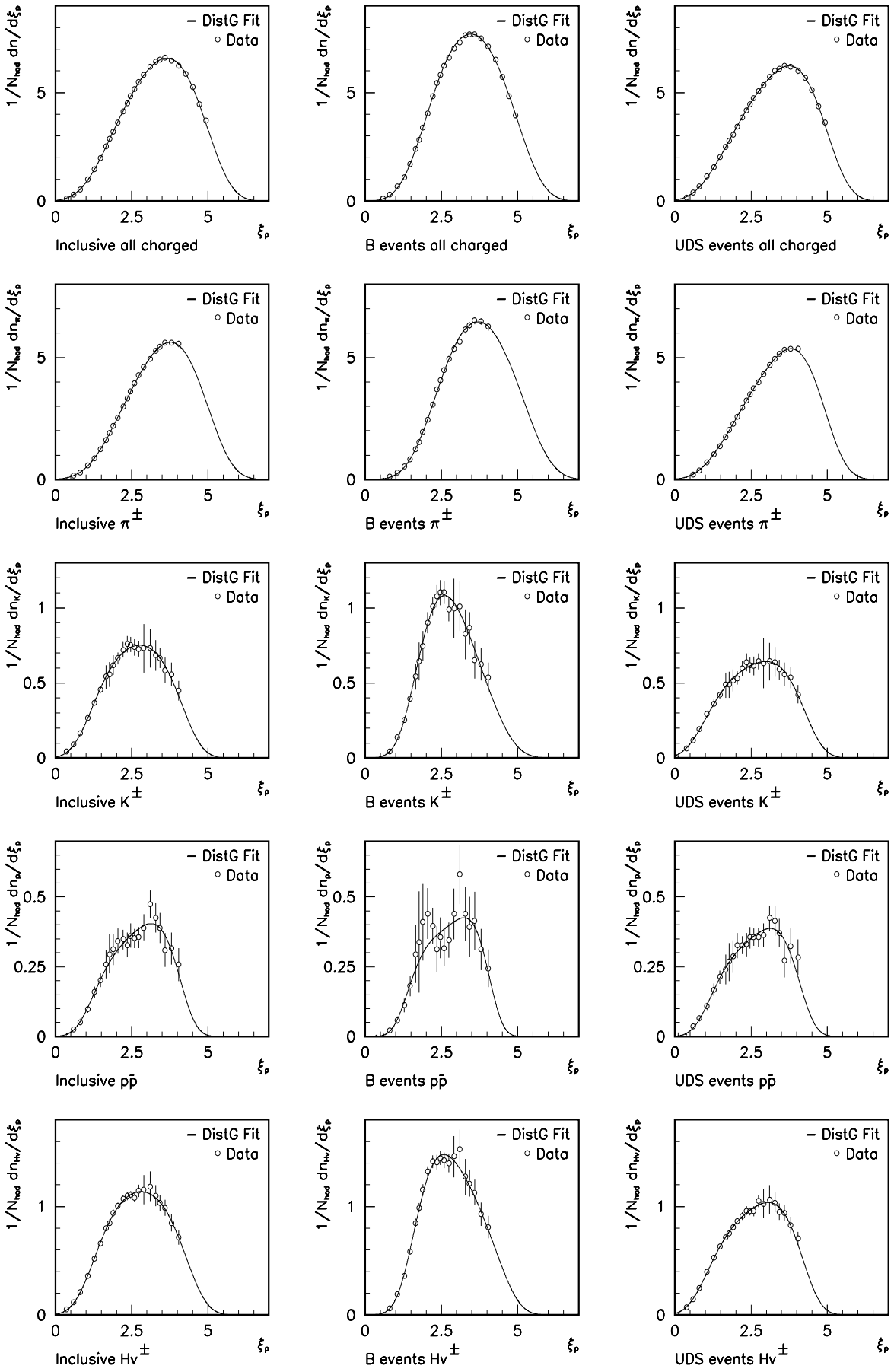


Figure 11: The fitted $\xi_p$ distributions for $\pi^{\pm}$, $\mathrm{K}^{\pm}$, $\mathrm{p\overline{p}}$ and $\mathrm{Hv}^{\pm}$ in $\mathrm{Z}^0 \to q\overline{q}$ , $\mathrm{Z}^0 \to b\overline{b}$ and $\mathrm{Z}^0 \to u\overline{u}, d\overline{d}, s\overline{s}$ events.

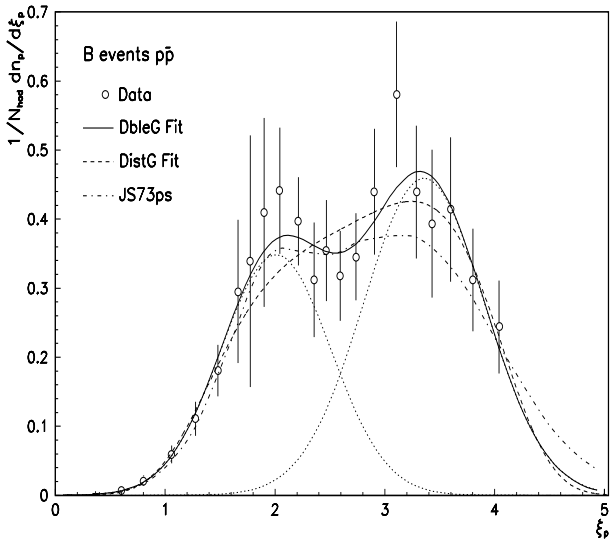


Figure 12: The distorted Gaussian (DistG) fit and a double Gaussian (DbleG) fit for protons in $b$ - events compared to the JETSET prediction (JS73PS).

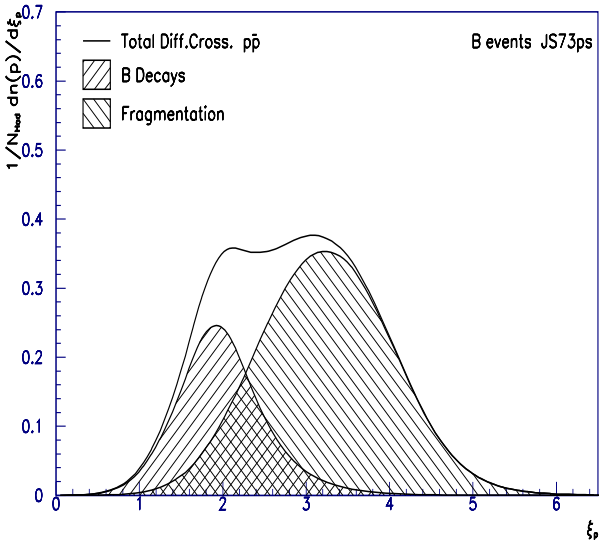


Figure 13: The JETSET prediction in $b$ - events for protons originating from fragmentation and from $b$ - decays.

good description of the measured spectra. Only for protons in $b$ - events the result is not satisfactory. This will be studied in more detail in the next section.

The extrapolation of the LPHD-MLLA prediction to the unmeasured high $\xi_p$ region, was tested using JETSET. Applying the fit procedure and using the same fit windows as for the data distributions, showed that the extrapolation of the fit was systematically below the JETSET prediction for the high $\xi_p$ region. The same was observed in comparing the JETSET prediction with the extrapolation of the fit to the data. For the proton spectrum in $b$ - events this is illustrated in figure 12: the 5 parameter distorted Gaussian fit result (dashed line) is below the JETSET prediction (dash-dot) for $\xi_p \gtrsim 4$.

# 9 Fragmentation and decays in flavour tagged events

As mentioned in section 7 above, the $\xi_p$ distribution for protons in $b$ - events shows two local maxima. JETSET predicts a similar shape, but less pronounced. Similar effects can be observed in the distributions of the (normalised) proton production rate in $b$ - events (fig. 9). The fit procedure based on the distorted Gaussian approximation in equation 9 clearly cannot account for the double-peaked structure (probably because the LPHD-MLLA considers only particles originating from fragmentation). Instead, a double Gaussian fit appears to be quite successful in describing the data. Figure 12 shows the result of a double Gaussian fit (full line) and the two constituent single Gaussians (dotted) together with the distorted Gaussian fit result (dashed) and the JETSET prediction (dash-dot).

The two-Gaussian composition may indicate two different origins of protons in $b$ - events. Protons with low $\xi_p$ values (i.e. high momenta) may come mostly from $b$ - decays while protons with high $\xi_p$ values come mostly from the fragmentation process. The two constituent single Gaussians (dotted lines) respectively cover 40.8% and 59.2% of the total fit result. This can be verified using JETSET by tracing back their production history. For comparison with figure 12, figure 13 shows the breakdown of the JETSET prediction for protons in $b$ - events into two parts: a) those protons originating from the decay of the particle which initially contained the primary quark and b) those protons originating – directly or indirectly[6] – from the string fragmentation process.

[6] the parent particle (or parents-parent etc.) may originate from the fragmentation e.g. $\Lambda^0 \to p\pi^-$ .

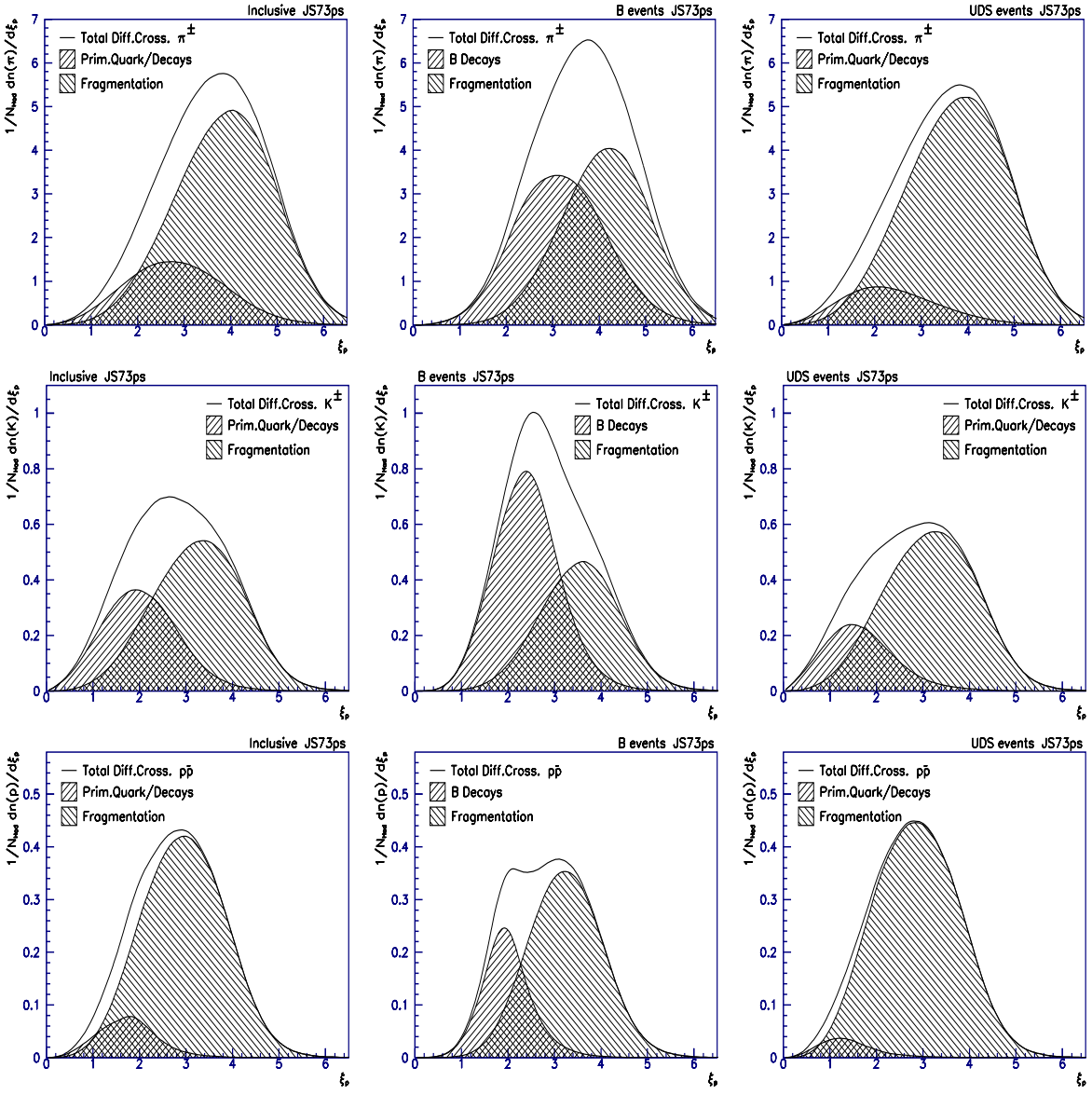


Figure 14: The JETSET 7.3 prediction for $Z^0 \to q\overline{q}$ , $Z^0 \to b\overline{b}$ and $Z^0 \to u\overline{u}, d\overline{d}, s\overline{s}$ of the differential cross-section versus $\xi_p$ for $\pi^{\pm}$, $K^{\pm}$, $p\overline{p}$ originating from fragmentation and from (decays of) particles containing the primary quark. The inclusive- and *uds* - distributions are obtained from 5 million generated $q\overline{q}$ - events. For the $b\overline{b}$ distributions, 10 million events have been generated. In the case of the inclusive- and the *uds* - distributions, Prim. Quark/Decays means particles produced directly from the primary quark as well as particles produced indirectly, i.e. produced from a decaying particle which contained the primary quark.

Both parts show also Gaussian-like shapes, similar to the constituent single Gaussian distributions resulting from the double Gaussian fit performed on the data. However, in the JETSET prediction, the two constituent Gaussians respectively cover 29.5% and 71.5% of the total distribution.

To illustrate why this effect may become visible only for proton production in $b$ - events, figure 14 shows the same breakdown of the JETSET $\xi_p$ distributions for the complete set of $\pi^{\pm}$, $K^{\pm}$ *and* $p\overline{p}$ spectra studied in this analysis.

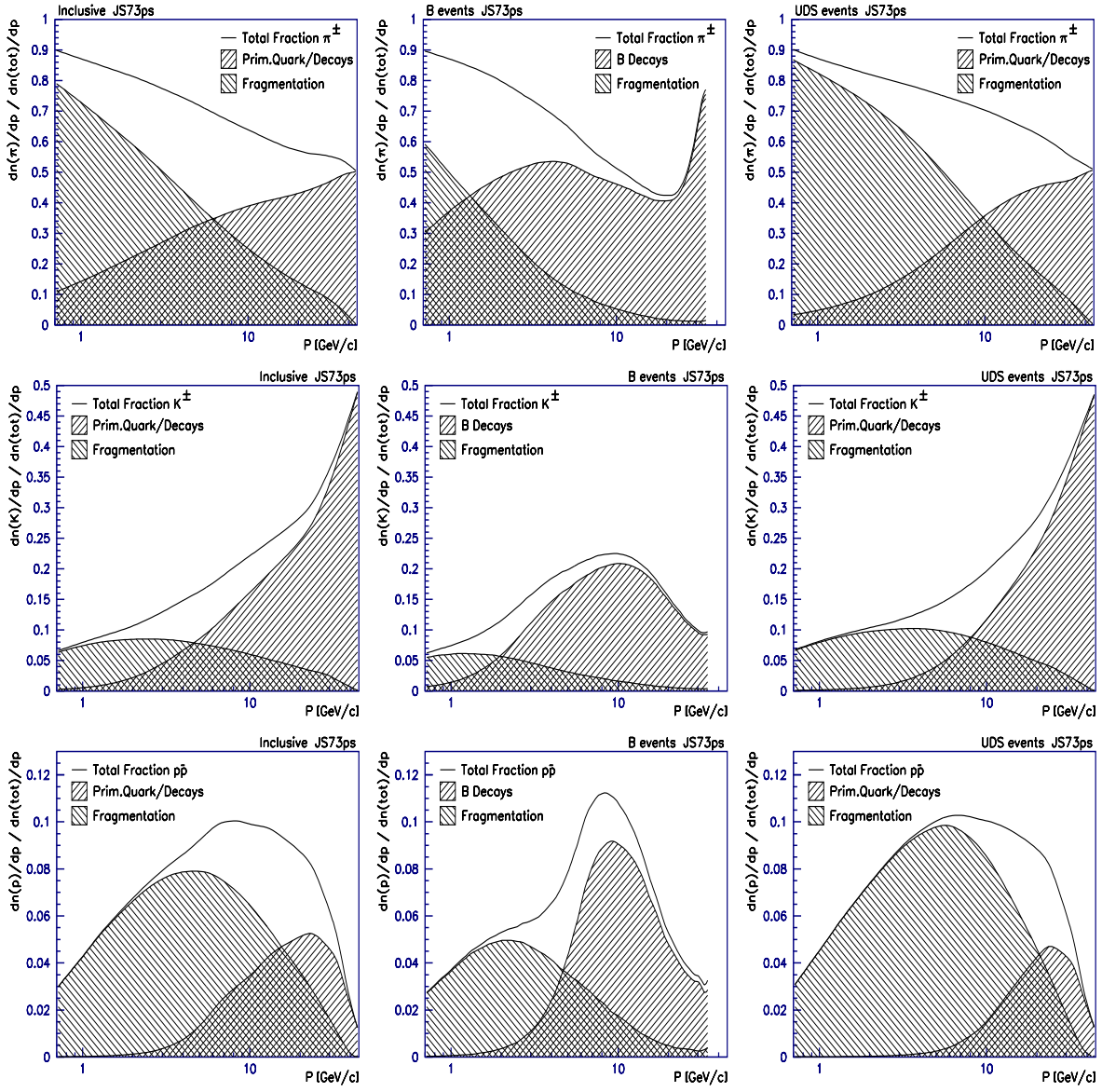


Figure 15: The JETSET 7.3 prediction for for $Z^0 \to q\overline{q}$ , $Z^0 \to b\overline{b}$ and $Z^0 \to u\overline{u}, d\overline{d}, s\overline{s}$ of the normalised production rates versus $p$ for $\pi^{\pm}, K^{\pm}, p\overline{p}$ originating from fragmentation and from (decays of) particles containing the primary quark.

In comparing the $\pi^{\pm}, K^{\pm}, p\overline{p}$ decay and fragmentation distributions for $b$ - and $uds$ - events, figure 14 also shows that decays and fragmentation contribute about equally to the total particle production in $b$ - events, whereas particle production in $uds$ - events is clearly dominated by string fragmentation.

Figure 15 shows the equivalent distributions for the normalised production rates versus momentum. As suggested in section 6 when comparing the $K^{\pm}$ distributions for the different event samples, a large fraction of the high momentum kaons ($p > 20$ GeV/$c$) in $uds$ - events originate from the primary quark.

| $Z^0 \to q\overline{q}$ | DELPHI | $\epsilon_{\rm stat}$ | $\epsilon_{\rm syst}$ | $\epsilon_{\rm extr}$ | $\epsilon_{\rm tot}$ | JS73 | HW58 |
|---|---|---|---|---|---|---|---|
| $< n_q >$ | 20.81 | $\pm 0.09$ | $\pm 0.19$ | $\pm 0.29$ | $\pm 0.35$ | 20.72 | 20.92 |
| $< \pi^{\pm} >$ | 17.26 | $\pm 0.10$ | $\pm 0.17$ | $\pm 0.86$ | $\pm 0.88$ | 17.23 | 17.66 |
| $< \mathrm{K}^{\pm} >^{*}$ | 2.21 | $\pm 0.05$ | $\pm 0.03$ | $\pm 0.04$ | $\pm 0.07$ | 2.09 | 2.11 |
| $< \mathrm{p\overline{p}} >^{*}$ | 1.08 | $\pm 0.04$ | $\pm 0.02$ | $\pm 0.02$ | $\pm 0.05$ | 1.09 | 0.78 |
| $< \mathrm{Hv}^{\pm} >^{**}$ | 3.30 | $\pm 0.05$ | $\pm 0.04$ | $\pm 0.05$ | $\pm 0.08$ | 3.18 | 3.03 |
| $Z^0 \to b\overline{b}$ | DELPHI | $\epsilon_{\rm stat}$ | $\epsilon_{\rm syst}$ | $\epsilon_{\rm extr}$ | $\epsilon_{\rm tot}$ | JS73 | HW58 |
| $< n_b >$ | 23.17 | $\pm 0.10$ | $\pm 0.21$ | $\pm 0.30$ | $\pm 0.38$ | 22.52 | 22.9 |
| $< \pi^{\pm} >^{**}$ | 18.56 | $\pm 0.12$ | $\pm 0.20$ | $\pm 0.92$ | $\pm 0.94$ | 18.28 | 18.6 |
| $< \mathrm{K}^{\pm} >^{*}$ | 2.59 | $\pm 0.08$ | $\pm 0.04$ | $\pm 0.04$ | $\pm 0.10$ | 2.35 | 2.85 |
| $< \mathrm{p\overline{p}} >^{*}$ | 1.07 | $\pm 0.06$ | $\pm 0.03$ | $\pm 0.02$ | $\pm 0.07$ | 1.01 | 0.61 |
| $< \mathrm{Hv}^{\pm} >^{**}$ | 3.69 | $\pm 0.07$ | $\pm 0.04$ | $\pm 0.05$ | $\pm 0.09$ | 3.36 | 3.46 |
| $Z^0 \to u\overline{u}, d\overline{d}, s\overline{s}$ | DELPHI | $\epsilon_{\rm stat}$ | $\epsilon_{\rm syst}$ | $\epsilon_{\rm extr}$ | $\epsilon_{\rm tot}$ | JS73 | HW58 |
| $< n_{uds} >$ | 19.94 | $\pm 0.09$ | $\pm 0.18$ | $\pm 0.28$ | $\pm 0.34$ | 19.97 | 18.6 |
| $< \pi^{\pm} >^{**}$ | 16.84 | $\pm 0.10$ | $\pm 0.19$ | $\pm 0.85$ | $\pm 0.87$ | 16.91 | 16.1 |
| $< \mathrm{K}^{\pm} >^{**}$ | 2.02 | $\pm 0.05$ | $\pm 0.03$ | $\pm 0.04$ | $\pm 0.07$ | 1.92 | 1.80 |
| $< \mathrm{p\overline{p}} >^{**}$ | 1.07 | $\pm 0.04$ | $\pm 0.02$ | $\pm 0.02$ | $\pm 0.05$ | 1.13 | 0.70 |
| $< \mathrm{Hv}^{\pm} >^{**}$ | 3.09 | $\pm 0.05$ | $\pm 0.04$ | $\pm 0.05$ | $\pm 0.08$ | 3.04 | 2.50 |

Table 3: The measured $\pi^{\pm}$, $\mathrm{K}^{\pm}$ *and* $\mathrm{p\overline{p}}$ average multiplicities in $Z^0 \to q\overline{q}$ , $Z^0 \to b\overline{b}$ , $Z^0 \to u\overline{u}, d\overline{d}, s\overline{s}$ compared to the JETSET and HERWIG prediction. Results with an improved accuracy compared to previous measurements are indicated by a '$*$'. New results are indicated by '$**$'.

# 10 Particle multiplicities

The particle multiplicities i.e. total particle production rates, can be obtained by integrating the differential cross-section distribution of any observable e.g. $p$, $X_p$ or $\xi_p$. The DELPHI particle multiplicities are determined through integration over the $\xi_p$ range of the above presented distorted Gaussian fit-results. The JETSET prediction was used to extrapolate into the regions not covered by the data. The final $\pi^{\pm}, \mathrm{K}^{\pm}, \mathrm{p\overline{p}}$ multiplicities are listed in table 3, including the values obtained for JETSET and HERWIG. Only for protons in $b$ - events the double Gaussian fit result from figure 12, which obviously yields a better description of the spectrum, was integrated. Within the uncertainties, the proton multiplicity using the distorted Gaussian fit ($1.08 \pm 0.05 \pm 0.04 \pm 0.02$) nevertheless agrees with the result obtained from the double Gaussian fit ($1.07 \pm 0.06 \pm 0.03 \pm 0.02$).

The total uncertainty ($\epsilon_{\rm tot}$) is the quadratic sum of the statistical ($\epsilon_{\rm stat}$), systematic ($\epsilon_{\rm syst}$) and extrapolation ($\epsilon_{\rm extr}$) uncertainties. The statistical uncertainty was estimated by repeating the fit procedure five times, each time reducing equation 9 to a four parameter expression by freezing one of the five parameters and adding one standard deviation (derived from the five parameter fit) to the frozen parameter. The systematic uncertainty is mainly determined by the track reconstruction efficiency, the RICH particle identification and the correction factors, as discussed in detail in section 5.3. The extrapolation uncertainty was obtained from the JETSET and HERWIG generators assuming an uncertainty of $\pm 15\%$ on the additions due to extrapolation, 15% being the difference between the JETSET and HERWIG predictions, averaged over all unmeasured areas of the distributions in figure 11.

| DELPHI | 5 parameter fit | | | | | 3 parameter fit | | | $\Delta\chi^2$/ndf |
|---|---|---|---|---|---|---|---|---|---|
| $Z^0 \to q\overline{q}$ | $\xi_p^*$ | $\epsilon_{\rm stat}$ | $\epsilon_{\rm syst}$ | JS73 | HW58 | $\xi_p^*$ | $\epsilon_{\rm stat}$ | $\epsilon_{\rm syst}$ | (3 p.-5 p.) |
| All charged | 3.66 | $\pm$ 0.01 | $\pm$ 0.02 | 3.64 | 3.66 | 3.61 | $\pm$ 0.01 | $\pm$ 0.02 | 3.7 |
| $\pi^\pm$ | 3.79 | $\pm$ 0.01 | $\pm$ 0.04 | 3.81 | 3.77 | 3.70 | $\pm$ 0.01 | $\pm$ 0.03 | 5.1 |
| $K^\pm$ | 2.69 | $\pm$ 0.03 | $\pm$ 0.05 | 2.72 | 2.80 | 2.69 | $\pm$ 0.01 | $\pm$ 0.03 | 0.1 |
| $p\overline{p}$ | 3.15 | $\pm$ 0.06 | $\pm$ 0.07 | 2.82 | 2.75 | 2.87 | $\pm$ 0.04 | $\pm$ 0.04 | 0.9 |
| $Hv^\pm$ | 2.78 | $\pm$ 0.03 | $\pm$ 0.04 | 2.76 | 2.77 | 2.75 | $\pm$ 0.01 | $\pm$ 0.02 | 2.0 |
| $Z^0 \to b\overline{b}$ | $\xi_p^*$ | $\epsilon_{\rm stat}$ | $\epsilon_{\rm syst}$ | JS73 | HW58 | $\xi_p^*$ | $\epsilon_{\rm stat}$ | $\epsilon_{\rm syst}$ | (3 p.-5 p.) |
| All charged | 3.45 | $\pm$ 0.02 | $\pm$ 0.03 | 3.54 | 3.63 | 3.49 | $\pm$ 0.01 | $\pm$ 0.01 | 2.5 |
| $\pi^\pm$ | 3.65 | $\pm$ 0.02 | $\pm$ 0.04 | 3.72 | 3.79 | 3.67 | $\pm$ 0.01 | $\pm$ 0.03 | 0.9 |
| $K^\pm$ | 2.58 | $\pm$ 0.04 | $\pm$ 0.03 | 2.59 | 2.69 | 2.56 | $\pm$ 0.02 | $\pm$ 0.02 | 0.4 |
| $p\overline{p}$ | 3.25 | $\pm$ 0.07 | $\pm$ 0.12 | 3.06 | 2.48 | 3.36 | $\pm$ 0.04 | $\pm$ 0.03 | see text |
| $Hv^\pm$ | 2.55 | $\pm$ 0.02 | $\pm$ 0.03 | 2.62 | 2.66 | 2.60 | $\pm$ 0.02 | $\pm$ 0.02 | 0.4 |
| $Z^0 \to u\overline{u}, d\overline{d}, s\overline{s}$ | $\xi_p^*$ | $\epsilon_{\rm stat}$ | $\epsilon_{\rm syst}$ | JS73 | HW58 | $\xi_p^*$ | $\epsilon_{\rm stat}$ | $\epsilon_{\rm syst}$ | (3 p.-5 p.) |
| All charged | 3.76 | $\pm$ 0.01 | $\pm$ 0.02 | 3.71 | 3.71 | 3.70 | $\pm$ 0.01 | $\pm$ 0.01 | 0.1 |
| $\pi^\pm$ | 3.85 | $\pm$ 0.01 | $\pm$ 0.04 | 3.81 | 3.81 | 3.79 | $\pm$ 0.01 | $\pm$ 0.03 | 1.4 |
| $K^\pm$ | 2.99 | $\pm$ 0.05 | $\pm$ 0.08 | 3.01 | 3.22 | 2.93 | $\pm$ 0.02 | $\pm$ 0.04 | 0.1 |
| $p\overline{p}$ | 3.16 | $\pm$ 0.06 | $\pm$ 0.07 | 2.81 | 2.77 | 2.87 | $\pm$ 0.04 | $\pm$ 0.05 | 1.9 |
| $Hv^\pm$ | 3.06 | $\pm$ 0.03 | $\pm$ 0.03 | 2.89 | 3.01 | 2.88 | $\pm$ 0.01 | $\pm$ 0.02 | 4.9 |

Table 4: The resulting $\xi_p^*$ values obtained from a five parameter fit and a reduced three parameter fit (see text) for the different particle distributions, compared to the JETSET and HERWIG prediction including the difference between the $\chi^2$/ndf of the two fits. For completeness the values for heavy particles are included.

Results with an improved accuracy compared to previous measurements are indicated by a '$*$' in the left hand column of the table and will be discussed in section 12. New results are indicated by a '$**$'.

The results in table 3 are consistent within their uncertainties. For example, in $Z^0 \to q\overline{q}$ , comparing the $<n_q>$ with the the sum of $<\pi^\pm + K^\pm + p\overline{p}>$ leaves $0.26 \pm 0.33$ (excluding $\epsilon_{\rm extr}$ ) for light leptons i.e. $<e^\pm + \mu^\pm>$. For $uds$ - events, the difference between $<n_{uds}>$ and $<\pi^\pm + K^\pm + p\overline{p}>$ is 0.01. This means that most leptons in hadronic $Z^0$ decays are produced in heavy flavour events through the semi-leptonic decay of heavy flavour hadrons. For $b$ - events, $<n_b> = 23.17 \pm 0.38$ and $<\pi^\pm + K^\pm + p\overline{p}> = 22.22 \pm 0.26$ (excluding $\epsilon_{\rm extr}$ ), leaving $0.95 \pm 0.35$ for $<e^\pm + \mu^\pm>$. The same exercise holds also for both JETSET and HERWIG. Similarly, the comparisons between the sum of $<K^\pm + p\overline{p}>$ and the results obtained for the heavy particle distributions $<Hv^\pm>$ are in good agreement.

# 11 Determination of $\xi_p^*$ values

The maximum $\xi_p^*$ of the $\xi_p$ distributions is considered an important observable with which one can test QCD predictions (for a detailed review see ref. [10]). To obtain $\xi_p^*$ values from the $\xi_p$ distributions, $\overline{\xi}_p$ was parametrised as a function of $\xi_p^*$ in equation 9 and the fits were repeated. The results are listed in table 4 together with the predictions from JETSET and HERWIG.

| DELPHI | $\triangle\xi_p^*(uds\text{ - }b)$ | JS73 | HW58 |
|---|---|---|---|
| All charged | $0.31 \pm 0.05$ | 0.17 | 0.08 |
| $\pi^{\pm}$ | $0.20 \pm 0.06$ | 0.09 | 0.02 |
| $K^{\pm}$ | $0.41 \pm 0.11$ | 0.42 | 0.53 |
| $p\overline{p}$ | $-0.20 \pm 0.10$ | $-0.25$ | 0.29 |
| $Hv^{\pm}$ | $0.51 \pm 0.06$ | 0.27 | 0.35 |

Table 5: The difference in $\xi_p^*$ values in $uds$ - and $b$ - events compared to JETSET (JS73) and HERWIG (HW58).

Also included are the results of a second fit, in which the $k$ and $s$ parameters have been set equal to their values obtained from the five parameter fit applied to the full spectrum of the equivalent JETSET distributions. Thus the five parameter fit is reduced to a three parameter (distorted Gaussian) fit. These 'reduced three parameter' fit results have been included to enable comparisons with future measurements of $\xi_p^*$ obtained from low statistics LEP-II data samples at various energies $\sqrt{s} > M_Z$, for which the reduced three parameter fit is most likely to be applied. The right hand column in table 4 gives the difference $\Delta\chi^2/\text{ndf}$ between the two fit procedures.

The reduced three parameter fit did not work for the proton distribution in $b$ - events. Here, the values given in table 4 are those obtained for the second constituent Gaussian of the double Gaussian fit in figure 12 (for the first constituent Gaussian the maximum was at $2.01 \pm 0.05 \pm 0.02$).

The statistical uncertainty was derived directly from the fit procedure. The systematic uncertainty was estimated by refitting over the same $\xi_p$ range, after having moved the individual data points by their systematic uncertainty, assuming the systematics to be linearly correlated from bin to bin, being zero at the maximum bin, and anti correlated on either side of the peak. The distribution around the peak in $\xi_p$, is often very flat or distorted so that the actual value of $\xi_p^*$ depends critically on the shape used to express LPHD-MLLA (eq. 9). This is particularly true when there is very little data to the right of the peak as in the pion distributions. The possibility that eq. 9 may not be correct is not taken into account in the systematic uncertainty.

The five parameter fit results for $\xi_p^*$ agree well with the JETSET results. The difference with HERWIG is generally a little larger but also agrees within the uncertainties. The $\xi_p^*$ dependence on the primary quark flavour, can be quantified by taking the difference between the $\xi_p^*$ values for $uds$ - events and $b$ - events. Table 5 shows $\triangle\xi_p^*(uds\text{ - }b)$ and the comparison with the results obtained from JETSET and HERWIG. For $p\overline{p}$ in $b$ - events, the $\xi_p^*$ values of the second peak from the double Gaussian fit is taken both in data and in JETSET. The difference $\triangle\xi_p^*(uds\text{ - }b)$ being positive for mesons and negative for baryons is confirmed only by JETSET.

# 12 Comparison with other experimental results

For the three event samples, figure 16 illustrates the good agreement of the total charged particle distributions versus $\xi_p$ obtained from this analysis in comparison with results obtained by the ALEPH Collaboration. The ALEPH distributions versus $\xi_p$ are obtained from $X_p$ distributions published in reference [11].

Previously published measurements of particle multiplicities, are listed in table 6. The multiplicities from this analysis are in good agreement with these results. The column $\triangle\epsilon$ gives the difference in standard deviations between the measurements.

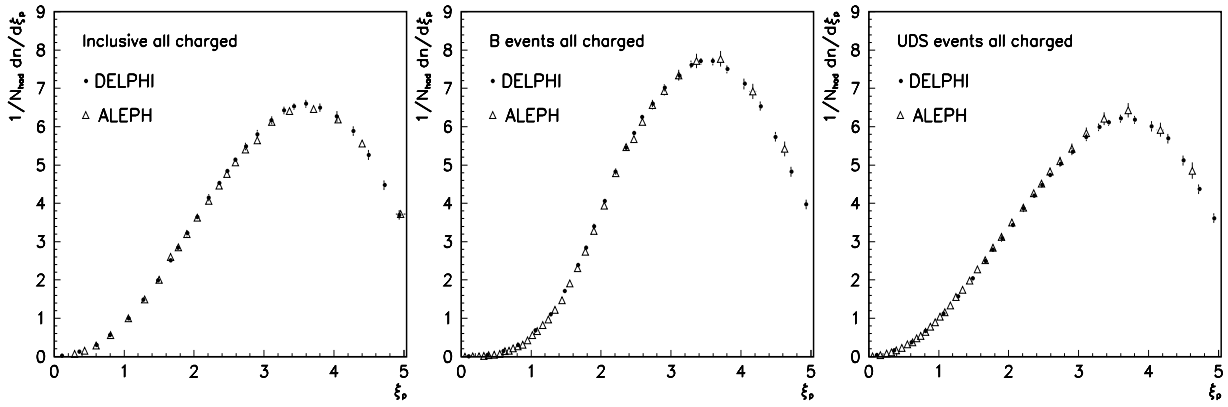


Figure 16: The charged particle distributions of DELPHI compared with the ALEPH results for $Z^0 \to q\overline{q}$ (left), $Z^0 \to b\overline{b}$ (middle) and $Z^0 \to u\overline{u}, d\overline{d}, s\overline{s}$ (right). The ALEPH distributions versus $\xi_p$ are obtained from the $X_p$ distributions published in [11].

| $Z^0 \to q\overline{q}$ | DELPHI | $\epsilon_{\rm tot}$ | OTHERS | $\epsilon_{\rm tot}$ | | $\triangle\epsilon$ |
|---|---|---|---|---|---|---|
| $< n_q >$ | 20.81 | $\pm$0.35 | 20.92 | $\pm$0.24 | LEP Av. [7] | 0.26 |
| $< \pi^{\pm} >$ | 17.26 | $\pm$0.88 | 17.1 | $\pm$0.4 | PDG'96 [12] | 0.17 |
| | | | 17.052 | $\pm$0.429 | OPAL [13] | 0.21 |
| $< \mathrm{K}^{\pm} >$ | 2.21 | $\pm$0.07 | 2.39 | $\pm$0.12 | PDG'96 [12] | 1.30 |
| | | | 2.421 | $\pm$0.133 | OPAL [13] | 1.40 |
| | | | 2.26 | $\pm$0.18 | DELPHI [14] | 0.26 |
| $< \mathrm{p\overline{p}} >$ | 1.08 | $\pm$0.05 | 0.964 | $\pm$0.102 | PDG'96 [12] | 1.02 |
| | | | 0.916 | $\pm$0.111 | OPAL [13] | 1.35 |
| | | | 1.07 | $\pm$0.14 | DELPHI [14] | 0.07 |
| $Z^0 \to b\overline{b}$ | DELPHI | $\epsilon_{\rm tot}$ | OTHERS | $\epsilon_{\rm tot}$ | | $\triangle\epsilon$ |
| $< n_b >$ | 23.17 | $\pm$0.38 | 23.47 | $\pm$0.37 | DELPHI [15] | 0.57 |
| | | | 23.62 | $\pm$0.48 | OPAL [16] | 0.74 |
| | | | 23.14 | $\pm$0.39 | SLD [17] | 0.06 |
| $< \mathrm{K}^{\pm} >$ | 2.59 | $\pm$0.10 | 2.74 | $\pm$0.50 | DELPHI [18] | 0.29 |
| $< \mathrm{p\overline{p}} >$ | 1.07 | $\pm$0.07 | 1.13 | $\pm$0.26 | DELPHI [18] | 0.22 |
| $Z^0 \to u\overline{u}, d\overline{d}, s\overline{s}$ | DELPHI | $\epsilon_{\rm tot}$ | OTHERS | $\epsilon_{\rm tot}$ | | $\triangle\epsilon$ |
| $< n_{uds} >$ | 19.94 | $\pm$0.34 | 20.35 | $\pm$0.19 | DELPHI [15] | 1.05 |
| | | | 20.21 | $\pm$0.24 | SLD [17] | 0.65 |

Table 6: The production rates from this analysis compared to published results from other sources. The measurements of $\pi^{\pm}$, $\mathrm{K}^{\pm}$ *and* $\mathrm{p\overline{p}}$ multiplicities in $b$ - and *uds* - events at LEP have so far been published only by DELPHI. The column $\triangle\epsilon$ gives the difference in standard deviations between the measurements.

| | DELPHI | | OTHERS | | | |
|---|---|---|---|---|---|---|
| $Z^0 \to q\overline{q}$ | $\xi_p^*$ | $\epsilon_{\rm tot}$ | $\xi_p^*$ | $\epsilon_{\rm tot}$ | | $\triangle\epsilon$ |
| All charged | 3.66 | $\pm$ 0.02 | 3.67 | $\pm$0.01 | ALEPH [11] | 0.44 |
| | | | 3.603 | $\pm$0.013 | OPAL [21] | 2.39 |
| | | | 3.71 | $\pm$0.05 | L3 [22] | 0.93 |
| $\pi^\pm$ | 3.79 | $\pm$ 0.04 | 3.78 | $\pm$0.02 | ALEPH [11] | 0.22 |
| $K^\pm$ | 2.69 | $\pm$ 0.06 | 2.70 | $\pm$0.09 | ALEPH [11] | 0.09 |
| | | | 2.63 | $\pm$0.07 | DELPHI [14] | 0.65 |
| $p\overline{p}$ | 3.15 | $\pm$ 0.09 | 2.85 | $\pm$0.15 | ALEPH [11] | 1.71 |
| | | | 2.96 | $\pm$0.16 | DELPHI [14] | 1.03 |

Table 7: The $\xi_p^*$ values from the 5 parameter fit result of this analysis compared to published results from other sources. The column $\triangle\epsilon$ gives the difference in standard deviations between the measurements.

The improvements in accuracy for $<K^\pm>$ and $<p\overline{p}>$ in $Z^0 \to q\overline{q}$ may be understood from figure 17. The left hand column compares the DELPHI-RICH $\pi^\pm, K^\pm, p\overline{p}$ distributions from this analysis with the measurements obtained by the ALEPH [11] and OPAL [13] $dE/dx$ identifications.

DELPHI data are seen to cover more of the $\xi_p$ space, ruling out uncertainties due to interpolations in areas where the integrated cross-section is high. The right hand column of the figure shows the comparison between the DELPHI-RICH and SLD-CRID [19]. The latter can not (yet) cover the identification window by applying veto-identification. Veto-identification was also not applied in a previously published DELPHI analysis for $<K^\pm>$ and $<p\overline{p}>$ in $Z^0 \to q\overline{q}$ (on 1992 data [14]). In addition, that data sample was about a factor of eight smaller than in this analysis. The previous DELPHI measurement of $<K^\pm>$ and $<p\overline{p}>$ in $b$ - events was performed using 1992 and 1993 data [18]. This analysis provides an improvement in accuracy for $K^\pm$ ($p\overline{p}$) by a factor $\sim 5$ ($\sim 4$). It should be noted that the apparent discrepancy of the OPAL proton data at low $\xi_p$ is absent in a more recent OPAL analysis based on increased statistics and an improved modelling of the $dE/dx$ distributions [20].

Previously published measurements of $\xi_p^*$ are listed in table 7. The column $\triangle\epsilon$ gives the difference in standard deviations between the measurements. In general, there is a good agreement between the different results.

# 13 Conclusions

The production of $\pi^\pm$, $K^\pm$ *and* $p\overline{p}$ in $Z^0 \to q\overline{q}$ , $Z^0 \to b\overline{b}$ and $Z^0 \to u\overline{u}, d\overline{d}, s\overline{s}$ has been studied using 1 400 000 $Z^0$ decays collected by DELPHI in 1994. The results have been compared with the predictions from the JETSET string fragmentation model and the HERWIG cluster fragmentation model. In general, JETSET describes the measured spectra better while HERWIG fails for the proton spectra. Both JETSET and HERWIG describe the inclusive $\pi^\pm$ and $K^\pm$ differential cross sections as a function of $\xi_p$ well. However, HERWIG over estimates $\pi^\pm$ and $K^\pm$ production for $Z^0 \to b\overline{b}$ and under estimates $\pi^\pm$ and $K^\pm$ production for $Z^0 \to u\overline{u}, d\overline{d}, s\overline{s}$ .

The prediction of the shape of the $\xi_p$ distributions, based on the Modified Leading Logarithm Approximation while assuming Local Hadron Parton Duality (LPHD-MLLA),

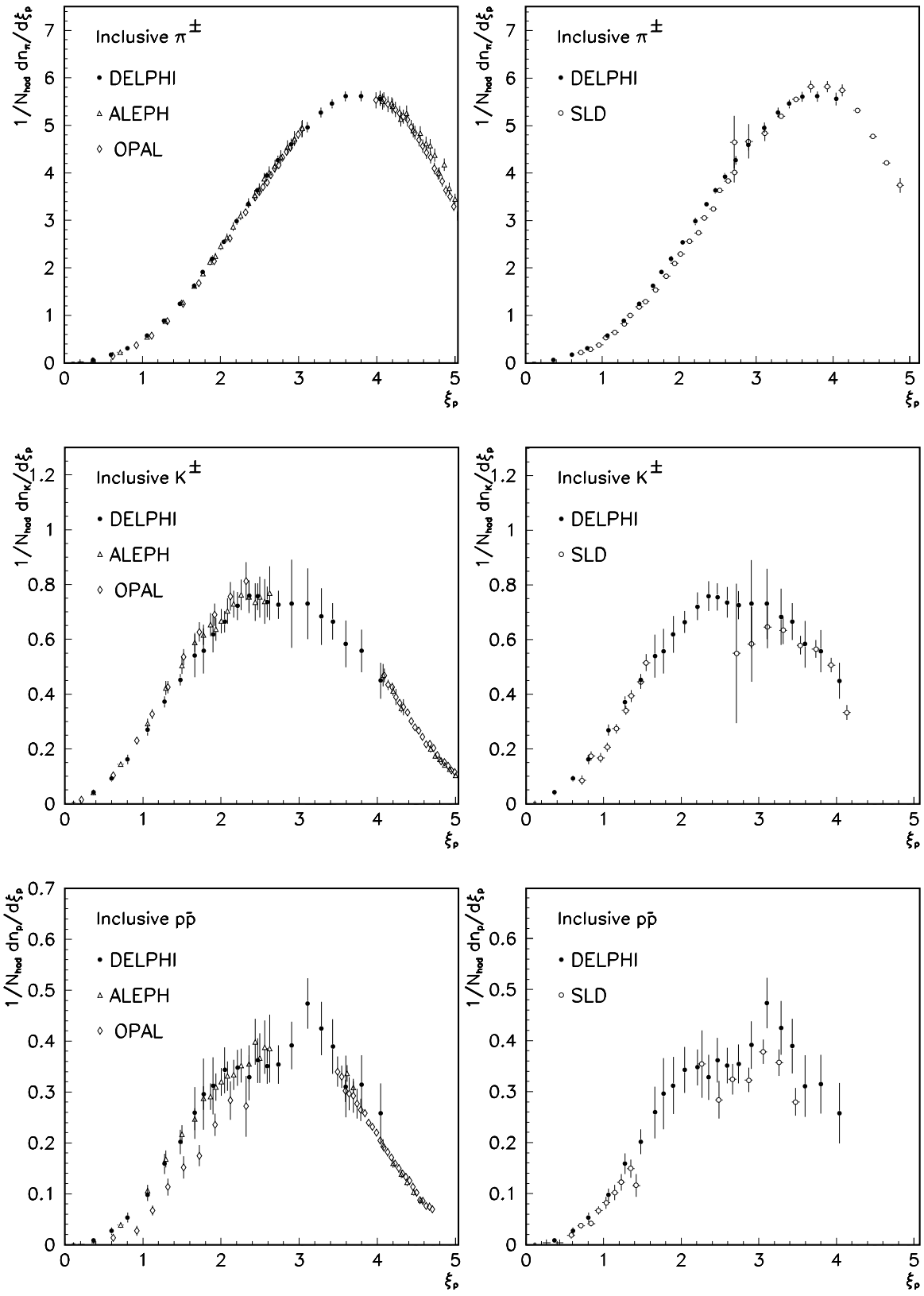


Figure 17: The $\pi^{\pm}$, $K^{\pm}$, $p\overline{p}$ $\xi_p$ distributions in $Z^0 \to q\overline{q}$ events from DELPHI compared with those from ALEPH, OPAL and SLD.

| $< n >$ | $Z^0 \to q\overline{q}$ | $Z^0 \to b\overline{b}$ | $Z^0 \to u\overline{u}, d\overline{d}, s\overline{s}$ |
|---|---|---|---|
| $< \pi^{\pm} >$ | 17.26 $\pm$0.88 | **18.56 $\pm$0.94 | **16.84 $\pm$0.87 |
| $< K^{\pm} >$ | *2.21 $\pm$0.07 | *2.59 $\pm$0.10 | **2.02 $\pm$0.07 |
| $< p\overline{p} >$ | *1.08 $\pm$0.05 | *1.07 $\pm$0.07 | **1.07 $\pm$0.05 |

Table 8: The measured particle production rates in $Z^0 \to q\overline{q}$ , $Z^0 \to b\overline{b}$ , $Z^0 \to u\overline{u}, d\overline{d}, s\overline{s}$ . Results with an improved accuracy compared to previous measurements are indicated by a '$*$'. New results are indicated by '$**$'.

| $\xi_p^*$ | $Z^0 \to q\overline{q}$ | $Z^0 \to b\overline{b}$ | $Z^0 \to u\overline{u}, d\overline{d}, s\overline{s}$ | $\triangle\xi_p^*(uds - b)$ |
|---|---|---|---|---|
| All charged | 3.66 $\pm$ 0.02 | 3.45 $\pm$ 0.04 | 3.76 $\pm$ 0.02 | 0.31 $\pm$0.05 |
| $\pi^{\pm}$ | 3.79 $\pm$ 0.04 | 3.65 $\pm$ 0.04 | 3.85 $\pm$ 0.04 | 0.20 $\pm$0.06 |
| $K^{\pm}$ | 2.69 $\pm$ 0.06 | 2.58 $\pm$ 0.05 | 2.99 $\pm$ 0.09 | 0.41 $\pm$0.11 |
| $p\overline{p}$ | 3.15 $\pm$ 0.09 | 3.36 $\pm$ 0.05 | 3.16 $\pm$ 0.09 | $-$0.20 $\pm$0.10 |

Table 9: The DELPHI $\xi_p^*$ values in $Z^0 \to q\overline{q}$ , $Z^0 \to b\overline{b}$ , $Z^0 \to u\overline{u}, d\overline{d}, s\overline{s}$ and the $\xi_p^*$ difference $\triangle\xi_p^*(uds - b)$ between $uds$ - and $b$ - events.

has been tested on all the measured distributions. The LPHD-MLLA generally describes the shapes of the measured areas very well apart from protons in $b$ - events, where the contribution from $b$ - decays becomes explicitly visible. In this specific case, a double-Gaussian approach has been shown to perform better, where the assumption of one Gaussian describing protons from fragmentation and the other describing protons from $b$ - decays is confirmed by JETSET.

The $\pi^{\pm}, K^{\pm}, p\overline{p}$ multiplicities in $Z^0 \to q\overline{q}$ , $Z^0 \to b\overline{b}$ and $Z^0 \to u\overline{u}, d\overline{d}, s\overline{s}$ are summarised in table 8. The results are obtained by integrating the outcome of the LPHD-MLLA analysis performed on the measured distributions. The results have been compared with the JETSET and HERWIG predictions. It has been shown that the results agree well with the available measurements presented in previous publications, but the uncertainties are in some cases significantly smaller. The accuracy has been improved by a factor $\sim$1.7 ($\sim$2.0) for $< K^{\pm} >$ ($< p\overline{p} >$) in $Z^0 \to q\overline{q}$ , and by a factor $\sim$5 ($\sim$4) for $< K^{\pm} >$ ($< p\overline{p} >$) in $Z^0 \to b\overline{b}$ . The $\pi^{\pm}, K^{\pm}, p\overline{p}$ multiplicities in $Z^0 \to u\overline{u}, d\overline{d}, s\overline{s}$ are presented for the first time.

The maxima $\xi_p^*$ of the measured distributions have been determined and are summarised in table 9. The results have again been compared with the JETSET and HERWIG predictions and with previously published measurements. The $\xi_p^*$ dependence on the primary quark flavour is quantified for the different particle distributions by $\triangle\xi_p^*(uds - b)$ measurements, also given in table 9.

# Acknowledgements

We are greatly indebted to our technical collaborators and to the funding agencies for their support in building and operating the DELPHI detector, and to the members of the CERN-SL Division for the excellent performance of the LEP collider.
We also acknowledge the support of
Austrian Federal Ministry of Science, Research and Arts,
FNRS–FWO, Belgium,
FINEP, CNPq, CAPES, FUJB and FAPERJ, Brazil,
Czech Ministry of Industry and Trade, GA CR 202/96/0450 and GA AVCR A1010521,
Danish Natural Research Council,
Commission of the European Communities (DG XII),
Direction des Sciences de la Matière, CEA, France,
Bundesministerium für Bildung, Wissenschaft, Forschung und Technologie, Germany,
General Secretariat for Research and Technology, Greece,
National Science Foundation (NWO) and Foundation for Research on Matter (FOM), The Netherlands,
Norwegian Research Council,
State Committee for Scientific Research, Poland, 2P03B00108, 2P03B03311 and 628/E–78–SPUB–P03–023/97,
JNICT–Junta Nacional de Investigação Científica e Tecnológica, Portugal,
Vedecka grantova agentura MS SR, Slovakia, Nr. 95/5195/134,
Ministry of Science and Technology of the Republic of Slovenia,
CICYT, Spain, AEN96–1661 and AEN96-1681,
The Swedish Natural Science Research Council,
Particle Physics and Astronomy Research Council, UK,
Department of Energy, USA, DE–FG02–94ER40817.

# Appendix I: Summary Tables Normalised Production Rates

| | DELPHI | | | | JS73 |
|---|---|---|---|---|---|
| $p$ (GeV/$c$) | $f_\pi$ % | $\epsilon_{\rm tot}$ | $\epsilon_{\rm stat}$ | $\epsilon_{\rm syst}$ | $f_\pi$ % |
| 0.70 - 0.91 | 88.72 | ± 0.73 | ± 0.44 | ± 0.58 | 89.49 |
| 0.91 - 1.14 | 86.41 | ± 0.89 | ± 0.44 | ± 0.77 | 87.58 |
| 1.14 - 1.37 | 85.08 | ± 0.88 | ± 0.50 | ± 0.73 | 86.09 |
| 1.37 - 1.60 | 83.60 | ± 0.90 | ± 0.54 | ± 0.72 | 84.84 |
| 1.60 - 1.82 | 82.04 | ± 0.95 | ± 0.60 | ± 0.74 | 83.81 |
| 1.82 - 2.28 | 80.37 | ± 1.16 | ± 0.52 | ± 1.04 | 82.46 |
| 2.28 - 2.74 | 79.11 | ± 1.60 | ± 0.60 | ± 1.48 | 80.79 |
| 2.74 - 3.19 | 77.89 | ± 0.94 | ± 0.49 | ± 0.80 | 79.28 |
| 3.19 - 3.65 | 76.45 | ± 1.14 | ± 0.48 | ± 1.04 | 78.02 |
| 3.65 - 4.10 | 74.74 | ± 1.02 | ± 0.50 | ± 0.89 | 76.94 |
| 4.10 - 4.56 | 73.56 | ± 0.88 | ± 0.54 | ± 0.70 | 75.83 |
| 4.56 - 5.47 | 71.82 | ± 0.82 | ± 0.43 | ± 0.70 | 74.55 |
| 5.47 - 6.38 | 69.92 | ± 0.85 | ± 0.50 | ± 0.69 | 72.78 |
| 6.38 - 7.29 | 68.19 | ± 0.96 | ± 0.58 | ± 0.76 | 71.26 |
| 7.29 - 8.21 | 66.89 | ± 0.99 | ± 0.70 | ± 0.70 | 70.15 |
| 8.21 - 9.12 | 64.57 | ± 1.35 | ± 0.65 | ± 1.18 | 69.03 |
| 9.12 - 11.85 | 62.47 | ± 0.79 | ± 0.38 | ± 0.69 | 67.83 |
| 11.85 - 13.68 | 59.71 | ± 0.94 | ± 0.58 | ± 0.73 | 66.10 |
| 13.68 - 18.24 | 57.67 | ± 1.13 | ± 0.51 | ± 1.01 | 64.67 |
| 18.24 - 22.80 | 54.66 | ± 1.48 | ± 0.81 | ± 1.24 | 62.52 |
| 22.80 - 27.36 | 55.36 | ± 2.18 | ± 1.41 | ± 1.66 | 60.46 |
| 27.36 - 36.47 | 55.69 | ± 4.10 | ± 2.41 | ± 3.31 | 57.01 |
| 36.47 - 45.00 | 56.11 | ± 13.30 | ± 9.72 | ± 9.09 | 53.23 |

Table 10: The normalised production rates for $\pi^\pm$ in $Z^0 \to q\overline{q}$ versus JETSET (JS73).

| | DELPHI | | | | JS73 |
|---|---|---|---|---|---|
| $p$ (GeV/$c$) | $f_{\rm K}$ % | $\epsilon_{\rm tot}$ | $\epsilon_{\rm stat}$ | $\epsilon_{\rm syst}$ | $f_{\rm K}$ % |
| 0.70 - 0.91 | 7.17 | ± 1.02 | ± 0.35 | ± 0.95 | 7.06 |
| 0.91 - 1.14 | 8.58 | ± 1.18 | ± 0.29 | ± 1.14 | 8.03 |
| 1.14 - 1.37 | 8.84 | ± 1.28 | ± 0.31 | ± 1.24 | 8.76 |
| 1.37 - 1.60 | 10.21 | ± 0.99 | ± 0.39 | ± 0.91 | 9.39 |
| 1.60 - 1.82 | 10.63 | ± 1.58 | ± 0.52 | ± 1.49 | 9.94 |
| 1.82 - 2.28 | 11.84 | ± 2.06 | ± 0.47 | ± 2.01 | 10.73 |
| 2.28 - 2.74 | 12.55 | ± 2.75 | ± 0.59 | ± 2.69 | 11.80 |
| 2.74 - 3.19 | 13.25 | ± 0.89 | ± 0.39 | ± 0.80 | 12.81 |
| 3.19 - 3.65 | 14.32 | ± 1.05 | ± 0.36 | ± 0.99 | 13.72 |
| 3.65 - 4.10 | 15.59 | ± 0.98 | ± 0.38 | ± 0.91 | 14.52 |
| 4.10 - 4.56 | 16.72 | ± 1.17 | ± 0.43 | ± 1.09 | 15.31 |
| 4.56 - 5.47 | 17.39 | ± 1.15 | ± 0.37 | ± 1.09 | 16.26 |
| 5.47 - 6.38 | 18.23 | ± 1.02 | ± 0.57 | ± 0.84 | 17.57 |
| 6.38 - 7.29 | 19.25 | ± 1.94 | ± 0.99 | ± 1.67 | 18.77 |
| 7.29 - 8.21 | 19.55 | ± 2.78 | ± 1.44 | ± 2.37 | 19.81 |
| 8.21 - 9.12 | 21.47 | ± 3.04 | ± 0.94 | ± 2.89 | 20.92 |
| 9.12 - 11.85 | 22.73 | ± 0.76 | ± 0.32 | ± 0.69 | 22.27 |
| 11.85 - 13.68 | 25.17 | ± 1.04 | ± 0.48 | ± 0.93 | 24.19 |
| 13.68 - 18.24 | 26.77 | ± 1.56 | ± 0.45 | ± 1.49 | 25.98 |
| 18.24 - 22.80 | 29.04 | ± 2.75 | ± 0.82 | ± 2.63 | 28.78 |
| 22.80 - 27.36 | 29.97 | ± 3.03 | ± 1.52 | ± 2.62 | 31.77 |
| 27.36 - 36.47 | 33.86 | ± 6.91 | ± 2.97 | ± 6.24 | 36.99 |
| 36.47 - 45.00 | 27.78 | ± 24.12 | ± 13.30 | ± 20.12 | 44.15 |

Table 11: The normalised production rates for $K^\pm$ in $Z^0 \to q\overline{q}$ versus JETSET (JS73).

| | DELPHI | | | | JS73 |
|---|---|---|---|---|---|
| $p$ (GeV/$c$) | $f_{\rm p}$ % | $\epsilon_{\rm tot}$ | $\epsilon_{\rm stat}$ | $\epsilon_{\rm syst}$ | $f_{\rm p}$ % |
| 0.70 - 0.91 | 4.11 | ± 0.93 | ± 0.18 | ± 0.92 | 3.45 |
| 0.91 - 1.14 | 4.85 | ± 0.87 | ± 0.25 | ± 0.84 | 4.39 |
| 1.14 - 1.37 | 4.71 | ± 0.90 | ± 0.38 | ± 0.82 | 5.15 |
| 1.37 - 1.60 | 5.97 | ± 0.79 | ± 0.42 | ± 0.67 | 5.77 |
| 1.60 - 1.82 | 6.61 | ± 0.79 | ± 0.36 | ± 0.70 | 6.25 |
| 1.82 - 2.28 | 7.68 | ± 0.77 | ± 0.34 | ± 0.69 | 6.80 |
| 2.28 - 2.74 | 6.73 | ± 0.79 | ± 0.24 | ± 0.75 | 7.41 |
| 2.74 - 3.19 | 6.46 | ± 0.68 | ± 0.17 | ± 0.66 | 7.90 |
| 3.19 - 3.65 | 6.83 | ± 0.67 | ± 0.22 | ± 0.63 | 8.26 |
| 3.65 - 4.10 | 7.46 | ± 0.89 | ± 0.26 | ± 0.85 | 8.54 |
| 4.10 - 4.56 | 7.23 | ± 0.96 | ± 0.31 | ± 0.91 | 8.86 |
| 4.56 - 5.47 | 8.37 | ± 0.82 | ± 0.29 | ± 0.77 | 9.19 |
| 5.47 - 6.38 | 9.40 | ± 1.21 | ± 0.52 | ± 1.09 | 9.64 |
| 6.38 - 7.29 | 9.70 | ± 1.64 | ± 1.02 | ± 1.29 | 9.97 |
| 7.29 - 8.21 | 10.37 | ± 2.29 | ± 1.56 | ± 1.67 | 10.04 |
| 8.21 - 9.12 | 10.30 | ± 1.88 | ± 1.08 | ± 1.54 | 10.05 |
| 9.12 - 11.85 | 10.12 | ± 1.12 | ± 0.41 | ± 1.04 | 9.91 |
| 11.85 - 13.68 | 10.75 | ± 1.24 | ± 0.50 | ± 1.14 | 9.71 |
| 13.68 - 18.24 | 9.71 | ± 1.04 | ± 0.43 | ± 0.95 | 9.35 |
| 18.24 - 22.80 | 9.54 | ± 1.68 | ± 0.57 | ± 1.58 | 8.69 |
| 22.80 - 27.36 | 8.72 | ± 2.11 | ± 0.95 | ± 1.88 | 7.77 |
| 27.36 - 36.47 | 7.00 | ± 3.16 | ± 1.61 | ± 2.72 | 5.99 |
| 36.47 - 45.00 | 8.68 | ± 6.69 | ± 4.26 | ± 5.16 | 2.62 |

Table 12: The normalised production rates for $p\overline{p}$ in $Z^0 \to q\overline{q}$ versus JETSET (JS73).

| | DELPHI | | | | JS73 |
|---|---|---|---|---|---|
| $p$ (GeV/$c$) | $f_{\rm Hv}$ % | $\epsilon_{\rm tot}$ | $\epsilon_{\rm stat}$ | $\epsilon_{\rm syst}$ | $f_{\rm Hv}$ % |
| 0.70 - 0.91 | 11.40 | ± 0.99 | ± 0.39 | ± 0.91 | 10.51 |
| 0.91 - 1.14 | 13.08 | ± 1.19 | ± 0.33 | ± 1.14 | 12.42 |
| 1.14 - 1.37 | 14.99 | ± 1.07 | ± 0.39 | ± 0.99 | 13.91 |
| 1.37 - 1.60 | 15.87 | ± 1.09 | ± 0.48 | ± 0.98 | 15.16 |
| 1.60 - 1.82 | 17.11 | ± 1.46 | ± 0.59 | ± 1.33 | 16.19 |
| 1.82 - 2.28 | 19.23 | ± 2.16 | ± 0.58 | ± 2.08 | 17.54 |
| 2.28 - 2.74 | 19.87 | ± 2.27 | ± 0.61 | ± 2.19 | 19.21 |
| 2.74 - 3.19 | 20.89 | ± 0.97 | ± 0.40 | ± 0.88 | 20.72 |
| 3.19 - 3.65 | 21.02 | ± 0.75 | ± 0.35 | ± 0.66 | 21.98 |
| 3.65 - 4.10 | 22.77 | ± 0.68 | ± 0.36 | ± 0.57 | 23.06 |
| 4.10 - 4.56 | 24.14 | ± 0.74 | ± 0.40 | ± 0.63 | 24.17 |
| 4.56 - 5.47 | 25.74 | ± 0.68 | ± 0.32 | ± 0.60 | 25.45 |
| 5.47 - 6.38 | 27.65 | ± 0.70 | ± 0.38 | ± 0.58 | 27.22 |
| 6.38 - 7.29 | 29.22 | ± 0.73 | ± 0.45 | ± 0.57 | 28.74 |
| 7.29 - 8.21 | 29.89 | ± 0.78 | ± 0.53 | ± 0.57 | 29.85 |
| 8.21 - 9.12 | 31.77 | ± 0.85 | ± 0.50 | ± 0.69 | 30.97 |
| 9.12 - 11.85 | 33.04 | ± 0.72 | ± 0.32 | ± 0.65 | 32.17 |
| 11.85 - 13.68 | 35.24 | ± 1.00 | ± 0.54 | ± 0.84 | 33.90 |
| 13.68 - 18.24 | 36.09 | ± 1.59 | ± 0.52 | ± 1.51 | 35.33 |
| 18.24 - 22.80 | 37.71 | ± 2.92 | ± 0.89 | ± 2.78 | 37.48 |
| 22.80 - 27.36 | 37.92 | ± 3.08 | ± 1.43 | ± 2.72 | 39.54 |
| 27.36 - 36.47 | 41.24 | ± 4.07 | ± 2.26 | ± 3.39 | 42.99 |
| 36.47 - 45.00 | 46.00 | ± 15.65 | ± 9.72 | ± 12.27 | 46.77 |

Table 13: normalised production rates for $Hv^\pm$ particles in $Z^0 \to q\overline{q}$ versus JETSET (JS73).

| | DELPHI | | | | JS73 |
|---|---|---|---|---|---|
| $p$ (GeV/$c$) | $f_\pi$ % | $\epsilon_{\rm tot}$ | $\epsilon_{\rm stat}$ | $\epsilon_{\rm syst}$ | $f_\pi$ % |
| 0.70 - 0.91 | 88.57 | ± 1.21 | ± 0.99 | ± 0.71 | 88.77 |
| 0.91 - 1.14 | 86.34 | ± 1.18 | ± 0.99 | ± 0.68 | 86.85 |
| 1.14 - 1.37 | 84.86 | ± 1.31 | ± 1.08 | ± 0.76 | 85.12 |
| 1.37 - 1.60 | 83.15 | ± 1.42 | ± 1.18 | ± 0.81 | 83.53 |
| 1.60 - 1.82 | 81.12 | ± 1.54 | ± 1.30 | ± 0.84 | 81.92 |
| 1.82 - 2.28 | 78.79 | ± 1.52 | ± 1.11 | ± 1.02 | 79.75 |
| 2.28 - 2.74 | 76.66 | ± 1.89 | ± 1.25 | ± 1.43 | 77.01 |
| 2.74 - 3.19 | 74.39 | ± 1.44 | ± 0.99 | ± 1.03 | 74.25 |
| 3.19 - 3.65 | 72.25 | ± 1.46 | ± 0.95 | ± 1.12 | 72.09 |
| 3.65 - 4.10 | 69.87 | ± 1.36 | ± 0.99 | ± 0.95 | 70.12 |
| 4.10 - 4.56 | 68.07 | ± 1.39 | ± 1.04 | ± 0.94 | 68.23 |
| 4.56 - 5.47 | 65.13 | ± 1.08 | ± 0.81 | ± 0.74 | 65.46 |
| 5.47 - 6.38 | 61.46 | ± 1.12 | ± 0.92 | ± 0.66 | 61.60 |
| 6.38 - 7.29 | 58.17 | ± 1.30 | ± 1.07 | ± 0.73 | 58.19 |
| 7.29 - 8.21 | 55.87 | ± 1.40 | ± 1.29 | ± 0.57 | 55.83 |
| 8.21 - 9.12 | 53.23 | ± 1.57 | ± 1.20 | ± 1.01 | 53.94 |
| 9.12 - 11.85 | 49.84 | ± 0.92 | ± 0.71 | ± 0.62 | 50.73 |
| 11.85 - 13.68 | 46.23 | ± 1.36 | ± 1.06 | ± 0.86 | 47.45 |
| 13.68 - 18.24 | 43.25 | ± 1.22 | ± 0.95 | ± 0.75 | 44.36 |
| 18.24 - 22.80 | 40.83 | ± 2.24 | ± 1.67 | ± 1.47 | 42.43 |
| 22.80 - 27.36 | 46.20 | ± 5.51 | ± 3.62 | ± 3.70 | 46.61 |
| 27.36 - 36.47 | 62.64 | ± 11.18 | ± 9.12 | ± 5.98 | 62.07 |
| 36.47 - 45.00 | 78.62 | ± 83.44 | ± 55.48 | ± 62.05 | 74.48 |

Table 14: The normalised production rates for $\pi^\pm$ in $Z^0 \to b\overline{b}$ versus JETSET (JS73).

| | DELPHI | | | | JS73 |
|---|---|---|---|---|---|
| $p$ (GeV/$c$) | $f_{\rm K}$ % | $\epsilon_{\rm tot}$ | $\epsilon_{\rm stat}$ | $\epsilon_{\rm syst}$ | $f_{\rm K}$ % |
| 0.70 - 0.91 | 6.70 | ± 1.14 | ± 0.79 | ± 0.81 | 6.60 |
| 0.91 - 1.14 | 8.05 | ± 1.23 | ± 0.61 | ± 1.09 | 7.53 |
| 1.14 - 1.37 | 8.51 | ± 1.45 | ± 0.68 | ± 1.30 | 8.43 |
| 1.37 - 1.60 | 10.11 | ± 1.21 | ± 0.88 | ± 0.85 | 9.31 |
| 1.60 - 1.82 | 11.03 | ± 2.08 | ± 1.18 | ± 1.71 | 10.32 |
| 1.82 - 2.28 | 12.98 | ± 2.32 | ± 1.16 | ± 2.00 | 11.77 |
| 2.28 - 2.74 | 14.59 | ± 3.20 | ± 1.48 | ± 2.85 | 13.71 |
| 2.74 - 3.19 | 16.08 | ± 1.38 | ± 1.04 | ± 0.91 | 15.55 |
| 3.19 - 3.65 | 17.76 | ± 1.45 | ± 0.99 | ± 1.08 | 17.01 |
| 3.65 - 4.10 | 19.43 | ± 1.74 | ± 1.06 | ± 1.40 | 18.10 |
| 4.10 - 4.56 | 20.67 | ± 1.66 | ± 1.19 | ± 1.15 | 18.93 |
| 4.56 - 5.47 | 21.23 | ± 1.47 | ± 1.02 | ± 1.03 | 19.85 |
| 5.47 - 6.38 | 21.73 | ± 2.03 | ± 1.53 | ± 1.34 | 20.94 |
| 6.38 - 7.29 | 22.19 | ± 3.45 | ± 2.81 | ± 1.88 | 21.64 |
| 7.29 - 8.21 | 21.76 | ± 5.01 | ± 3.96 | ± 3.04 | 22.04 |
| 8.21 - 9.12 | 23.09 | ± 3.98 | ± 2.43 | ± 3.12 | 22.50 |
| 9.12 - 11.85 | 22.77 | ± 1.00 | ± 0.75 | ± 0.69 | 22.31 |
| 11.85 - 13.68 | 22.24 | ± 1.32 | ± 0.98 | ± 0.86 | 21.37 |
| 13.68 - 18.24 | 19.85 | ± 1.36 | ± 0.80 | ± 1.03 | 19.26 |
| 18.24 - 22.80 | 15.47 | ± 1.99 | ± 1.16 | ± 1.59 | 15.33 |
| 22.80 - 27.36 | 11.50 | ± 1.97 | ± 1.73 | ± 0.72 | 12.18 |
| 27.36 - 36.47 | 9.38 | ± 2.93 | ± 2.76 | ± 0.83 | 10.25 |
| 36.47 - 45.00 | 5.86 | ± 9.04 | ± 5.95 | ± 6.71 | 9.31 |

Table 15: Normalised production rates for $K^\pm$ in $Z^0 \to b\overline{b}$ versus JETSET (JS73).

| | DELPHI | | | | JS73 |
|---|---|---|---|---|---|
| $p$ (GeV/$c$) | $f_{\rm p}$ % | $\epsilon_{\rm tot}$ | $\epsilon_{\rm stat}$ | $\epsilon_{\rm syst}$ | $f_{\rm p}$ % |
| 0.70 - 0.91 | 3.65 | ± 0.84 | ± 0.35 | ± 0.78 | 3.05 |
| 0.91 - 1.14 | 4.20 | ± 0.81 | ± 0.48 | ± 0.68 | 3.81 |
| 1.14 - 1.37 | 3.99 | ± 1.06 | ± 0.70 | ± 0.82 | 4.36 |
| 1.37 - 1.60 | 4.94 | ± 0.96 | ± 0.82 | ± 0.54 | 4.77 |
| 1.60 - 1.82 | 5.36 | ± 0.86 | ± 0.67 | ± 0.58 | 5.07 |
| 1.82 - 2.28 | 6.00 | ± 0.88 | ± 0.63 | ± 0.65 | 5.31 |
| 2.28 - 2.74 | 5.06 | ± 0.82 | ± 0.40 | ± 0.74 | 5.57 |
| 2.74 - 3.19 | 4.78 | ± 0.59 | ± 0.25 | ± 0.57 | 5.84 |
| 3.19 - 3.65 | 4.96 | ± 0.65 | ± 0.33 | ± 0.59 | 6.00 |
| 3.65 - 4.10 | 5.54 | ± 0.78 | ± 0.41 | ± 0.68 | 6.34 |
| 4.10 - 4.56 | 5.60 | ± 0.99 | ± 0.51 | ± 0.87 | 6.87 |
| 4.56 - 5.47 | 7.11 | ± 0.91 | ± 0.57 | ± 0.68 | 7.81 |
| 5.47 - 6.38 | 9.16 | ± 1.69 | ± 1.18 | ± 1.21 | 9.39 |
| 6.38 - 7.29 | 10.34 | ± 3.10 | ± 2.86 | ± 1.20 | 10.62 |
| 7.29 - 8.21 | 11.50 | ± 5.13 | ± 4.50 | ± 2.42 | 11.14 |
| 8.21 - 9.12 | 11.38 | ± 3.32 | ± 2.84 | ± 1.72 | 11.11 |
| 9.12 - 11.85 | 10.88 | ± 1.64 | ± 1.08 | ± 1.25 | 10.65 |
| 11.85 - 13.68 | 10.43 | ± 1.49 | ± 1.18 | ± 0.94 | 9.42 |
| 13.68 - 18.24 | 7.87 | ± 1.11 | ± 0.85 | ± 0.71 | 7.57 |
| 18.24 - 22.80 | 5.71 | ± 1.34 | ± 0.95 | ± 0.91 | 5.20 |
| 22.80 - 27.36 | 4.72 | ± 2.05 | ± 1.68 | ± 1.15 | 4.21 |
| 27.36 - 36.47 | 4.08 | ± 5.28 | ± 3.74 | ± 3.70 | 3.49 |
| 36.47 - 45.00 | 29.72 | ± 137.3 | ± 77.8 | ± 113.0 | 8.97 |

Table 16: The normalised production rates for $p\overline{p}$ in $Z^0 \to b\overline{b}$ versus JETSET (JS73).

| | DELPHI | | | | JS73 |
|---|---|---|---|---|---|
| $p$ (GeV/$c$) | $f_{\rm Hv}$ % | $\epsilon_{\rm tot}$ | $\epsilon_{\rm stat}$ | $\epsilon_{\rm syst}$ | $f_{\rm Hv}$ % |
| 0.70 - 0.91 | 10.47 | ± 1.20 | ± 0.84 | ± 0.80 | 9.66 |
| 0.91 - 1.14 | 11.95 | ± 1.18 | ± 0.69 | ± 0.98 | 11.34 |
| 1.14 - 1.37 | 13.79 | ± 1.27 | ± 0.80 | ± 1.01 | 12.79 |
| 1.37 - 1.60 | 14.73 | ± 1.30 | ± 0.98 | ± 0.87 | 14.08 |
| 1.60 - 1.82 | 16.26 | ± 1.83 | ± 1.23 | ± 1.37 | 15.39 |
| 1.82 - 2.28 | 18.73 | ± 2.12 | ± 1.26 | ± 1.69 | 17.08 |
| 2.28 - 2.74 | 19.94 | ± 2.50 | ± 1.34 | ± 2.12 | 19.28 |
| 2.74 - 3.19 | 21.57 | ± 1.16 | ± 0.90 | ± 0.73 | 21.40 |
| 3.19 - 3.65 | 22.01 | ± 1.11 | ± 0.80 | ± 0.80 | 23.01 |
| 3.65 - 4.10 | 24.13 | ± 1.02 | ± 0.83 | ± 0.62 | 24.44 |
| 4.10 - 4.56 | 25.76 | ± 1.23 | ± 0.91 | ± 0.83 | 25.79 |
| 4.56 - 5.47 | 27.97 | ± 1.15 | ± 0.77 | ± 0.87 | 27.66 |
| 5.47 - 6.38 | 30.82 | ± 1.16 | ± 0.95 | ± 0.70 | 30.34 |
| 6.38 - 7.29 | 32.80 | ± 1.43 | ± 1.14 | ± 0.72 | 32.26 |
| 7.29 - 8.21 | 33.22 | ± 1.47 | ± 1.31 | ± 0.69 | 33.19 |
| 8.21 - 9.12 | 34.47 | ± 1.43 | ± 1.23 | ± 0.74 | 33.61 |
| 9.12 - 11.85 | 33.85 | ± 1.02 | ± 0.73 | ± 0.74 | 32.96 |
| 11.85 - 13.68 | 32.01 | ± 1.41 | ± 1.13 | ± 0.80 | 30.79 |
| 13.68 - 18.24 | 27.42 | ± 1.46 | ± 0.96 | ± 1.08 | 26.84 |
| 18.24 - 22.80 | 20.66 | ± 2.33 | ± 1.30 | ± 1.94 | 20.53 |
| 22.80 - 27.36 | 15.72 | ± 2.25 | ± 1.75 | ± 1.17 | 16.39 |
| 27.36 - 36.47 | 13.18 | ± 3.12 | ± 2.34 | ± 1.94 | 13.74 |
| 36.47 - 45.00 | 17.98 | ± 20.28 | ± 16.79 | ± 11.29 | 18.28 |

Table 17: The normalised production rates for $Hv^\pm$ particles in $Z^0 \to b\overline{b}$ versus JETSET (JS73).

| | DELPHI | | | | JS73 |
|---|---|---|---|---|---|
| $p$ (GeV/$c$) | $f_\pi$ % | $\epsilon_{\rm tot}$ | $\epsilon_{\rm stat}$ | $\epsilon_{\rm syst}$ | $f_\pi$ % |
| 0.70 - 0.91 | 88.87 | ± 0.80 | ± 0.56 | ± 0.60 | 88.77 |
| 0.91 - 1.14 | 86.56 | ± 0.98 | ± 0.57 | ± 0.81 | 86.85 |
| 1.14 - 1.37 | 85.28 | ± 0.95 | ± 0.64 | ± 0.73 | 85.12 |
| 1.37 - 1.60 | 83.90 | ± 0.99 | ± 0.70 | ± 0.72 | 83.53 |
| 1.60 - 1.82 | 82.51 | ± 1.07 | ± 0.78 | ± 0.76 | 81.92 |
| 1.82 - 2.28 | 81.13 | ± 1.21 | ± 0.67 | ± 1.03 | 79.75 |
| 2.28 - 2.74 | 80.34 | ± 1.78 | ± 0.78 | ± 1.60 | 77.01 |
| 2.74 - 3.19 | 79.71 | ± 0.99 | ± 0.65 | ± 0.77 | 74.25 |
| 3.19 - 3.65 | 78.77 | ± 1.31 | ± 0.64 | ± 1.16 | 72.09 |
| 3.65 - 4.10 | 77.50 | ± 1.13 | ± 0.68 | ± 0.92 | 70.12 |
| 4.10 - 4.56 | 76.73 | ± 1.06 | ± 0.74 | ± 0.78 | 68.23 |
| 4.56 - 5.47 | 75.61 | ± 1.00 | ± 0.59 | ± 0.83 | 65.46 |
| 5.47 - 6.38 | 74.60 | ± 1.04 | ± 0.69 | ± 0.80 | 61.60 |
| 6.38 - 7.29 | 73.55 | ± 1.16 | ± 0.81 | ± 0.85 | 58.19 |
| 7.29 - 8.21 | 72.56 | ± 1.24 | ± 0.98 | ± 0.78 | 55.83 |
| 8.21 - 9.12 | 70.47 | ± 1.54 | ± 0.90 | ± 1.27 | 53.94 |
| 9.12 - 11.85 | 68.81 | ± 0.93 | ± 0.53 | ± 0.79 | 50.73 |
| 11.85 - 13.68 | 66.22 | ± 1.15 | ± 0.80 | ± 0.84 | 47.45 |
| 13.68 - 18.24 | 64.12 | ± 1.22 | ± 0.69 | ± 1.03 | 44.36 |
| 18.24 - 22.80 | 60.17 | ± 1.73 | ± 1.07 | ± 1.37 | 42.43 |
| 22.80 - 27.36 | 59.25 | ± 2.25 | ± 1.80 | ± 1.32 | 46.61 |
| 27.36 - 36.47 | 56.75 | ± 5.45 | ± 2.86 | ± 4.61 | 62.07 |
| 36.47 - 45.00 | 56.19 | ± 14.56 | ± 11.31 | ± 9.00 | 74.48 |

Table 18: Normalised production rates for $\pi^{\pm}$ in $Z^0 \to u\overline{u}, d\overline{d}, s\overline{s}$ versus JETSET (JS73).

| | DELPHI | | | | JS73 |
|---|---|---|---|---|---|
| $p$ (GeV/$c$) | $f_{\rm K}$ % | $\epsilon_{\rm tot}$ | $\epsilon_{\rm stat}$ | $\epsilon_{\rm syst}$ | $f_{\rm K}$ % |
| 0.70 - 0.91 | 7.34 | ± 1.03 | ± 0.45 | ± 0.95 | 7.24 |
| 0.91 - 1.14 | 8.78 | ± 1.18 | ± 0.37 | ± 1.13 | 8.21 |
| 1.14 - 1.37 | 8.98 | ± 1.27 | ± 0.40 | ± 1.22 | 8.89 |
| 1.37 - 1.60 | 10.27 | ± 1.05 | ± 0.51 | ± 0.93 | 9.45 |
| 1.60 - 1.82 | 10.52 | ± 1.61 | ± 0.65 | ± 1.48 | 9.84 |
| 1.82 - 2.28 | 11.43 | ± 2.06 | ± 0.58 | ± 1.98 | 10.37 |
| 2.28 - 2.74 | 11.72 | ± 2.77 | ± 0.70 | ± 2.69 | 11.02 |
| 2.74 - 3.19 | 11.99 | ± 0.86 | ± 0.44 | ± 0.76 | 11.60 |
| 3.19 - 3.65 | 12.65 | ± 1.07 | ± 0.40 | ± 1.01 | 12.12 |
| 3.65 - 4.10 | 13.57 | ± 0.90 | ± 0.42 | ± 0.82 | 12.64 |
| 4.10 - 4.56 | 14.45 | ± 1.09 | ± 0.46 | ± 1.00 | 13.23 |
| 4.56 - 5.47 | 14.91 | ± 1.00 | ± 0.40 | ± 0.92 | 13.94 |
| 5.47 - 6.38 | 15.59 | ± 0.97 | ± 0.62 | ± 0.76 | 15.02 |
| 6.38 - 7.29 | 16.52 | ± 1.86 | ± 1.03 | ± 1.53 | 16.11 |
| 7.29 - 8.21 | 17.01 | ± 2.53 | ± 1.55 | ± 2.00 | 17.23 |
| 8.21 - 9.12 | 18.86 | ± 2.84 | ± 1.02 | ± 2.65 | 18.38 |
| 9.12 - 11.85 | 20.33 | ± 0.75 | ± 0.36 | ± 0.68 | 19.92 |
| 11.85 - 13.68 | 23.14 | ± 1.21 | ± 0.55 | ± 1.09 | 22.23 |
| 13.68 - 18.24 | 25.60 | ± 1.66 | ± 0.53 | ± 1.58 | 24.84 |
| 18.24 - 22.80 | 28.87 | ± 2.79 | ± 0.98 | ± 2.62 | 28.62 |
| 22.80 - 27.36 | 30.59 | ± 3.82 | ± 1.84 | ± 3.34 | 32.43 |
| 27.36 - 36.47 | 34.77 | ± 6.80 | ± 3.53 | ± 5.79 | 37.98 |
| 36.47 - 45.00 | 27.88 | ± 24.47 | ± 16.19 | ± 18.19 | 44.30 |

Table 19: Normalised production rates for $K^{\pm}$ in $Z^0 \to u\overline{u}, d\overline{d}, s\overline{s}$ versus JETSET (JS73).

| | DELPHI | | | | JS73 |
|---|---|---|---|---|---|
| $p$ (GeV/$c$) | $f_{\rm p}$ % | $\epsilon_{\rm tot}$ | $\epsilon_{\rm stat}$ | $\epsilon_{\rm syst}$ | $f_{\rm p}$ % |
| 0.70 - 0.91 | 4.30 | ± 1.06 | ± 0.24 | ± 1.04 | 3.60 |
| 0.91 - 1.14 | 5.10 | ± 1.06 | ± 0.34 | ± 1.00 | 4.62 |
| 1.14 - 1.37 | 5.02 | ± 1.05 | ± 0.52 | ± 0.93 | 5.48 |
| 1.37 - 1.60 | 6.40 | ± 0.89 | ± 0.57 | ± 0.71 | 6.19 |
| 1.60 - 1.82 | 7.13 | ± 0.96 | ± 0.50 | ± 0.85 | 6.75 |
| 1.82 - 2.28 | 8.40 | ± 0.88 | ± 0.47 | ± 0.76 | 7.44 |
| 2.28 - 2.74 | 7.45 | ± 0.91 | ± 0.35 | ± 0.86 | 8.19 |
| 2.74 - 3.19 | 7.17 | ± 0.79 | ± 0.25 | ± 0.78 | 8.77 |
| 3.19 - 3.65 | 7.62 | ± 0.78 | ± 0.32 | ± 0.73 | 9.22 |
| 3.65 - 4.10 | 8.31 | ± 1.03 | ± 0.38 | ± 0.98 | 9.51 |
| 4.10 - 4.56 | 7.99 | ± 1.17 | ± 0.44 | ± 1.10 | 9.79 |
| 4.56 - 5.47 | 9.11 | ± 0.90 | ± 0.41 | ± 0.81 | 10.01 |
| 5.47 - 6.38 | 9.91 | ± 1.42 | ± 0.69 | ± 1.25 | 10.16 |
| 6.38 - 7.29 | 10.00 | ± 1.92 | ± 1.25 | ± 1.47 | 10.27 |
| 7.29 - 8.21 | 10.55 | ± 2.48 | ± 1.92 | ± 1.57 | 10.21 |
| 8.21 - 9.12 | 10.41 | ± 2.09 | ± 1.34 | ± 1.61 | 10.16 |
| 9.12 - 11.85 | 10.22 | ± 1.18 | ± 0.52 | ± 1.07 | 10.00 |
| 11.85 - 13.68 | 10.84 | ± 1.40 | ± 0.62 | ± 1.27 | 9.79 |
| 13.68 - 18.24 | 9.74 | ± 1.15 | ± 0.53 | ± 1.03 | 9.37 |
| 18.24 - 22.80 | 9.70 | ± 1.71 | ± 0.69 | ± 1.57 | 8.84 |
| 22.80 - 27.36 | 8.74 | ± 2.03 | ± 1.09 | ± 1.71 | 7.79 |
| 27.36 - 36.47 | 6.76 | ± 2.71 | ± 1.72 | ± 2.09 | 5.79 |
| 36.47 - 45.00 | 8.17 | ± 5.93 | ± 4.19 | ± 4.20 | 2.46 |

Table 20: Normalised production rates for $p\overline{p}$ in $Z^0 \to u\overline{u}, d\overline{d}, s\overline{s}$ versus JETSET (JS73).

| | DELPHI | | | | JS73 |
|---|---|---|---|---|---|
| $p$ (GeV/$c$) | $f_{\rm Hv}$ % | $\epsilon_{\rm tot}$ | $\epsilon_{\rm stat}$ | $\epsilon_{\rm syst}$ | $f_{\rm Hv}$ % |
| 0.70 - 0.91 | 11.75 | ± 0.98 | ± 0.50 | ± 0.86 | 10.84 |
| 0.91 - 1.14 | 13.52 | ± 1.26 | ± 0.43 | ± 1.20 | 12.84 |
| 1.14 - 1.37 | 15.50 | ± 1.14 | ± 0.51 | ± 1.04 | 14.38 |
| 1.37 - 1.60 | 16.36 | ± 1.27 | ± 0.63 | ± 1.11 | 15.63 |
| 1.60 - 1.82 | 17.53 | ± 1.53 | ± 0.78 | ± 1.34 | 16.59 |
| 1.82 - 2.28 | 19.52 | ± 2.33 | ± 0.75 | ± 2.21 | 17.81 |
| 2.28 - 2.74 | 19.87 | ± 2.44 | ± 0.78 | ± 2.32 | 19.22 |
| 2.74 - 3.19 | 20.53 | ± 1.02 | ± 0.50 | ± 0.91 | 20.36 |
| 3.19 - 3.65 | 20.41 | ± 0.87 | ± 0.44 | ± 0.78 | 21.34 |
| 3.65 - 4.10 | 21.87 | ± 0.70 | ± 0.45 | ± 0.57 | 22.16 |
| 4.10 - 4.56 | 22.99 | ± 0.80 | ± 0.48 | ± 0.66 | 23.03 |
| 4.56 - 5.47 | 24.21 | ± 0.67 | ± 0.38 | ± 0.58 | 23.95 |
| 5.47 - 6.38 | 25.59 | ± 0.75 | ± 0.45 | ± 0.61 | 25.18 |
| 6.38 - 7.29 | 26.82 | ± 0.79 | ± 0.52 | ± 0.58 | 26.37 |
| 7.29 - 8.21 | 27.48 | ± 0.83 | ± 0.62 | ± 0.56 | 27.45 |
| 8.21 - 9.12 | 29.28 | ± 0.89 | ± 0.59 | ± 0.70 | 28.54 |
| 9.12 - 11.85 | 30.72 | ± 0.74 | ± 0.37 | ± 0.67 | 29.92 |
| 11.85 - 13.68 | 33.29 | ± 1.17 | ± 0.64 | ± 1.00 | 32.02 |
| 13.68 - 18.24 | 34.96 | ± 1.69 | ± 0.63 | ± 1.58 | 34.22 |
| 18.24 - 22.80 | 37.69 | ± 3.00 | ± 1.07 | ± 2.81 | 37.46 |
| 22.80 - 27.36 | 38.56 | ± 3.99 | ± 1.73 | ± 3.59 | 40.21 |
| 27.36 - 36.47 | 41.99 | ± 3.98 | ± 2.66 | ± 2.95 | 43.77 |
| 36.47 - 45.00 | 46.00 | ± 15.98 | ± 10.83 | ± 11.70 | 46.77 |

Table 21: Normalised production rates for $Hv^{\pm}$ particles in $Z^0 \to u\overline{u}, d\overline{d}, s\overline{s}$ versus JETSET (JS73).

# Appendix II: Summary Tables Differential Cross-sections

| | DELPHI | | | | DELPHI | | JS73 |
|---|---|---|---|---|---|---|---|
| $p$ (GeV/$c$) | $\frac{1}{N_h}\frac{dn_{tot}}{dp}$ | $\epsilon_{stat}$ | $\epsilon_{syst}$ | $X_p$ | $\frac{1}{N_h}\frac{dn_{tot}}{dx_p}$ | $\epsilon_{tot}$ | $\frac{1}{N_h}\frac{dn_{tot}}{dx_p}$ |
| 0.30 - 0.36 | 11.22 | ± 0.47 | ± 0.74 | 0.007 - 0.008 | 511.8 | ± 39.8 | 510.5 |
| 0.36 - 0.46 | 10.95 | ± 0.30 | ± 0.52 | 0.008 - 0.010 | 499.4 | ± 27.4 | 498.9 |
| 0.46 - 0.57 | 10.30 | ± 0.16 | ± 0.24 | 0.010 - 0.012 | 470.0 | ± 13.0 | 468.9 |
| 0.57 - 0.70 | 9.25 | ± 0.16 | ± 0.23 | 0.012 - 0.015 | 422.1 | ± 12.8 | 424.6 |
| 0.70 - 0.91 | 7.79 | ± 0.15 | ± 0.22 | 0.015 - 0.020 | 355.1 | ± 12.1 | 361.1 |
| 0.91 - 1.14 | 6.360 | ± 0.062 | ± 0.082 | 0.020 - 0.025 | 290.08 | ± 4.67 | 295.22 |
| 1.14 - 1.37 | 5.273 | ± 0.065 | ± 0.079 | 0.025 - 0.030 | 240.50 | ± 4.67 | 243.31 |
| 1.37 - 1.60 | 4.412 | ± 0.035 | ± 0.041 | 0.030 - 0.035 | 201.22 | ± 2.43 | 203.35 |
| 1.60 - 1.82 | 3.764 | ± 0.035 | ± 0.039 | 0.035 - 0.040 | 171.70 | ± 2.41 | 172.46 |
| 1.82 - 2.28 | 3.018 | ± 0.028 | ± 0.030 | 0.040 - 0.050 | 137.68 | ± 1.88 | 138.12 |
| 2.28 - 2.74 | 2.325 | ± 0.023 | ± 0.024 | 0.050 - 0.060 | 106.03 | ± 1.50 | 106.25 |
| 2.74 - 3.19 | 1.853 | ± 0.021 | ± 0.021 | 0.060 - 0.070 | 84.52 | ± 1.35 | 83.96 |
| 3.19 - 3.65 | 1.506 | ± 0.019 | ± 0.019 | 0.070 - 0.080 | 68.71 | ± 1.22 | 67.79 |
| 3.65 - 4.10 | 1.253 | ± 0.018 | ± 0.017 | 0.080 - 0.090 | 57.15 | ± 1.13 | 56.06 |
| 4.10 - 4.56 | 1.049 | ± 0.017 | ± 0.016 | 0.090 - 0.100 | 47.84 | ± 1.04 | 46.96 |
| 4.56 - 5.47 | 0.830 | ± 0.015 | ± 0.014 | 0.100 - 0.120 | 37.86 | ± 0.93 | 36.88 |
| 5.47 - 6.38 | 0.616 | ± 0.013 | ± 0.011 | 0.120 - 0.140 | 28.09 | ± 0.76 | 27.23 |
| 6.38 - 7.29 | 0.471 | ± 0.011 | ± 0.009 | 0.140 - 0.160 | 21.48 | ± 0.63 | 20.72 |
| 7.29 - 8.21 | 0.3684 | ± 0.0090 | ± 0.0074 | 0.160 - 0.180 | 16.80 | ± 0.53 | 16.10 |
| 8.21 - 9.12 | 0.2907 | ± 0.0074 | ± 0.0060 | 0.180 - 0.200 | 13.26 | ± 0.43 | 12.68 |
| 9.12 - 11.9 | 0.1911 | ± 0.0055 | ± 0.0043 | 0.200 - 0.260 | 8.72 | ± 0.32 | 8.33 |
| 11.9 - 13.7 | 0.1159 | ± 0.0036 | ± 0.0027 | 0.260 - 0.300 | 5.29 | ± 0.20 | 5.00 |
| 13.7 - 18.2 | 0.0635 | ± 0.0021 | ± 0.0015 | 0.300 - 0.400 | 2.90 | ± 0.12 | 2.72 |
| 18.2 - 22.8 | 0.0273 | ± 0.0011 | ± 0.0007 | 0.400 - 0.500 | 1.243 | ± 0.058 | 1.170 |
| 22.8 - 27.4 | 0.01216 | ± 0.00057 | ± 0.00037 | 0.500 - 0.600 | 0.554 | ± 0.031 | 0.517 |
| 27.4 - 36.5 | 0.00384 | ± 0.00039 | ± 0.00027 | 0.600 - 0.800 | 0.175 | ± 0.022 | 0.161 |
| 36.5 - 45.6 | 0.000530 | ± 0.000096 | ± 0.000050 | 0.800 - 1.000 | 0.0242 | ± 0.0050 | 0.0227 |

Table 22: Differential cross-section for charged particles in $Z^0 \to q\overline{q}$ versus JETSET (JS73).

| | DELPHI | | | | DELPHI | | JS73 |
|---|---|---|---|---|---|---|---|
| $p$ (GeV/$c$) | $\frac{1}{N_h}\frac{dn_{\pi}}{dp}$ | $\epsilon_{stat}$ | $\epsilon_{syst}$ | $X_p$ | $\frac{1}{N_h}\frac{dn_{\pi}}{dx_p}$ | $\epsilon_{tot}$ | $\frac{1}{N_h}\frac{dn_{\pi}}{dx_p}$ |
| 0.70 - 0.91 | 6.908 | ± 0.039 | ± 0.239 | 0.015 - 0.020 | 315.1 | ± 11.1 | 321.1 |
| 0.91 - 1.14 | 5.495 | ± 0.032 | ± 0.101 | 0.020 - 0.025 | 250.66 | ± 4.83 | 256.60 |
| 1.14 - 1.37 | 4.486 | ± 0.030 | ± 0.095 | 0.025 - 0.030 | 204.61 | ± 4.54 | 207.63 |
| 1.37 - 1.60 | 3.688 | ± 0.027 | ± 0.055 | 0.030 - 0.035 | 168.23 | ± 2.79 | 170.77 |
| 1.60 - 1.82 | 3.088 | ± 0.025 | ± 0.051 | 0.035 - 0.040 | 140.85 | ± 2.61 | 142.88 |
| 1.82 - 2.28 | 2.426 | ± 0.018 | ± 0.046 | 0.040 - 0.050 | 110.65 | ± 2.23 | 112.35 |
| 2.28 - 2.74 | 1.839 | ± 0.016 | ± 0.043 | 0.050 - 0.060 | 83.88 | ± 2.10 | 84.44 |
| 2.74 - 3.19 | 1.443 | ± 0.010 | ± 0.027 | 0.060 - 0.070 | 65.83 | ± 1.33 | 65.28 |
| 3.19 - 3.65 | 1.1517 | ± 0.0083 | ± 0.0257 | 0.070 - 0.080 | 52.53 | ± 1.23 | 51.71 |
| 3.65 - 4.10 | 0.9364 | ± 0.0072 | ± 0.0216 | 0.080 - 0.090 | 42.71 | ± 1.04 | 42.04 |
| 4.10 - 4.56 | 0.7714 | ± 0.0065 | ± 0.0183 | 0.090 - 0.100 | 35.19 | ± 0.89 | 34.63 |
| 4.56 - 5.47 | 0.5961 | ± 0.0042 | ± 0.0157 | 0.100 - 0.120 | 27.19 | ± 0.74 | 26.62 |
| 5.47 - 6.38 | 0.4306 | ± 0.0036 | ± 0.0124 | 0.120 - 0.140 | 19.64 | ± 0.59 | 19.08 |
| 6.38 - 7.29 | 0.3211 | ± 0.0032 | ± 0.0101 | 0.140 - 0.160 | 14.65 | ± 0.48 | 14.13 |
| 7.29 - 8.21 | 0.2464 | ± 0.0030 | ± 0.0082 | 0.160 - 0.180 | 11.24 | ± 0.40 | 10.76 |
| 8.21 - 9.12 | 0.1877 | ± 0.0024 | ± 0.0070 | 0.180 - 0.200 | 8.56 | ± 0.34 | 8.30 |
| 9.12 - 11.9 | 0.1194 | ± 0.0012 | ± 0.0045 | 0.200 - 0.260 | 5.45 | ± 0.21 | 5.30 |
| 11.9 - 13.7 | 0.06922 | ± 0.00096 | ± 0.00277 | 0.260 - 0.300 | 3.16 | ± 0.13 | 3.06 |
| 13.7 - 18.2 | 0.03661 | ± 0.00066 | ± 0.00154 | 0.300 - 0.400 | 1.670 | ± 0.077 | 1.612 |
| 18.2 - 22.8 | 0.01490 | ± 0.00042 | ± 0.00071 | 0.400 - 0.500 | 0.680 | ± 0.038 | 0.664 |
| 22.8 - 27.4 | 0.00673 | ± 0.00030 | ± 0.00037 | 0.500 - 0.600 | 0.307 | ± 0.022 | 0.289 |
| 27.4 - 36.5 | 0.00214 | ± 0.00020 | ± 0.00024 | 0.600 - 0.800 | 0.097 | ± 0.014 | 0.089 |
| 36.5 - 45.6 | 0.000298 | ± 0.000084 | ± 0.000056 | 0.800 - 1.000 | 0.0136 | ± 0.0046 | 0.0121 |

Table 23: Differential cross-section for $\pi^{\pm}$ in $Z^0 \to q\overline{q}$ versus JETSET (JS73).

| | DELPHI | | | | DELPHI | | JS73 |
|---|---|---|---|---|---|---|---|
| $p$ (GeV/$c$) | $\frac{1}{N_h}\frac{dn_K}{dp}$ | $\epsilon_{stat}$ | $\epsilon_{syst}$ | $X_p$ | $\frac{1}{N_h}\frac{dn_K}{dx_p}$ | $\epsilon_{tot}$ | $\frac{1}{N_h}\frac{dn_K}{dx_p}$ |
| 0.70 - 0.91 | 0.558 | ± 0.031 | ± 0.077 | 0.015 - 0.020 | 25.46 | ± 3.77 | 25.51 |
| 0.91 - 1.14 | 0.546 | ± 0.021 | ± 0.073 | 0.020 - 0.025 | 24.90 | ± 3.46 | 23.70 |
| 1.14 - 1.37 | 0.466 | ± 0.018 | ± 0.066 | 0.025 - 0.030 | 21.27 | ± 3.13 | 21.32 |
| 1.37 - 1.60 | 0.450 | ± 0.020 | ± 0.040 | 0.030 - 0.035 | 20.54 | ± 2.05 | 19.09 |
| 1.60 - 1.82 | 0.400 | ± 0.022 | ± 0.056 | 0.035 - 0.040 | 18.26 | ± 2.76 | 17.15 |
| 1.82 - 2.28 | 0.357 | ± 0.016 | ± 0.061 | 0.040 - 0.050 | 16.30 | ± 2.87 | 14.83 |
| 2.28 - 2.74 | 0.292 | ± 0.015 | ± 0.063 | 0.050 - 0.060 | 13.31 | ± 2.94 | 12.54 |
| 2.74 - 3.19 | 0.2455 | ± 0.0080 | ± 0.0154 | 0.060 - 0.070 | 11.20 | ± 0.79 | 10.76 |
| 3.19 - 3.65 | 0.2157 | ± 0.0061 | ± 0.0154 | 0.070 - 0.080 | 9.84 | ± 0.76 | 9.30 |
| 3.65 - 4.10 | 0.1953 | ± 0.0054 | ± 0.0120 | 0.080 - 0.090 | 8.91 | ± 0.60 | 8.14 |
| 4.10 - 4.56 | 0.1754 | ± 0.0052 | ± 0.0121 | 0.090 - 0.100 | 8.00 | ± 0.60 | 7.19 |
| 4.56 - 5.47 | 0.1443 | ± 0.0035 | ± 0.0097 | 0.100 - 0.120 | 6.58 | ± 0.47 | 6.00 |
| 5.47 - 6.38 | 0.1123 | ± 0.0040 | ± 0.0060 | 0.120 - 0.140 | 5.12 | ± 0.33 | 4.79 |
| 6.38 - 7.29 | 0.0906 | ± 0.0052 | ± 0.0083 | 0.140 - 0.160 | 4.13 | ± 0.45 | 3.89 |
| 7.29 - 8.21 | 0.0720 | ± 0.0060 | ± 0.0090 | 0.160 - 0.180 | 3.29 | ± 0.49 | 3.19 |
| 8.21 - 9.12 | 0.0624 | ± 0.0033 | ± 0.0086 | 0.180 - 0.200 | 2.85 | ± 0.42 | 2.65 |
| 9.12 - 11.9 | 0.04344 | ± 0.00082 | ± 0.00204 | 0.200 - 0.260 | 1.98 | ± 0.10 | 1.86 |
| 11.9 - 13.7 | 0.02917 | ± 0.00073 | ± 0.00155 | 0.260 - 0.300 | 1.331 | ± 0.078 | 1.209 |
| 13.7 - 18.2 | 0.01699 | ± 0.00044 | ± 0.00115 | 0.300 - 0.400 | 0.775 | ± 0.056 | 0.708 |
| 18.2 - 22.8 | 0.00791 | ± 0.00033 | ± 0.00079 | 0.400 - 0.500 | 0.361 | ± 0.039 | 0.337 |
| 22.8 - 27.4 | 0.00364 | ± 0.00025 | ± 0.00036 | 0.500 - 0.600 | 0.166 | ± 0.020 | 0.164 |
| 27.4 - 36.5 | 0.00130 | ± 0.00017 | ± 0.00027 | 0.600 - 0.800 | 0.059 | ± 0.015 | 0.060 |
| 36.5 - 45.6 | 0.000147 | ± 0.000082 | ± 0.000108 | 0.800 - 1.000 | 0.0067 | ± 0.0062 | 0.0100 |

Table 24: Differential cross-section for $K^{\pm}$ in $Z^0 \to q\overline{q}$ versus JETSET (JS73).

| | DELPHI | | | | DELPHI | | JS73 |
|---|---|---|---|---|---|---|---|
| $p$ (GeV/$c$) | $\frac{1}{N_h}\frac{dn_p}{dp}$ | $\epsilon_{stat}$ | $\epsilon_{syst}$ | $X_p$ | $\frac{1}{N_h}\frac{dn_p}{dx_p}$ | $\epsilon_{tot}$ | $\frac{1}{N_h}\frac{dn_p}{dx_p}$ |
| 0.70 - 0.91 | 0.320 | ± 0.016 | ± 0.072 | 0.015 - 0.020 | 14.61 | ± 3.37 | 12.44 |
| 0.91 - 1.14 | 0.308 | ± 0.018 | ± 0.053 | 0.020 - 0.025 | 14.06 | ± 2.58 | 12.96 |
| 1.14 - 1.37 | 0.249 | ± 0.022 | ± 0.043 | 0.025 - 0.030 | 11.34 | ± 2.22 | 12.53 |
| 1.37 - 1.60 | 0.263 | ± 0.021 | ± 0.030 | 0.030 - 0.035 | 12.01 | ± 1.66 | 11.73 |
| 1.60 - 1.82 | 0.249 | ± 0.015 | ± 0.027 | 0.035 - 0.040 | 11.35 | ± 1.40 | 10.78 |
| 1.82 - 2.28 | 0.232 | ± 0.012 | ± 0.021 | 0.040 - 0.050 | 10.58 | ± 1.10 | 9.40 |
| 2.28 - 2.74 | 0.1566 | ± 0.0062 | ± 0.0175 | 0.050 - 0.060 | 7.14 | ± 0.85 | 7.87 |
| 2.74 - 3.19 | 0.1198 | ± 0.0034 | ± 0.0123 | 0.060 - 0.070 | 5.46 | ± 0.58 | 6.64 |
| 3.19 - 3.65 | 0.1028 | ± 0.0036 | ± 0.0097 | 0.070 - 0.080 | 4.69 | ± 0.47 | 5.60 |
| 3.65 - 4.10 | 0.0934 | ± 0.0036 | ± 0.0108 | 0.080 - 0.090 | 4.26 | ± 0.52 | 4.79 |
| 4.10 - 4.56 | 0.0758 | ± 0.0035 | ± 0.0097 | 0.090 - 0.100 | 3.46 | ± 0.47 | 4.16 |
| 4.56 - 5.47 | 0.0695 | ± 0.0027 | ± 0.0066 | 0.100 - 0.120 | 3.17 | ± 0.32 | 3.39 |
| 5.47 - 6.38 | 0.0579 | ± 0.0036 | ± 0.0069 | 0.120 - 0.140 | 2.64 | ± 0.35 | 2.63 |
| 6.38 - 7.29 | 0.0457 | ± 0.0054 | ± 0.0062 | 0.140 - 0.160 | 2.08 | ± 0.37 | 2.06 |
| 7.29 - 8.21 | 0.0382 | ± 0.0065 | ± 0.0063 | 0.160 - 0.180 | 1.74 | ± 0.41 | 1.62 |
| 8.21 - 9.12 | 0.0299 | ± 0.0038 | ± 0.0046 | 0.180 - 0.200 | 1.37 | ± 0.27 | 1.27 |
| 9.12 - 11.9 | 0.0193 | ± 0.0010 | ± 0.0021 | 0.200 - 0.260 | 0.88 | ± 0.11 | 0.83 |
| 11.9 - 13.7 | 0.01246 | ± 0.00076 | ± 0.00140 | 0.260 - 0.300 | 0.569 | ± 0.073 | 0.486 |
| 13.7 - 18.2 | 0.00616 | ± 0.00036 | ± 0.00065 | 0.300 - 0.400 | 0.281 | ± 0.034 | 0.255 |
| 18.2 - 22.8 | 0.00260 | ± 0.00021 | ± 0.00044 | 0.400 - 0.500 | 0.119 | ± 0.022 | 0.102 |
| 22.8 - 27.4 | 0.00106 | ± 0.00015 | ± 0.00023 | 0.500 - 0.600 | 0.048 | ± 0.013 | 0.040 |
| 27.4 - 36.5 | 0.000269 | ± 0.000084 | ± 0.000107 | 0.600 - 0.800 | 0.0123 | ± 0.0062 | 0.0097 |
| 36.5 - 45.6 | 0.000046 | ± 0.000059 | ± 0.000028 | 0.800 - 1.000 | 0.0021 | ± 0.0030 | 0.0006 |

Table 25: Differential cross-section for protons in $Z^0 \to q\overline{q}$ versus JETSET (JS73).

| | DELPHI | | | | DELPHI | | JS73 |
|---|---|---|---|---|---|---|---|
| $p$ (GeV/$c$) | $\frac{1}{N_h}\frac{dn_{tot}}{dp}$ | $\epsilon_{stat}$ | $\epsilon_{syst}$ | $X_p$ | $\frac{1}{N_h}\frac{dn_{tot}}{dx_p}$ | $\epsilon_{tot}$ | $\frac{1}{N_h}\frac{dn_{tot}}{dx_p}$ |
| 0.30 - 0.36 | 12.05 | ± 0.46 | ± 0.74 | 0.007 - 0.008 | 549.5 | ± 39.7 | 542.2 |
| 0.36 - 0.46 | 11.80 | ± 0.30 | ± 0.52 | 0.008 - 0.010 | 538.4 | ± 27.3 | 534.4 |
| 0.46 - 0.57 | 11.23 | ± 0.16 | ± 0.24 | 0.010 - 0.012 | 512.3 | ± 13.0 | 507.7 |
| 0.57 - 0.70 | 10.28 | ± 0.16 | ± 0.23 | 0.012 - 0.015 | 469.1 | ± 12.8 | 466.8 |
| 0.70 - 0.91 | 8.84 | ± 0.16 | ± 0.22 | 0.015 - 0.020 | 403.2 | ± 12.3 | 403.6 |
| 0.91 - 1.14 | 7.336 | ± 0.064 | ± 0.082 | 0.020 - 0.025 | 334.61 | ± 4.73 | 333.93 |
| 1.14 - 1.37 | 6.159 | ± 0.065 | ± 0.079 | 0.025 - 0.030 | 280.93 | ± 4.68 | 276.66 |
| 1.37 - 1.60 | 5.208 | ± 0.034 | ± 0.041 | 0.030 - 0.035 | 237.57 | ± 2.42 | 231.68 |
| 1.60 - 1.82 | 4.466 | ± 0.034 | ± 0.040 | 0.035 - 0.040 | 203.70 | ± 2.38 | 196.91 |
| 1.82 - 2.28 | 3.586 | ± 0.027 | ± 0.030 | 0.040 - 0.050 | 163.57 | ± 1.84 | 157.90 |
| 2.28 - 2.74 | 2.806 | ± 0.021 | ± 0.024 | 0.050 - 0.060 | 127.98 | ± 1.46 | 121.90 |
| 2.74 - 3.19 | 2.235 | ± 0.019 | ± 0.021 | 0.060 - 0.070 | 101.95 | ± 1.29 | 96.61 |
| 3.19 - 3.65 | 1.831 | ± 0.017 | ± 0.019 | 0.070 - 0.080 | 83.53 | ± 1.16 | 78.50 |
| 3.65 - 4.10 | 1.510 | ± 0.016 | ± 0.017 | 0.080 - 0.090 | 68.89 | ± 1.07 | 64.74 |
| 4.10 - 4.56 | 1.259 | ± 0.015 | ± 0.016 | 0.090 - 0.100 | 57.43 | ± 0.98 | 53.87 |
| 4.56 - 5.47 | 0.966 | ± 0.013 | ± 0.014 | 0.100 - 0.120 | 44.04 | ± 0.86 | 41.31 |
| 5.47 - 6.38 | 0.687 | ± 0.011 | ± 0.011 | 0.120 - 0.140 | 31.32 | ± 0.70 | 29.33 |
| 6.38 - 7.29 | 0.4967 | ± 0.0086 | ± 0.0092 | 0.140 - 0.160 | 22.66 | ± 0.57 | 21.28 |
| 7.29 - 8.21 | 0.3681 | ± 0.0070 | ± 0.0077 | 0.160 - 0.180 | 16.79 | ± 0.46 | 15.74 |
| 8.21 - 9.12 | 0.2764 | ± 0.0057 | ± 0.0063 | 0.180 - 0.200 | 12.61 | ± 0.38 | 11.85 |
| 9.12 - 11.9 | 0.1637 | ± 0.0043 | ± 0.0047 | 0.200 - 0.260 | 7.46 | ± 0.28 | 7.17 |
| 11.9 - 13.7 | 0.0882 | ± 0.0028 | ± 0.0034 | 0.260 - 0.300 | 4.02 | ± 0.18 | 3.87 |
| 13.7 - 18.2 | 0.0431 | ± 0.0022 | ± 0.0025 | 0.300 - 0.400 | 1.96 | ± 0.12 | 1.91 |
| 18.2 - 22.8 | 0.0152 | ± 0.0012 | ± 0.0021 | 0.400 - 0.500 | 0.694 | ± 0.064 | 0.714 |
| 22.8 - 27.4 | 0.00577 | ± 0.00071 | ± 0.00203 | 0.500 - 0.600 | 0.263 | ± 0.037 | 0.261 |
| 27.4 - 36.5 | 0.00120 | ± 0.00041 | ± 0.00202 | 0.600 - 0.800 | 0.055 | ± 0.022 | 0.048 |
| 36.5 - 45.6 | 0.0000201 | ± 0.0000085 | ± 0.0020006 | 0.800 - 1.000 | 0.0009 | ± 0.0023 | 0.0006 |

Table 26: Differential cross-section for charged particles in $Z^0 \to b\bar{b}$ versus JETSET (JS73).

| | DELPHI | | | | DELPHI | | JS73 |
|---|---|---|---|---|---|---|---|
| $p$ (GeV/$c$) | $\frac{1}{N_h}\frac{dn_{\pi}}{dp}$ | $\epsilon_{stat}$ | $\epsilon_{syst}$ | $X_p$ | $\frac{1}{N_h}\frac{dn_{\pi}}{dx_p}$ | $\epsilon_{tot}$ | $\frac{1}{N_h}\frac{dn_{\pi}}{dx_p}$ |
| 0.70 - 0.91 | 7.781 | ± 0.096 | ± 0.246 | 0.015 - 0.020 | 354.9 | ± 12.0 | 358.3 |
| 0.91 - 1.14 | 6.334 | ± 0.078 | ± 0.102 | 0.020 - 0.025 | 288.90 | ± 5.87 | 290.00 |
| 1.14 - 1.37 | 5.205 | ± 0.072 | ± 0.098 | 0.025 - 0.030 | 237.41 | ± 5.55 | 235.49 |
| 1.37 - 1.60 | 4.280 | ± 0.066 | ± 0.060 | 0.030 - 0.035 | 195.20 | ± 4.09 | 193.52 |
| 1.60 - 1.82 | 3.595 | ± 0.063 | ± 0.056 | 0.035 - 0.040 | 163.96 | ± 3.84 | 161.31 |
| 1.82 - 2.28 | 2.768 | ± 0.044 | ± 0.047 | 0.040 - 0.050 | 126.27 | ± 2.96 | 125.92 |
| 2.28 - 2.74 | 2.140 | ± 0.039 | ± 0.047 | 0.050 - 0.060 | 97.59 | ± 2.76 | 93.88 |
| 2.74 - 3.19 | 1.674 | ± 0.025 | ± 0.031 | 0.060 - 0.070 | 76.35 | ± 1.83 | 71.74 |
| 3.19 - 3.65 | 1.312 | ± 0.020 | ± 0.027 | 0.070 - 0.080 | 59.83 | ± 1.55 | 56.59 |
| 3.65 - 4.10 | 1.049 | ± 0.017 | ± 0.022 | 0.080 - 0.090 | 47.84 | ± 1.26 | 45.39 |
| 4.10 - 4.56 | 0.853 | ± 0.015 | ± 0.019 | 0.090 - 0.100 | 38.92 | ± 1.10 | 36.76 |
| 4.56 - 5.47 | 0.6166 | ± 0.0095 | ± 0.0138 | 0.100 - 0.120 | 28.13 | ± 0.76 | 27.04 |
| 5.47 - 6.38 | 0.4124 | ± 0.0077 | ± 0.0101 | 0.120 - 0.140 | 18.81 | ± 0.58 | 18.07 |
| 6.38 - 7.29 | 0.2861 | ± 0.0066 | ± 0.0079 | 0.140 - 0.160 | 13.05 | ± 0.47 | 12.38 |
| 7.29 - 8.21 | 0.2010 | ± 0.0057 | ± 0.0058 | 0.160 - 0.180 | 9.17 | ± 0.37 | 8.79 |
| 8.21 - 9.12 | 0.1457 | ± 0.0044 | ± 0.0051 | 0.180 - 0.200 | 6.64 | ± 0.30 | 6.39 |
| 9.12 - 11.9 | 0.0810 | ± 0.0018 | ± 0.0029 | 0.200 - 0.260 | 3.70 | ± 0.16 | 3.64 |
| 11.9 - 13.7 | 0.0409 | ± 0.0014 | ± 0.0018 | 0.260 - 0.300 | 1.87 | ± 0.10 | 1.84 |
| 13.7 - 18.2 | 0.01858 | ± 0.00093 | ± 0.00088 | 0.300 - 0.400 | 0.848 | ± 0.058 | 0.849 |
| 18.2 - 22.8 | 0.00629 | ± 0.00051 | ± 0.00042 | 0.400 - 0.500 | 0.287 | ± 0.030 | 0.303 |
| 22.8 - 27.4 | 0.00252 | ± 0.00035 | ± 0.00028 | 0.500 - 0.600 | 0.115 | ± 0.020 | 0.122 |
| 27.4 - 36.5 | 0.00081 | ± 0.00030 | ± 0.00018 | 0.600 - 0.800 | 0.037 | ± 0.016 | 0.030 |
| 36.5 - 45.6 | 0.000016 | ± 0.000042 | ± 0.000013 | 0.800 - 1.000 | 0.0007 | ± 0.0020 | 0.0004 |

Table 27: Differential cross-section for $\pi^{\pm}$ in $Z^0 \to b\bar{b}$ versus JETSET (JS73).

| | DELPHI | | | | DELPHI | | JS73 |
|---|---|---|---|---|---|---|---|
| $p$ (GeV/$c$) | $\frac{1}{N_h}\frac{dn_K}{dp}$ | $\epsilon_{stat}$ | $\epsilon_{syst}$ | $X_p$ | $\frac{1}{N_h}\frac{dn_K}{dx_p}$ | $\epsilon_{tot}$ | $\frac{1}{N_h}\frac{dn_K}{dx_p}$ |
| 0.70 - 0.91 | 0.667 | ± 0.090 | ± 0.084 | 0.015 - 0.020 | 30.42 | ± 5.61 | 26.66 |
| 0.91 - 1.14 | 0.612 | ± 0.064 | ± 0.083 | 0.020 - 0.025 | 27.93 | ± 4.80 | 25.15 |
| 1.14 - 1.37 | 0.523 | ± 0.060 | ± 0.080 | 0.025 - 0.030 | 23.84 | ± 4.57 | 23.32 |
| 1.37 - 1.60 | 0.585 | ± 0.051 | ± 0.050 | 0.030 - 0.035 | 26.68 | ± 3.27 | 21.56 |
| 1.60 - 1.82 | 0.483 | ± 0.061 | ± 0.075 | 0.035 - 0.040 | 22.02 | ± 4.44 | 20.32 |
| 1.82 - 2.28 | 0.494 | ± 0.025 | ± 0.076 | 0.040 - 0.050 | 22.55 | ± 3.67 | 18.59 |
| 2.28 - 2.74 | 0.398 | ± 0.016 | ± 0.078 | 0.050 - 0.060 | 18.17 | ± 3.63 | 16.72 |
| 2.74 - 3.19 | 0.335 | ± 0.018 | ± 0.020 | 0.060 - 0.070 | 15.26 | ± 1.22 | 15.03 |
| 3.19 - 3.65 | 0.3225 | ± 0.0096 | ± 0.0203 | 0.070 - 0.080 | 14.71 | ± 1.02 | 13.36 |
| 3.65 - 4.10 | 0.2845 | ± 0.0055 | ± 0.0211 | 0.080 - 0.090 | 12.97 | ± 0.99 | 11.72 |
| 4.10 - 4.56 | 0.249 | ± 0.010 | ± 0.015 | 0.090 - 0.100 | 11.34 | ± 0.81 | 10.20 |
| 4.56 - 5.47 | 0.2022 | ± 0.0061 | ± 0.0106 | 0.100 - 0.120 | 9.22 | ± 0.56 | 8.20 |
| 5.47 - 6.38 | 0.1526 | ± 0.0070 | ± 0.0101 | 0.120 - 0.140 | 6.96 | ± 0.56 | 6.14 |
| 6.38 - 7.29 | 0.109 | ± 0.011 | ± 0.010 | 0.140 - 0.160 | 4.98 | ± 0.68 | 4.60 |
| 7.29 - 8.21 | 0.083 | ± 0.011 | ± 0.012 | 0.160 - 0.180 | 3.79 | ± 0.75 | 3.47 |
| 8.21 - 9.12 | 0.0625 | ± 0.0050 | ± 0.0087 | 0.180 - 0.200 | 2.85 | ± 0.46 | 2.67 |
| 9.12 - 11.9 | 0.0379 | ± 0.0013 | ± 0.0017 | 0.200 - 0.260 | 1.727 | ± 0.099 | 1.600 |
| 11.9 - 13.7 | 0.0199 | ± 0.0011 | ± 0.0011 | 0.260 - 0.300 | 0.907 | ± 0.071 | 0.827 |
| 13.7 - 18.2 | 0.00868 | ± 0.00068 | ± 0.00059 | 0.300 - 0.400 | 0.396 | ± 0.041 | 0.368 |
| 18.2 - 22.8 | 0.00231 | ± 0.00041 | ± 0.00027 | 0.400 - 0.500 | 0.105 | ± 0.023 | 0.109 |
| 22.8 - 27.4 | 0.00062 | ± 0.00023 | ± 0.00006 | 0.500 - 0.600 | 0.028 | ± 0.011 | 0.032 |
| 27.4 - 36.5 | 0.000024 | ± 0.000062 | ± 0.000005 | 0.600 - 0.800 | 0.0011 | ± 0.0028 | 0.0049 |
| 36.5 - 45.6 | 0.0000007 | ± 0.0000036 | ± 0.0000009 | 0.800 - 1.000 | 0.00003 | ± 0.00017 | 0.00005 |

Table 28: Differential cross-section for $K^{\pm}$ in $Z^0 \to b\bar{b}$ versus JETSET (JS73).

| | DELPHI | | | | DELPHI | | JS73 |
|---|---|---|---|---|---|---|---|
| $p$ (GeV/$c$) | $\frac{1}{N_h}\frac{dn_p}{dp}$ | $\epsilon_{stat}$ | $\epsilon_{syst}$ | $X_p$ | $\frac{1}{N_h}\frac{dn_p}{dx_p}$ | $\epsilon_{tot}$ | $\frac{1}{N_h}\frac{dn_p}{dx_p}$ |
| 0.70 - 0.91 | 0.303 | ± 0.051 | ± 0.066 | 0.015 - 0.020 | 13.82 | ± 3.83 | 12.33 |
| 0.91 - 1.14 | 0.305 | ± 0.053 | ± 0.050 | 0.020 - 0.025 | 13.93 | ± 3.32 | 12.72 |
| 1.14 - 1.37 | 0.331 | ± 0.049 | ± 0.068 | 0.025 - 0.030 | 15.11 | ± 3.82 | 12.07 |
| 1.37 - 1.60 | 0.266 | ± 0.066 | ± 0.029 | 0.030 - 0.035 | 12.14 | ± 3.31 | 11.05 |
| 1.60 - 1.82 | 0.257 | ± 0.049 | ± 0.028 | 0.035 - 0.040 | 11.73 | ± 2.56 | 9.99 |
| 1.82 - 2.28 | 0.284 | ± 0.042 | ± 0.030 | 0.040 - 0.050 | 12.96 | ± 2.35 | 8.39 |
| 2.28 - 2.74 | 0.176 | ± 0.026 | ± 0.025 | 0.050 - 0.060 | 8.02 | ± 1.66 | 6.79 |
| 2.74 - 3.19 | 0.117 | ± 0.016 | ± 0.014 | 0.060 - 0.070 | 5.32 | ± 0.97 | 5.65 |
| 3.19 - 3.65 | 0.093 | ± 0.016 | ± 0.011 | 0.070 - 0.080 | 4.24 | ± 0.87 | 4.71 |
| 3.65 - 4.10 | 0.092 | ± 0.015 | ± 0.011 | 0.080 - 0.090 | 4.18 | ± 0.86 | 4.11 |
| 4.10 - 4.56 | 0.072 | ± 0.016 | ± 0.011 | 0.090 - 0.100 | 3.29 | ± 0.88 | 3.70 |
| 4.56 - 5.47 | 0.079 | ± 0.010 | ± 0.008 | 0.100 - 0.120 | 3.62 | ± 0.58 | 3.23 |
| 5.47 - 6.38 | 0.075 | ± 0.012 | ± 0.010 | 0.120 - 0.140 | 3.40 | ± 0.71 | 2.76 |
| 6.38 - 7.29 | 0.060 | ± 0.019 | ± 0.007 | 0.140 - 0.160 | 2.74 | ± 0.91 | 2.26 |
| 7.29 - 8.21 | 0.044 | ± 0.022 | ± 0.009 | 0.160 - 0.180 | 2.00 | ± 1.07 | 1.75 |
| 8.21 - 9.12 | 0.034 | ± 0.011 | ± 0.005 | 0.180 - 0.200 | 1.56 | ± 0.55 | 1.32 |
| 9.12 - 11.9 | 0.0173 | ± 0.0029 | ± 0.0021 | 0.200 - 0.260 | 0.79 | ± 0.16 | 0.76 |
| 11.9 - 13.7 | 0.0089 | ± 0.0018 | ± 0.0009 | 0.260 - 0.300 | 0.406 | ± 0.091 | 0.365 |
| 13.7 - 18.2 | 0.00371 | ± 0.00071 | ± 0.00037 | 0.300 - 0.400 | 0.169 | ± 0.037 | 0.145 |
| 18.2 - 22.8 | 0.00102 | ± 0.00033 | ± 0.00017 | 0.400 - 0.500 | 0.046 | ± 0.017 | 0.037 |
| 22.8 - 27.4 | 0.00027 | ± 0.00019 | ± 0.00007 | 0.500 - 0.600 | 0.0124 | ± 0.0092 | 0.0110 |
| 27.4 - 36.5 | 0.000083 | ± 0.000074 | ± 0.000077 | 0.600 - 0.800 | 0.0038 | ± 0.0049 | 0.0017 |
| 36.5 - 45.6 | 0.0000045 | ± 0.0000060 | ± 0.0000173 | 0.800 - 1.000 | 0.00021 | ± 0.00084 | 0.00005 |

Table 29: Differential cross-section for protons in $Z^0 \to b\bar{b}$ versus JETSET (JS73).

| DELPHI | | | | DELPHI | | | JS73 |
|---|---|---|---|---|---|---|---|
| $p$ (GeV/$c$) | $\frac{1}{N_h}\frac{dn_{tot}}{dp}$ | $\epsilon_{stat}$ | $\epsilon_{syst}$ | $X_p$ | $\frac{1}{N_h}\frac{dn_{tot}}{dx_p}$ | $\epsilon_{tot}$ | $\frac{1}{N_h}\frac{dn_{tot}}{dx_p}$ |
| 0.30 - 0.36 | 10.97 | ± 0.47 | ± 0.74 | 0.007 - 0.008 | 500.6 | ± 40.0 | 497.9 |
| 0.36 - 0.46 | 10.69 | ± 0.31 | ± 0.52 | 0.008 - 0.010 | 487.8 | ± 27.5 | 485.6 |
| 0.46 - 0.57 | 10.02 | ± 0.16 | ± 0.24 | 0.010 - 0.012 | 457.0 | ± 13.1 | 454.5 |
| 0.57 - 0.70 | 8.95 | ± 0.16 | ± 0.23 | 0.012 - 0.015 | 408.0 | ± 12.8 | 409.6 |
| 0.70 - 0.91 | 7.46 | ± 0.15 | ± 0.22 | 0.015 - 0.020 | 340.5 | ± 12.0 | 346.1 |
| 0.91 - 1.14 | 6.046 | ± 0.061 | ± 0.082 | 0.020 - 0.025 | 275.76 | ± 4.64 | 281.34 |
| 1.14 - 1.37 | 4.966 | ± 0.063 | ± 0.079 | 0.025 - 0.030 | 226.53 | ± 4.63 | 230.68 |
| 1.37 - 1.60 | 4.124 | ± 0.034 | ± 0.041 | 0.030 - 0.035 | 188.13 | ± 2.41 | 192.00 |
| 1.60 - 1.82 | 3.506 | ± 0.034 | ± 0.040 | 0.035 - 0.040 | 159.91 | ± 2.38 | 162.38 |
| 1.82 - 2.28 | 2.801 | ± 0.028 | ± 0.030 | 0.040 - 0.050 | 127.76 | ± 1.87 | 129.70 |
| 2.28 - 2.74 | 2.141 | ± 0.023 | ± 0.024 | 0.050 - 0.060 | 97.66 | ± 1.49 | 99.62 |
| 2.74 - 3.19 | 1.708 | ± 0.021 | ± 0.021 | 0.060 - 0.070 | 77.90 | ± 1.34 | 78.78 |
| 3.19 - 3.65 | 1.390 | ± 0.019 | ± 0.019 | 0.070 - 0.080 | 63.39 | ± 1.22 | 63.54 |
| 3.65 - 4.10 | 1.156 | ± 0.018 | ± 0.017 | 0.080 - 0.090 | 52.73 | ± 1.14 | 52.58 |
| 4.10 - 4.56 | 0.968 | ± 0.017 | ± 0.016 | 0.090 - 0.100 | 44.15 | ± 1.05 | 44.08 |
| 4.56 - 5.47 | 0.774 | ± 0.015 | ± 0.014 | 0.100 - 0.120 | 35.28 | ± 0.93 | 34.88 |
| 5.47 - 6.38 | 0.581 | ± 0.013 | ± 0.011 | 0.120 - 0.140 | 26.52 | ± 0.77 | 26.03 |
| 6.38 - 7.29 | 0.451 | ± 0.011 | ± 0.009 | 0.140 - 0.160 | 20.56 | ± 0.64 | 20.08 |
| 7.29 - 8.21 | 0.3597 | ± 0.0093 | ± 0.0077 | 0.160 - 0.180 | 16.41 | ± 0.54 | 15.86 |
| 8.21 - 9.12 | 0.2877 | ± 0.0076 | ± 0.0063 | 0.180 - 0.200 | 13.12 | ± 0.44 | 12.65 |
| 9.12 - 11.9 | 0.1948 | ± 0.0058 | ± 0.0047 | 0.200 - 0.260 | 8.89 | ± 0.33 | 8.57 |
| 11.9 - 13.7 | 0.1232 | ± 0.0038 | ± 0.0034 | 0.260 - 0.300 | 5.62 | ± 0.21 | 5.35 |
| 13.7 - 18.2 | 0.0707 | ± 0.0024 | ± 0.0025 | 0.300 - 0.400 | 3.22 | ± 0.13 | 3.04 |
| 18.2 - 22.8 | 0.0324 | ± 0.0013 | ± 0.0021 | 0.400 - 0.500 | 1.477 | ± 0.068 | 1.389 |
| 22.8 - 27.4 | 0.01528 | ± 0.00076 | ± 0.00203 | 0.500 - 0.600 | 0.697 | ± 0.038 | 0.659 |
| 27.4 - 36.5 | 0.00530 | ± 0.00057 | ± 0.00202 | 0.600 - 0.800 | 0.242 | ± 0.029 | 0.230 |
| 36.5 - 45.6 | 0.00079 | ± 0.00017 | ± 0.00200 | 0.800 - 1.000 | 0.0360 | ± 0.0079 | 0.0366 |

Table 30: Differential cross-section for charged particles in $Z^0 \to u\overline{u}, d\overline{d}, s\overline{s}$ versus JETSET (JS73).

| DELPHI | | | | DELPHI | | | JS73 |
|---|---|---|---|---|---|---|---|
| $p$ (GeV/$c$) | $\frac{1}{N_h}\frac{dn_{\pi}}{dp}$ | $\epsilon_{stat}$ | $\epsilon_{syst}$ | $X_p$ | $\frac{1}{N_h}\frac{dn_{\pi}}{dx_p}$ | $\epsilon_{tot}$ | $\frac{1}{N_h}\frac{dn_{\pi}}{dx_p}$ |
| 0.70 - 0.91 | 6.65 | ± 0.13 | ± 0.20 | 0.015 - 0.020 | 303.4 | ± 11.1 | 308.3 |
| 0.91 - 1.14 | 5.231 | ± 0.065 | ± 0.086 | 0.020 - 0.025 | 238.58 | ± 4.91 | 244.96 |
| 1.14 - 1.37 | 4.245 | ± 0.061 | ± 0.080 | 0.025 - 0.030 | 193.64 | ± 4.58 | 197.31 |
| 1.37 - 1.60 | 3.487 | ± 0.043 | ± 0.046 | 0.030 - 0.035 | 159.03 | ± 2.86 | 161.82 |
| 1.60 - 1.82 | 2.902 | ± 0.040 | ± 0.043 | 0.035 - 0.040 | 132.35 | ± 2.70 | 135.31 |
| 1.82 - 2.28 | 2.296 | ± 0.031 | ± 0.038 | 0.040 - 0.050 | 104.73 | ± 2.23 | 106.51 |
| 2.28 - 2.74 | 1.729 | ± 0.030 | ± 0.037 | 0.050 - 0.060 | 78.85 | ± 2.15 | 80.40 |
| 2.74 - 3.19 | 1.351 | ± 0.019 | ± 0.023 | 0.060 - 0.070 | 61.63 | ± 1.34 | 62.68 |
| 3.19 - 3.65 | 1.101 | ± 0.017 | ± 0.023 | 0.070 - 0.080 | 50.22 | ± 1.29 | 49.94 |
| 3.65 - 4.10 | 0.901 | ± 0.014 | ± 0.019 | 0.080 - 0.090 | 41.09 | ± 1.08 | 40.89 |
| 4.10 - 4.56 | 0.747 | ± 0.013 | ± 0.016 | 0.090 - 0.100 | 34.06 | ± 0.94 | 33.90 |
| 4.56 - 5.47 | 0.590 | ± 0.010 | ± 0.014 | 0.100 - 0.120 | 26.91 | ± 0.80 | 26.50 |
| 5.47 - 6.38 | 0.4369 | ± 0.0083 | ± 0.0115 | 0.120 - 0.140 | 19.93 | ± 0.65 | 19.46 |
| 6.38 - 7.29 | 0.3324 | ± 0.0070 | ± 0.0094 | 0.140 - 0.160 | 15.16 | ± 0.53 | 14.77 |
| 7.29 - 8.21 | 0.2635 | ± 0.0062 | ± 0.0077 | 0.160 - 0.180 | 12.02 | ± 0.45 | 11.50 |
| 8.21 - 9.12 | 0.2037 | ± 0.0050 | ± 0.0066 | 0.180 - 0.200 | 9.29 | ± 0.38 | 9.03 |
| 9.12 - 11.9 | 0.1333 | ± 0.0031 | ± 0.0043 | 0.200 - 0.260 | 6.08 | ± 0.24 | 6.00 |
| 11.9 - 13.7 | 0.0812 | ± 0.0022 | ± 0.0027 | 0.260 - 0.300 | 3.70 | ± 0.16 | 3.64 |
| 13.7 - 18.2 | 0.0449 | ± 0.0014 | ± 0.0015 | 0.300 - 0.400 | 2.046 | ± 0.094 | 2.002 |
| 18.2 - 22.8 | 0.01938 | ± 0.00084 | ± 0.00073 | 0.400 - 0.500 | 0.884 | ± 0.051 | 0.868 |
| 22.8 - 27.4 | 0.00930 | ± 0.00057 | ± 0.00037 | 0.500 - 0.600 | 0.424 | ± 0.031 | 0.394 |
| 27.4 - 36.5 | 0.00290 | ± 0.00040 | ± 0.00028 | 0.600 - 0.800 | 0.132 | ± 0.022 | 0.129 |
| 36.5 - 45.6 | 0.00042 | ± 0.00015 | ± 0.00006 | 0.800 - 1.000 | 0.0194 | ± 0.0075 | 0.0195 |

Table 31: Differential cross-section for pions in $Z^0 \to u\overline{u}, d\overline{d}, s\overline{s}$ versus JETSET (JS73).

| | DELPHI | | | | DELPHI | | JS73 |
|---|---|---|---|---|---|---|---|
| $p$ (GeV/$c$) | $\frac{1}{N_h}\frac{dn_K}{dp}$ | $\epsilon_{stat}$ | $\epsilon_{syst}$ | $X_p$ | $\frac{1}{N_h}\frac{dn_K}{dx_p}$ | $\epsilon_{tot}$ | $\frac{1}{N_h}\frac{dn_K}{dx_p}$ |
| 0.70 - 0.91 | 0.527 | ± 0.047 | ± 0.061 | 0.015 - 0.020 | 24.06 | ± 3.51 | 25.05 |
| 0.91 - 1.14 | 0.524 | ± 0.037 | ± 0.058 | 0.020 - 0.025 | 23.88 | ± 3.15 | 23.10 |
| 1.14 - 1.37 | 0.447 | ± 0.033 | ± 0.052 | 0.025 - 0.030 | 20.37 | ± 2.84 | 20.51 |
| 1.37 - 1.60 | 0.398 | ± 0.031 | ± 0.031 | 0.030 - 0.035 | 18.16 | ± 2.00 | 18.14 |
| 1.60 - 1.82 | 0.374 | ± 0.036 | ± 0.045 | 0.035 - 0.040 | 17.07 | ± 2.64 | 15.98 |
| 1.82 - 2.28 | 0.314 | ± 0.040 | ± 0.047 | 0.040 - 0.050 | 14.33 | ± 2.80 | 13.44 |
| 2.28 - 2.74 | 0.253 | ± 0.045 | ± 0.049 | 0.050 - 0.060 | 11.55 | ± 3.04 | 10.98 |
| 2.74 - 3.19 | 0.217 | ± 0.014 | ± 0.012 | 0.060 - 0.070 | 9.91 | ± 0.83 | 9.14 |
| 3.19 - 3.65 | 0.180 | ± 0.014 | ± 0.013 | 0.070 - 0.080 | 8.19 | ± 0.85 | 7.70 |
| 3.65 - 4.10 | 0.160 | ± 0.010 | ± 0.009 | 0.080 - 0.090 | 7.30 | ± 0.62 | 6.65 |
| 4.10 - 4.56 | 0.147 | ± 0.010 | ± 0.009 | 0.090 - 0.100 | 6.72 | ± 0.63 | 5.83 |
| 4.56 - 5.47 | 0.1189 | ± 0.0078 | ± 0.0068 | 0.100 - 0.120 | 5.43 | ± 0.47 | 4.86 |
| 5.47 - 6.38 | 0.0901 | ± 0.0064 | ± 0.0043 | 0.120 - 0.140 | 4.11 | ± 0.35 | 3.91 |
| 6.38 - 7.29 | 0.0756 | ± 0.0088 | ± 0.0063 | 0.140 - 0.160 | 3.45 | ± 0.49 | 3.23 |
| 7.29 - 8.21 | 0.0629 | ± 0.0093 | ± 0.0065 | 0.160 - 0.180 | 2.87 | ± 0.52 | 2.73 |
| 8.21 - 9.12 | 0.0561 | ± 0.0071 | ± 0.0069 | 0.180 - 0.200 | 2.56 | ± 0.45 | 2.32 |
| 9.12 - 11.9 | 0.0401 | ± 0.0015 | ± 0.0017 | 0.200 - 0.260 | 1.83 | ± 0.10 | 1.71 |
| 11.9 - 13.7 | 0.0287 | ± 0.0013 | ± 0.0015 | 0.260 - 0.300 | 1.308 | ± 0.090 | 1.189 |
| 13.7 - 18.2 | 0.01838 | ± 0.00082 | ± 0.00112 | 0.300 - 0.400 | 0.838 | ± 0.063 | 0.756 |
| 18.2 - 22.8 | 0.00927 | ± 0.00055 | ± 0.00077 | 0.400 - 0.500 | 0.423 | ± 0.043 | 0.397 |
| 22.8 - 27.4 | 0.00471 | ± 0.00036 | ± 0.00047 | 0.500 - 0.600 | 0.215 | ± 0.027 | 0.214 |
| 27.4 - 36.5 | 0.00211 | ± 0.00026 | ± 0.00033 | 0.600 - 0.800 | 0.096 | ± 0.019 | 0.087 |
| 36.5 - 45.6 | 0.00027 | ± 0.00012 | ± 0.00015 | 0.800 - 1.000 | 0.0125 | ± 0.0088 | 0.0162 |

Table 32: Differential cross-section for kaons in $Z^0 \to u\overline{u}, d\overline{d}, s\overline{s}$ versus JETSET (JS73).

| | DELPHI | | | | DELPHI | | JS73 |
|---|---|---|---|---|---|---|---|
| $p$ (GeV/$c$) | $\frac{1}{N_h}\frac{dn_p}{dp}$ | $\epsilon_{stat}$ | $\epsilon_{syst}$ | $X_p$ | $\frac{1}{N_h}\frac{dn_p}{dx_p}$ | $\epsilon_{tot}$ | $\frac{1}{N_h}\frac{dn_p}{dx_p}$ |
| 0.70 - 0.91 | 0.354 | ± 0.028 | ± 0.075 | 0.015 - 0.020 | 16.13 | ± 3.64 | 12.45 |
| 0.91 - 1.14 | 0.317 | ± 0.031 | ± 0.054 | 0.020 - 0.025 | 14.46 | ± 2.82 | 13.01 |
| 1.14 - 1.37 | 0.219 | ± 0.035 | ± 0.035 | 0.025 - 0.030 | 9.98 | ± 2.26 | 12.65 |
| 1.37 - 1.60 | 0.251 | ± 0.025 | ± 0.024 | 0.030 - 0.035 | 11.44 | ± 1.58 | 11.88 |
| 1.60 - 1.82 | 0.243 | ± 0.018 | ± 0.025 | 0.035 - 0.040 | 11.07 | ± 1.41 | 10.95 |
| 1.82 - 2.28 | 0.208 | ± 0.015 | ± 0.017 | 0.040 - 0.050 | 9.49 | ± 1.00 | 9.65 |
| 2.28 - 2.74 | 0.1451 | ± 0.0082 | ± 0.0145 | 0.050 - 0.060 | 6.62 | ± 0.76 | 8.16 |
| 2.74 - 3.19 | 0.1200 | ± 0.0021 | ± 0.0113 | 0.060 - 0.070 | 5.47 | ± 0.52 | 6.91 |
| 3.19 - 3.65 | 0.1043 | ± 0.0030 | ± 0.0088 | 0.070 - 0.080 | 4.76 | ± 0.42 | 5.86 |
| 3.65 - 4.10 | 0.0914 | ± 0.0041 | ± 0.0093 | 0.080 - 0.090 | 4.17 | ±0.47 | 5.00 |
| 4.10 - 4.56 | 0.0762 | ± 0.0035 | ± 0.0091 | 0.090 - 0.100 | 3.47 | ± 0.44 | 4.32 |
| 4.56 - 5.47 | 0.0655 | ± 0.0036 | ± 0.0052 | 0.100 - 0.120 | 2.99 | ± 0.29 | 3.49 |
| 5.47 - 6.38 | 0.0552 | ± 0.0048 | ± 0.0061 | 0.120 - 0.140 | 2.52 | ± 0.36 | 2.64 |
| 6.38 - 7.29 | 0.0419 | ± 0.0066 | ± 0.0054 | 0.140 - 0.160 | 1.91 | ± 0.39 | 2.06 |
| 7.29 - 8.21 | 0.0345 | ± 0.0077 | ± 0.0045 | 0.160 - 0.180 | 1.57 | ± 0.41 | 1.62 |
| 8.21 - 9.12 | 0.0277 | ± 0.0049 | ± 0.0037 | 0.180 - 0.200 | 1.27 | ± 0.28 | 1.28 |
| 9.12 - 11.9 | 0.0204 | ± 0.0013 | ± 0.0019 | 0.200 - 0.260 | 0.93 | ± 0.11 | 0.86 |
| 11.9 - 13.7 | 0.0132 | ± 0.0010 | ± 0.0014 | 0.260 - 0.300 | 0.602 | ± 0.079 | 0.524 |
| 13.7 - 18.2 | 0.00681 | ± 0.00048 | ± 0.00065 | 0.300 - 0.400 | 0.311 | ± 0.037 | 0.285 |
| 18.2 - 22.8 | 0.00315 | ± 0.00028 | ± 0.00045 | 0.400 - 0.500 | 0.144 | ± 0.024 | 0.123 |
| 22.8 - 27.4 | 0.00143 | ± 0.00021 | ± 0.00024 | 0.500 - 0.600 | 0.065 | ± 0.015 | 0.051 |
| 27.4 - 36.5 | 0.00027 | ± 0.00014 | ± 0.00007 | 0.600 - 0.800 | 0.0124 | ± 0.0071 | 0.0133 |
| 36.5 - 45.6 | 0.00007 | ± 0.00029 | ± 0.00003 | 0.800 - 1.000 | 0.003 | ± 0.013 | 0.001 |

Table 33: Differential cross-section for protons in $Z^0 \to u\overline{u}, d\overline{d}, s\overline{s}$ versus JETSET (JS73).

# References


[1] T. Sjöstrand, Comp. Phys. Comm. 39 (1986) 347;
T. Sjöstrand, M. Bengtsson, Comp. Phys. Comm. 43 (1987) 367;
T. Sjöstrand, Comp. Phys. Comm. 82 (1994) 74;
T. Sjöstrand, JETSET manual CERN–TH/7112/93 (1994).

[2] G. Marchesini and B. Webber, Nucl. Phys. B238 (1984) 1;
G. Marchesini et al., Comp. Phys. Comm. 67 (1992) 465;
G. Marchesini et al., HERWIG 5.8c manual.

[3] DELPHI Collaboration, Nucl. Instr. and Meth. A303 (1991) 233-276.

[4] DELPHI Collaboration, P. Abreu et al., Nucl. Instr. and Meth. A378 (1996) 57-100, and references therein.

[5] E.G. Anassontzis et al., Nucl. Instr. and Meth. A323 (1992) 351;
W. Adam et al., Nucl. Instr. and Meth. A343 (1994) 68;
DELPHI RICH Collaboration, Nucl. Instr. and Meth. A371 (1996).

[6] E. Schyns, PhD thesis, WUB-DIS 96-22, University of Wuppertal, Germany.

[7] DELPHI Collaboration, P. Abreu et al., Z. Phys. C73 (1996) 11.

[8] E. Schyns, NEWTAG - $\pi$, K, p Tagging for DELPHI RICHes.
DELPHI-Note 96-103 RICH 89 (1996).

[9] Y. Azimov et al., Z. Phys. C31 (1986) 213-218, and references therein;
C.P. Fong and B.R. Webber, Phys. Lett. B229 (1989) 289;
C.P. Fong and B.R. Webber, Nucl. Phys. B355 (1991) 54;
Y.Dokshitzer, V. Khoze and S. Troyan, Z. Phys. C55 (1992) 107, and ref. [19] therein.

[10] V.A. Khoze and W. Ochs, Int. J. mod. phys. A12 (1997) 2949-3119.

[11] ALEPH Collaboration, Phys. Rep. 294 (1998) 1, and references [72,161] therein.

[12] Particle Data Group, R. Barnett et al., Phys. Rev. D54, (1996) 1.

[13] OPAL Collaboration, R. Akers et al., Z. Phys. C63 (1994) 181-195.

[14] DELPHI Collaboration, P. Abreu et al., Phys. Lett. B444(1995) 3.

[15] DELPHI Collaboration, P. Abreu et al., Measurement of the Quark and Gluon Fragmentation Functions in $Z^0$ Hadronic Decays,
CERN–PPE/97-108, Accepted by E. Phys. J. C.

[16] OPAL Collaboration, R. Akers et al., Phys. Lett. B352 (1995) 176-186.

[17] SLD Collaboration, K. Abe et al., SLAC-PUB-96-7172.

[18] DELPHI Collaboration, P. Abreu et al., Phys. Lett. B347(1995) 447-466.

[19] SLD Collaboration, K. Abe et al., SLAC-PUB-95-6920.

[20] OPAL Collaboration, Identified Charged Particle Production in Quark and Gluon Jets, OPAL Physics Note PN 299, Preliminary results submitted to the XVIII International Symposium on Lepton-Photon Interactions,
28 July - 1 August 1997, Hamburg, Germany.

[21] OPAL Collaboration, M.Z. Akrawy et al., Phys. Lett. B247 (1990) 617-628.

[22] L3 Collaboration, O. Adriani et al., Phys. Lett. B259 (1991) 199.